CHAPTER 9

Imaging

Conventional Radiographic Procedures

INTRODUCTION

The last two decades have witnessed extraordinary advances in medical imaging, but conventional radiographic procedures remain the keystone in diagnosing musculoskeletal disorders. With the exception of ultrasonography, used in assessing congenital hip dysplasia, plain radiography should be the first imaging study performed in working up musculoskeletal problems. The plain film may lead to a definitive diagnosis, with no other radiologic test required. If not, the conventional radiographic findings are essential for planning subsequent imaging studies. Additional imaging modalities may better delineate the extent and aggressiveness of musculoskeletal disease, but prior to biopsy most bone diseases have been and continue to be identified from characteristic plain film findings. Even biopsy material often has limited value without x-ray correlation. As the renowned surgeon and pathologist James Ewing stated more than 75 years ago, the gross anatomy (as revealed in radiographs) is often a safer guide to a correct clinical conception of the disease than the variable and uncertain structure of a small piece of tissue.[4,7] Ewing's statement remains correct, supporting plain radiography as the first-line test in diagnosing musculoskeletal disease.

AN APPROACH TO INTERPRETING PEDIATRIC ORTHOPAEDIC FILMS

An adequate knowledge of the pediatric skeletal system is the most important factor in interpreting pediatric orthopaedic films. Generally, pediatric orthopaedists have a proficient knowledge of this organ system, which dramatically changes from birth to approximately 20 years of life. But there are additional factors, not always employed by orthopaedic surgeons, that help to enhance the interpretation of pediatric orthopaedic radiographs. A discussion of these guidelines follows.

Viewing Conditions. The room in which x-rays are viewed should be as dimly illuminated as possible. Visual acuity markedly improves as the ambient light is decreased. Subtle bony and soft tissue changes can be missed if this simple rule is not followed.

Impact of Clinical History on Film Interpretation. If possible, pertinent clinical information should be known before the examiner views the pediatric patient's x-rays. Knowledge of the patient's age, sex, race, and symptoms facilitates a more accurate diagnosis.

AGE. Age is one of the most important parts of the clinical history, as many pediatric skeletal disorders or manifestations of a particular disorder occur only within certain age ranges. The patient's age, in combination with the skeletal findings, often leads to a diagnosis or helps to limit the differential diagnosis. The patient's age should be printed on all x-rays, but if it is not, every effort should be made to obtain the patient's age before a final radiographic diagnosis is made. The importance of knowing the patient's age is demonstrated by the following scenario. An infant's anteroposterior (AP) pelvic radiograph, obtained at an outside institution, is submitted for evaluation of possible congenital hip dysplasia. The patient's age is not given. Both capital femoral epiphyses are symmetrically ossified and both hips are conjugated, with no acetabular dysplasia identified. A false assumption is made that the infant is age 4 to 6 months (the normal age range for ossification of the capital femoral ossific nuclei), and a radiographic diagnosis of normal hips is made. The pelvic film submitted, however, was obtained when the infant was 1 week old. The age in combination with the radiographic appearance points to advanced bone maturation, whose multiple causes in the newborn period include hyperthyroidism, Beckwith-Wiedemann syndrome, congenital adrenal hyperplasia, and other disorders. The patient is then deprived of an early intervention that could ameliorate or rectify the disorder.

SEX. Knowing the patient's sex also proves helpful in many instances. For example, skeletal maturation occurs on differ-

ent time lines in male and female pediatric populations. Also, knowledge of the patient's sex can help the clinician include or to exclude certain X-linked disorders such as spondyloepiphyseal dysplasia tarda. For still unknown reasons, many skeletal disorders are more commonly associated with one of the sexes. Some of the skeletal disorders that occur much more frequently in males are Legg-Calvé-Perthes disease, slipped capital femoral epiphyses (SCFE), and Poland's syndrome. Madelung's deformity, idiopathic scoliosis, and congenital hip dysplasia occur much more frequently in females. Knowing some of these more common associations may be useful in certain instances.

RACE. The patient's race is often less helpful in the diagnosis than age and sex, yet it may occasionally be useful. For example, certain tropical populations tend to walk earlier than those in more temperate areas and have a higher incidence of infantile Blount's disease. Knowing that the young patient is black may be helpful in grouping multiple radiographic findings relating to sickle cell disease.

SIGNS AND SYMPTOMS. Quite different disease processes may produce similar bony radiographic changes, and without knowledge of the patient's signs and symptoms, a definite diagnosis cannot always be determined. For example, Ewing's sarcoma and osteomyelitis may be indistinguishable radiographically. An acute onset of osseous pain and febrile episodes favors osteomyelitis, whereas a chronic and indolent course favors Ewing's sarcoma. The importance of clinical correlation with radiographic findings is illustrated by the scenario of a 5-year-old white boy who presents with a painful hip. The age and sex of the patient make Legg-Calvé-Perthes disease the most likely diagnosis before the film is read. But on first inspection of the AP pelvic film, the hips appear unremarkable. The clinical record notes that the patient had a febrile illness several weeks before the onset of pain, thought to have represented some type of viral syndrome. A subsequent hip sonogram reveals a hip effusion, which is then tapped and an organism is isolated. Is a septic hip the end of the story? If the symptoms are relatively acute, the answer is probably yes. If, however, the clinical history reveals that the patient has been lethargic for several months and has recently developed easy bruisability, a second look at the whole pelvis may reveal "leukemia lines" around the ilia (Fig. 9–1). It is extremely important to examine the bones carefully when leukemia (most commonly acute lymphoblastic leukemia) is considered, as the bone marrow and peripheral blood smear may initially be negative, with only radiographic changes being present. The last example is an uncommon scenario but not unheard of, which underscores the importance of integrating the clinical history and *all* of the radiographic findings. Looking at the entire radiograph leads to the next guideline.

AVOIDING TUNNEL VISION. Optimally, the radiographs should be viewed in a room with little ambient light and interpreted in the context of the patient's clinical history. With or with-

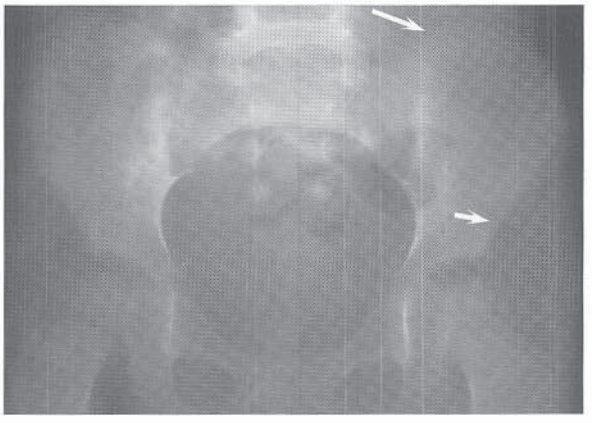

A

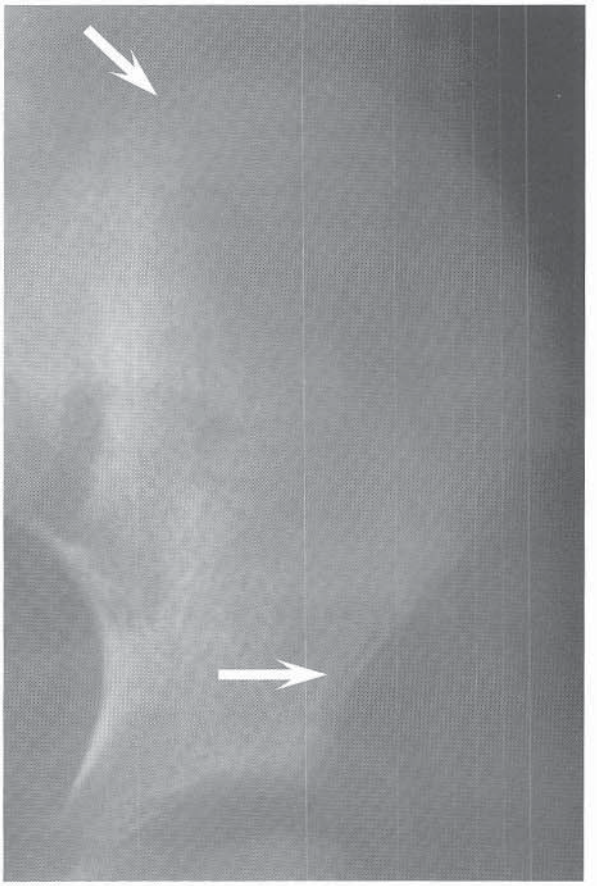

B

FIGURE 9–1 Leukemia lines present about the ilia.

out these requisites, however, the entire film should be scrutinized, not just the area of interest or of obvious pathology. Using some type of patterned search encourages the interpreter to analyze all parts of the film and not to fall prey to tunnel vision. The radiographic examiner may wish to cover the obvious finding with a piece of paper or may use some mnemonic device to remember to look at all areas of the film. Whatever the method used, all pattern searches should include (1) an examination of the soft tissues, (2) an examination of all organ systems included in the radiographic study, and (3) an examination of the portion of the skeletal system not obviously involved by pathology.

Examination of the Soft Tissues. Examination of the soft tissues may direct the interpreter to evaluate or reevaluate an adjacent osseous structure that at first glance appears normal. For example, detecting soft tissue edema or a joint effusion should direct the examiner to look for a subtle fracture that is not immediately recognizable. In addition, the soft tissues should be scrutinized for masses, calcifications, and foreign bodies. If the films are too dark—that is, overexposed for adequate soft tissue evaluation—they should be examined with a hot light or "windowed and leveled" on a computed radiography workstation.

Examination of All Organ Systems Included in the Radiographic Study. For example, following the evaluation of the spine on a scoliosis film, the radiographic interpreter should undertake a systematic pattern search of the remaining areas included on the film. A "head-to-toe" search first directs the observer to the lung fields for evaluation of intrinsic lung disease as well as for evaluation of bowel above the diaphragm (hiatal, paraesophageal, Morgagni, or posttraumatic hernias), which should be identified before surgery. Mediastinal lymph node involvement may represent primary tuberculosis, lymphoma, Castleman's disease, or sarcoidosis. Then the abdomen is evaluated for abnormal bowel gas patterns and abnormal intra-abdominal calcifications such as appendicoliths, gallstones, urinary calculi, hepatic and splenic calcification, ovarian calcifications (most commonly teratomas), calcification within the scrotal sac (meconium peritonitis or testicular teratoma), and psoas abscess calcification. A last look at the pelvic region should include scrutiny of the presacral region, for fetal skeletal parts may rarely be detected if the patient is pregnant.

Evaluation of the Skeletal System Not Obviously Involved by Pathology. A frequent cause of hip pain in the overweight adolescent (most commonly black males) is SCFE. Most cases of SCFE are idiopathic, but the entire pelvis should be scrutinized for rare causes such as primary hyperparathyroidism (very rare in children), secondary hyperparathyroidism associated with chronic renal failure, or vitamin D–deficient rickets (Fig. 9–2). Also, 10 percent of patients with pseudohypoparathyroidism have associated hyperparathyroidism and may develop SCFE. In all of these patients, subperiosteal, endosteal, subcortical, and subchondral resorption may occur. An underlying cause of SCFE may be missed if the entire film is not evaluated.

FIGURE 9–2 Pelvic film of a 14-year-old black girl with primary hyperparathyroidism (parathyroid adenoma) demonstrates bilateral slipped capital femoral epiphysis (SCFE) as well as subperiosteal resorption of bone at the public symphysis. The latter finding may be seen with hyperparathyroidism but not with idiopathic SCFE.

THE IMPORTANCE OF PREVIOUS STUDIES

The importance of comparing the current radiographic study with previous studies, if available, cannot be overemphasized. The reasons for such a comparison are: First, a slowly enlarging lesion may not be recognized as significant unless all previous studies are viewed together in chronological sequence. For example, a 9-year-old boy presents with knee pain after falling off his bicycle. Radiographs of his knees show no fracture, but a 1-cm, well-circumscribed sclerotic lesion is identified and thought to represent a bone island. The patient returns after 4 weeks with persistent knee pain. Another set of knee films is taken and compared with the previous study. The report issued at this time states that no change since the previous study is noted and no fractures are identified. Incidental note of the bone island is again made. The patient returns a third time 9 weeks after the initial injury. A third set of films is obtained that show no change when compared with the most previous study. When the third set of knee films (obtained 9 weeks post injury) is compared with the initial set of films, however, the previously diagnosed bone island is seen to have slightly enlarged. Although bone islands may occasionally enlarge, the differential diagnosis now includes osteoid osteoma, Garré's sclerosing osteomyelitis, low-grade sclerosing osteogenic sarcoma, and fibrous dysplasia. Subtle changes in the size of any lesion may only be appreciated when all previous examinations are compared with the current study.

Second, a subtle lesion not detectable on a current radiograph may become obvious when the current study is compared with an older study that may demonstrate the lesion more clearly because of a different projection or technique. For example, radiographs of an adolescent's lumbosacral spine are submitted, along with a history of pain and a request to evaluate for spondylolysis. The current study does not clearly delineate a pars intra-articularis defect, but on review of the previous lateral scoliosis film the examiner identifies a definite spondylolysis that was overlooked by the previous examiner. More times than any radiographic examiner likes to admit, the answer is on an old study, already in the x-ray jacket.

Third, if older studies are not reviewed in their entirety when bone dysplasia is considered, a correct diagnosis may be delayed or never made. Many bone dysplasias have similar or indistinguishable appearances during the various stages of their development. For example, the radiographic appearances of spondyloepiphyseal dysplasia congenita and Strudwick's spondyloepimetaphyseal dysplasia are indistinguishable in the early years of life. In the past, Morquio's syndrome was confused with Koslowski's spondylometaphyseal dysplasia during certain stages of its development. The overlapping

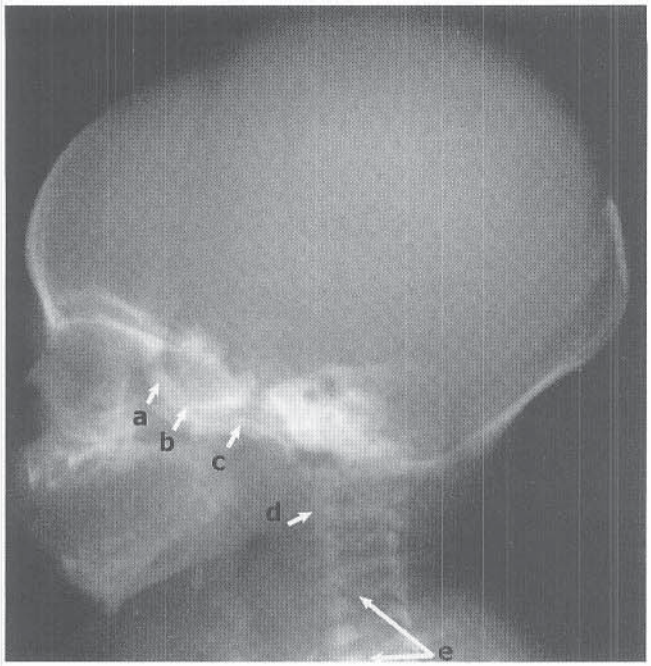

FIGURE 9–3 Frontosphenoid synchondrosis (*a*); intersphenoid synchondrosis (*b*); spheno-occipital synchondrosis (*c*); synchondrosis between the odontoid and body of C2 (*d*); synchondrosis between vertebral bodies and neural arches (*e*).

radiographic appearances of many bone dysplasias direct the examiner to closely observe the patient's radiographic findings over time in order to make a correct diagnosis.

A final caveat concerning previous radiographic studies: Expert witnesses always review the entire case. It behooves practitioners to do the same.

WHEN PLAIN FILMS STAND ALONE

Plain radiography may be the only imaging modality needed for diagnosis. It is the only study needed to assess many fractures, to evaluate bone age, to diagnose bone dysplasias, and to identify normal variants. The first three topics are discussed in other chapters. This section addresses some of the more common roentgen variants of normal. The reader is referred to *Atlas of Normal Roentgen Variants That May Simulate Disease* (6th ed., 1995), by Theodore Keats, for an exhaustive review of the subject. This radiographic atlas shows the appearance of normal variants in all organ systems from infancy through adulthood. Using this atlas when unusual bony findings are encountered helps the practitioner determine whether the osseous structure in question is a normal variant, and so may help avoid further imaging studies. If Keats's atlas or another atlas of normal variants is not available, the analogous anatomic part may be imaged for comparison. For example, if the same peculiar bone is present in both feet, it is almost always a normal variant. Rarely, normal variants may be involved by traumatic, infectious, or neoplastic changes. The patient's history and clinical findings then help to determine the subsequent imaging studies needed, if any.

Normal Radiographic Variants of the Immature Skeleton

SEVERAL SYNCHONDROSES COMMONLY MISTAKEN FOR FRACTURES

Sphenoid Bone Synchondroses. An infant is born with three synchondroses of the sphenoid bone. The frontosphenoid synchondrosis and the intersphenoid synchondrosis close by several months to 1 year of life. The spheno-occipital synchondrosis, however, may remain patent until early adulthood (Figs. 9–3, *a* to *c*). These synchondroses generally are not attended to by the orthopaedic surgeon except when assessing the cervical spine for trauma. The most common question then asked is, Do these synchondroses represent basilar skull fractures? Knowing the existence of these synchondroses and when they close eliminates the need to do other time-intensive and expensive studies.

Body of C2 and Odontoid Synchondrosis. The synchondrosis between the odontoid and body of C2 may simulate a fracture from birth until it closes, at between 3 and 7 years of life (Fig. 9–3, *d*; see also Fig. 9–7, *b*). When it is partially fused it may appear as an incomplete fracture of the odontoid. Assessment of the odontoid's alignment with the body of C2 then becomes extremely important. If the alignment is not anatomic, further evaluation with com-

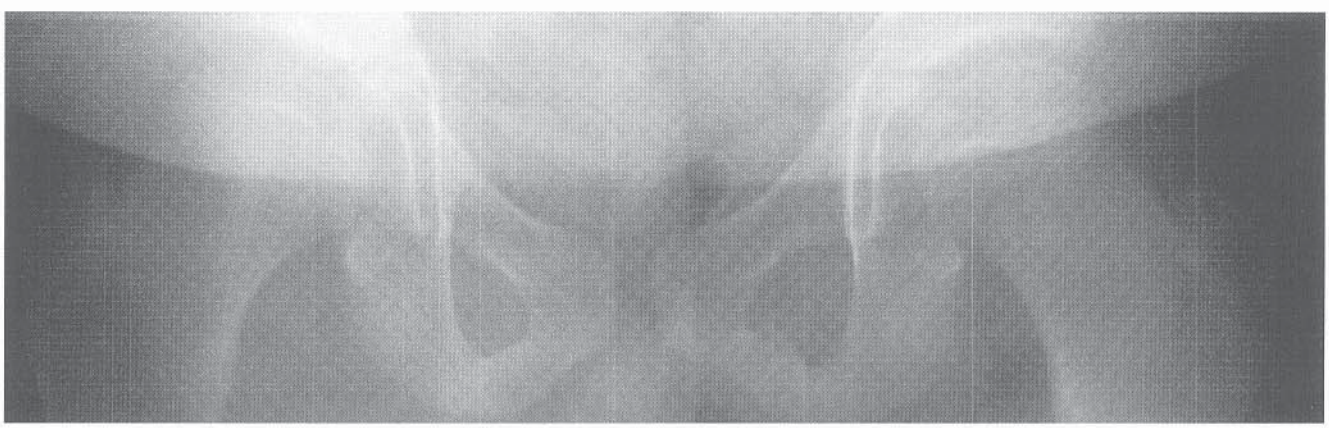

FIGURE 9–4 Asymmetrically mineralized ischiopubic synchondroses.

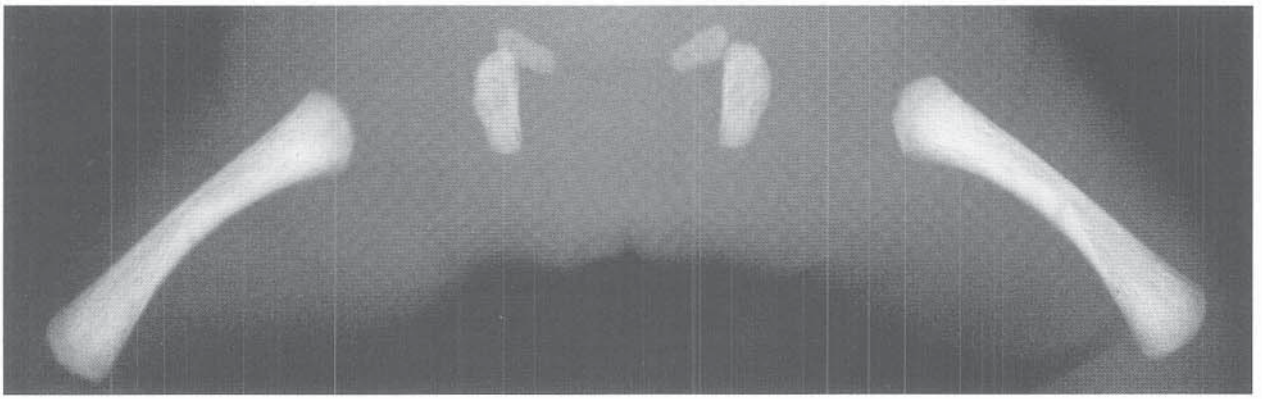

FIGURE 9–5 Osteosclerosis of the newborn.

puted tomography (CT) or magnetic resonance imaging (MRI) is indicated.

Synchondroses Between Vertebral Bodies and Neural Arches. These synchondroses appear as lucent lines between the vertebral bodies and neural arches from birth until mid-childhood, when they generally close (Fig. 9–3, *e*). They become particularly noticeable on oblique views of the infant's cervical spine and may mimic fractures. Reference to Keats's atlas is reassuring and instructive.

A SYNCHONDROSIS COMMONLY CONFUSED WITH INFECTIONS OR NEOPLASTIC CHANGE

Ischiopubic Synchondrosis. The ischiopubic synchondroses may have irregular mineralization and may be asymmetrically expanded (Fig. 9–4). The asymmetry is unusual, for most normal variants tend to be symmetric. Complete bilateral ossification occurs as early as age 4 years or as late as 14 years. Pain and tenderness may be associated with an irregularly mineralized and expanded ischiopubic synchondrosis, but without positive laboratory findings, further workup is unnecessary. Biopsy of this synchondrosis should not be done, as false positive results for neoplastic changes frequently occur. Not uncommonly, however, osteomyelitis may involve the ischiopubic synchondrosis, with positive blood cultures, elevated sedimentation rates, or increased C-reactive protein levels confirming the diagnosis. With adequate antibiotic therapy, the prognosis is good.

SEVERAL BONY NORMAL VARIANTS THAT ARE FREQUENTLY CONFUSED WITH PATHOLOGIC CHANGES

Osteosclerosis of the Newborn. A neonate's long bones may appear very dense and can be mistaken for pathologic conditions such as osteopetrosis (Fig. 9–5). In general, however, significant clinical findings are associated with pathologic osteosclerotic conditions. For example, jaundice, hepatosplenomegaly, anemia, or pancytopenia are associated with osteopetrosis manifesting in the newborn period. Normal osteosclerosis of the newborn has no associated signs or symptoms and resolves several weeks after birth.

Physiologic Periosteal New Bone Formation of the Newborn. Physiologic periosteal new bone is not present before 1 month of life and is most commonly noted between 1 and 6 months of life. It is almost always bilateral and symmetric, involving the femur, humerus, and tibia most frequently. The periosteal new bone formation is thin and separated by a lucent line from the diaphyseal cortex (Fig. 9–6). The patient's age, the bilateral symmetry, and the benign radiographic image differentiate this condition from pathologic entities such as trauma, congenital syphilis, osteomyelitis, prostaglandin therapy, infantile cortical hyperostosis (Caffey's disease), leukemia, and neuroblastoma.

Cervical Spine Pseudosubluxation. Owing to ligamentous laxity and horizontally positioned facet joints, the upper cervical spine in infants and children may appear to sublux-

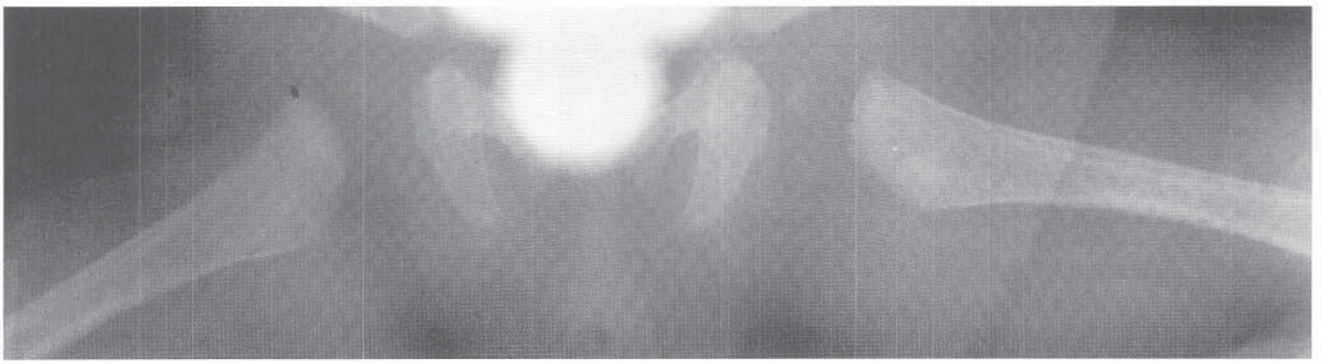

FIGURE 9–6 Physiologic periosteal new bone formation in a 5-month-old infant.

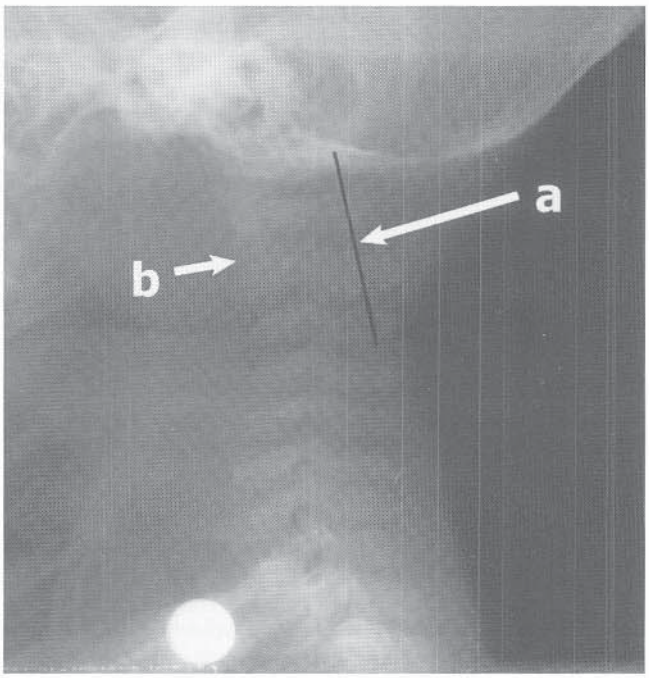

FIGURE 9–7 Physiologic subluxation of C2 on C3 confirmed by using the posterior cervical line. The posterior cervical line (*a*). Synchondrosis between odontoid and body of C2 is well demonstrated (*b*).

ate during flexion. When multiple cervical vertebral bodies are involved, physiologic subluxation is clearly the diagnosis. Subluxation limited to C2 on C3, however, may be physiologic or associated with a hangman's fracture. To differentiate these conditions, Swischuk devised the posterior cervical line.[9] This line is drawn from the anterior cortex of the C1 posterior ring to the anterior cortex of the spinous process of C3 (Fig. 9–7). If the line misses the anterior cortex of the spinous process of C2 by more than 2 mm, a true dislocation is present. This line should be used only to assess C2–3 subluxation and should not be applied at any other level. Moreover, a normal posterior cervical line does not exclude significant ligamentous injury.

Dense Transverse Metaphyseal Lines. Normal children have dense transverse metaphyseal lines, especially between ages 2 and 6 years, that may be confused with radiodense metaphyseal bands associated with lead poisoning (Fig. 9–8). Two radiographic findings, however, may help to distinguish normal radiodense metaphyseal lines from those seen in lead poisoning: (1) normal dense metaphyseal lines are no denser than the metaphyseal or diaphyseal bony cortex, whereas the dense metaphyseal bands associated with lead poisoning are generally denser than the metaphyseal or diaphyseal bony cortex, and (2) a dense metaphyseal line commonly involves the proximal fibula with lead poisoning, but the proximal fibula is usually not involved in the normal patient with dense metaphyseal lines.[1] Lead poisoning, however, cannot be definitively diagnosed from radiographic findings. Chemical tests of blood and urine must be employed to diagnose plumbism.

Avulsive Cortical Irregularity. The avulsive cortical irregularity generally involves the posterior aspect of the medial femoral condyle, appearing as an irregular and concave defect that may simulate a malignancy (Fig. 9–9). The lesion most probably results from repetitive avulsive-type trauma. This defect is most frequently seen in 10- to 15-year-olds, is more common in males, and is often bilateral. An avulsive cortical irregularity should not be biopsied, as a misdiagnosis of osteosarcoma may be made. A correct diagnosis is made by knowing the general age ranges as well as the characteristic location and radiographic features of the avulsive cortical defect.

Radiographic Technique

CHILD-FRIENDLY RADIOLOGY DEPARTMENT AND TECHNICAL STAFF

A well-trained technical staff that is experienced in working with children is essential to the running of a pediatric radiology department. A technologist who is comfortable in caring for children can allay both the child's and the parent's apprehensions and thereby decrease the time and effort required

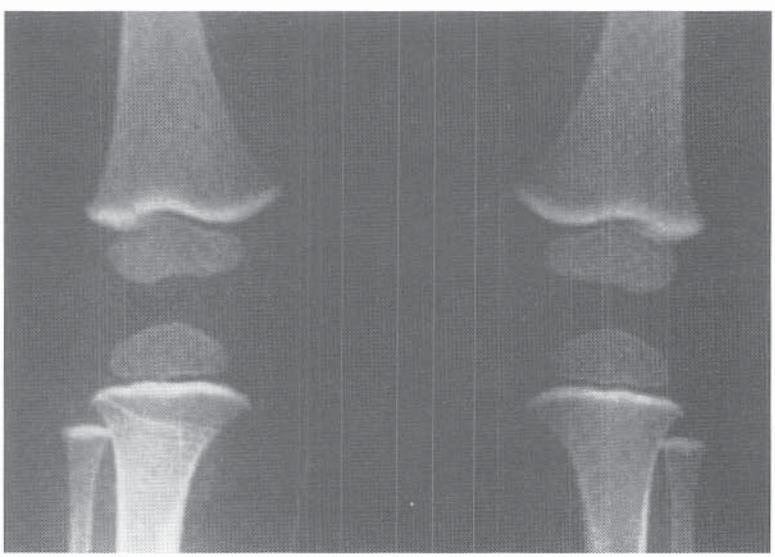

FIGURE 9–8 Transverse radiodense metaphyseal bands in the femur, tibia, and fibula in a child with lead poisoning. (From Resnick D (ed): Diagnosis of Bone and Joint Disorders, 3rd ed. Philadelphia, WB Saunders Co, 1995. Courtesy of F. Silverman, M.D., Stanford, CA.)

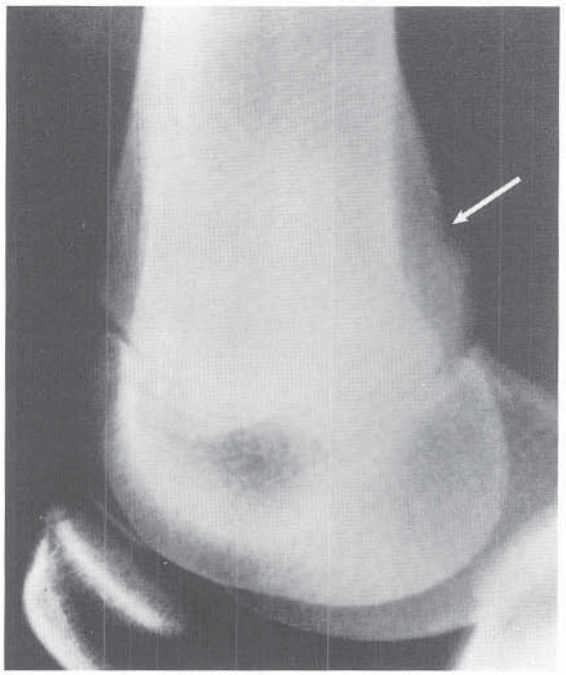

FIGURE 9–9 Normal cortical irregularities on the posterior aspect of the distal femur. Cortical irregularities are also present on the anterior aspect of the distal femur in this patient. (From Resnick D (ed): Diagnosis of Bone and Joint Disorders, 3rd ed. Philadelphia, WB Saunders Co, 1995.)

to obtain optimal radiographs. Pediatric radiology technologists generally allow parents to be present in the examining rooms and even to assist with some studies. This decreases the repeat rate and so decreases the total radiation dose to the young patient. In addition, the radiology technologist employs radiation-limiting techniques such as patient immobilization and gonadal and breast shielding. Cheerful uniforms and departmental decors with bright juvenile motifs help to distract and calm the child. But the essential component of a child-friendly department is a skilled technical staff that enjoys caring for children.

EQUIPMENT REQUISITES FOR X-RAY PRODUCTION

The basic equipment items necessary to produce a standard radiograph are an x-ray generator, an x-ray tube, collimators, grids, cassettes, and a screen-film combination (Fig. 9–10). The screen-film combination is currently being replaced by computed radiography, which employs a reusable phosphor plate. A brief description of each item follows.

X-Ray Generators. An x-ray generator modifies an already existent electrical source of alternating current into direct current high voltage or potential, which provides energy to an x-ray tube for (1) heating electrons off the cathode filament and (2) accelerating electrons from the cathode filament to the anode target. In addition to the electrical circuit utilized in boiling electrons off the cathode filament (filament current) and the separate electrical circuit applied for electron acceleration, an x-ray generator also has a third circuit, a timer, which controls the length of an x-ray exposure. For most pediatric radiographic and fluoroscopic procedures, x-ray generators should provide the following capabilities: (1) operator-controlled tube currents or milliamperage from 100 to 1,200 mA (50 kW rating at 100 kVp), (2) a maximum kVp of 150, (3) minimum switchable exposure times of 1 msec, and (4) 12-pulse three-phase power.

X-Ray Tube. An x-ray tube is composed of two metal electrodes, a cathode and an anode (target), which are mounted in a glass vacuum tube or a metal vacuum casing. The cathode is heated by the filament current, which is controlled by the filament power supply. When the cathode is heated to 2,000°C or higher, electrons are emitted. These electrons are propelled to the anode when the exposure switch is closed. The amplitude of the tube current is dependent on the emission rate of electrons from the cathode, which is determined by the cathode temperature. Therefore, the tube current control or milliampere control functions by altering the cathode's temperature. The speed of the electrons as they are propelled from the cathode to the anode is determined by the x-ray tube potential, or kVp.

On impacting the anode, 99 percent or more of the high-velocity electrons result in heating the anode. If the heat is not readily dissipated, damage to the anode may result within seconds. To circumvent overheating of any one portion of the anode's surface, most x-ray tubes utilize a rotating anode. The remaining 1 percent or less of electrons that collide with the anode produce the x-ray beam used for radiographic production. The higher the energy (kVp) of the impacting electrons, the more energetic and penetrating is the x-ray beam produced.

Collimators. Collimators protect the patient from excessive radiation and decrease scatter radiation, which degrades the image. Patient protection is achieved by decreasing the x-ray field, which is a square function. For example, if a 30 × 30-cm field is collimated to a 20 × 20-cm field, the area decreases from 900 cm^2 to 400 cm^2, more than a twofold decrease in area and a proportionate decrease in patient volume irradiated. Film quality is improved by decreasing the field size as scatter radiation increases up to a 30 × 30-cm field, after which scatter radiation increases only slowly.

Grids. Grids allow passage of primary radiation and absorption of scatter radiation. They are composed of a series of lead foil strips alternating with x-ray-transparent spaces. The grid ratio is the ratio of the depth of the lead stripes to the distance between them. The higher the grid ratio, the less the scatter radiation, but increased primary radiation must be used to penetrate the patient and grid in order to reach the film-screen system. In small pediatric patients, small irradiated fields produce low scatter levels, which often obviates the use of a grid and thereby significantly decreases the radiation dose. But patients 5 years old or older generally require grids for radiographic examinations of the abdomen, pelvis, spine, and skull. Grid ratios of 8 : 1 are usually sufficient for general pediatric radiology.

Cassettes. Cassettes are containers for film-screen combinations that produce good screen-film contact. If the contact is good between the screen and film, a dot of light emitted from the screen will produce a corresponding dot on the film. If the contact is poor, the dot of light will diffuse before reaching the film and result in a fuzzy rather than a sharp image.

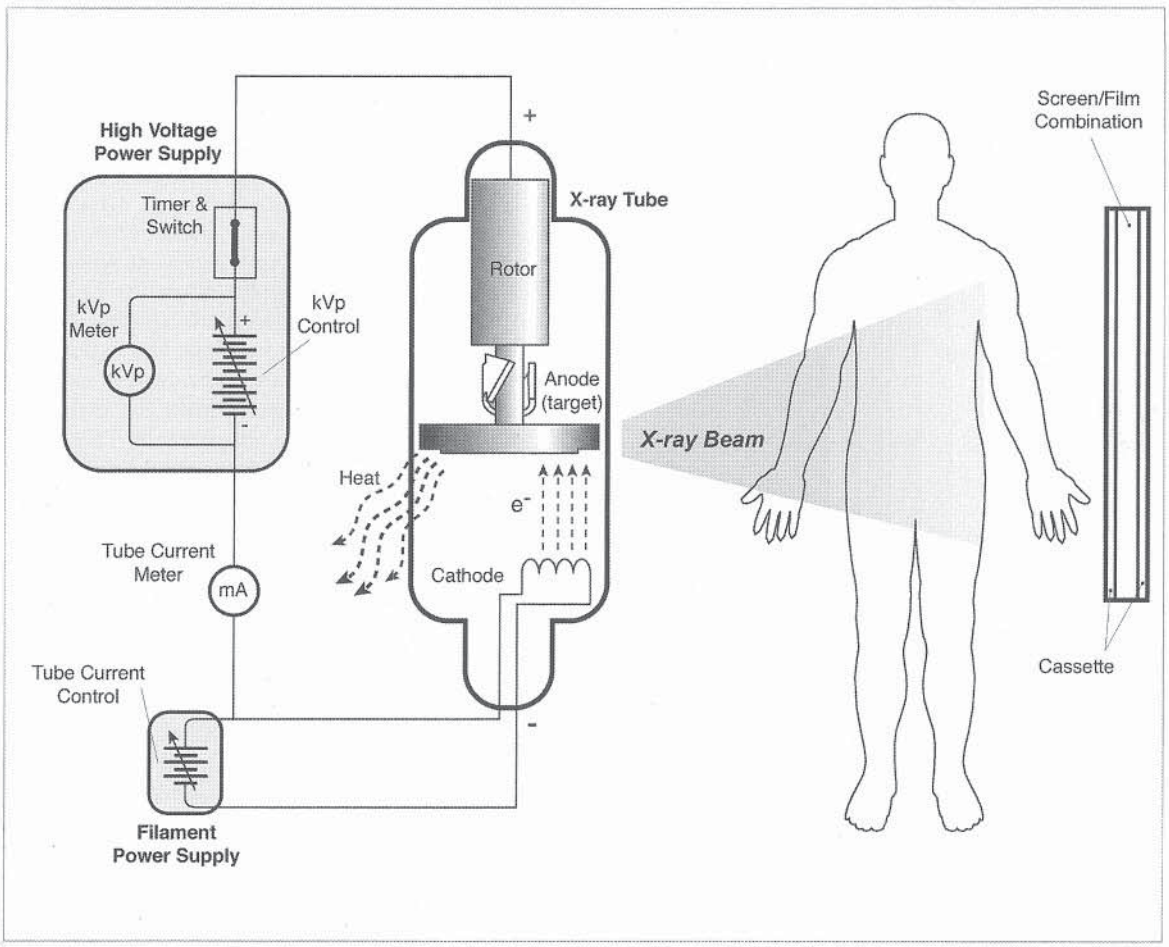

FIGURE 9–10 Basic equipment for x-ray production.

Luminescent Screen-Film Combinations. Luminescent screens convert x-rays into radiation in the visible light spectrum, which exposes the x-ray film and greatly reduces the patient dose, as x-ray film is very insensitive to direct x-ray exposure and requires prohibitive patient doses. Since the 1970s, rare earth screens have increased x-ray absorption efficiency and x-ray-to-light conversion efficiency with a resultant decrease in radiation dose of up to 50 percent. Special screen-film combinations are now available that reduce patient dose by as much as 85 percent. But a newer development, computed radiography, has in the last few years begun to replace screen-film combinations with reusable phosphor plates. It is estimated that most plain radiographic imaging systems will be filmless—that is, of the computed radiography variety—within 10 years.

COMPUTED RADIOGRAPHY

Storage phosphor computed radiography (CR) uses a standard x-ray tube to expose an image on a reusable phosphor image plate (several thousand exposures). Instead of a screen-film combination, a phosphor plate is placed in a cassette, similar to a standard film-screen cassette. Basically, the phosphor plate within a cassette is first exposed by x-ray photons, which elevate phosphor electrons to higher but stable energy levels. The exposed phosphor plate is then placed in a laser image reader. In the reader, the plate is removed from the cassette and transported to a laser scanner, where a laser beam scans the phosphor plate, causing electrons to return to their low-energy state. As these electrons return to lower energy states, they emit energy in the form of visible light. This light energy is collected and transmitted to a photo multiplier tube that converts light into electrical current and then converts current into voltage. The light intensity is proportional to the voltage, with the voltage variations representing an analog signal (information represented in a continuous fashion). Conversion to a digital signal (information represented in discrete units) is accomplished by an analog-to-digital converter. Next, an image processor enhances the digital image, which may then be sent to a workstation monitor or exposed and processed as hard film. CR images can be stored on laser-sensitive film by laser film recorders or on optical disks, digital tape, compact disks, or a computer's hard drive.

Advantages of CR over Conventional Radiography. The phosphor image plate responds in linear fashion to a wide range of exposures, which allows accurate depiction of differences in density. Simply stated, both low-density structures (soft tissues) and high-density structures (bone) may be accurately depicted on the same image. Conventional screen-film systems, on the other hand, have a nonlinear response and narrow range to x-ray exposure. This necessi-

tates that the x-ray technologist use a precise exposure technique to obtain an optimal bone image, and a second precise but different exposure technique to obtain an optimal soft tissue image. Overall, film-screen systems have an exposure range on the order of 1,000 : 1, whereas the CR plate exposure range is about 10,000 : 1.[6] Not only is contrast resolution improved using a CR system, but repeat films due to exposure errors can almost be eliminated, which decreases the total radiation dose to the patient. A further reduction in the radiation dose results from the phosphor plate being a more efficient detector than a film-screen system. That is, the phosphor plate detects a greater percentage of photons that have passed through a patient for image formation than even the fastest film, the rare screen systems that are generally used for musculoskeletal imaging.

In addition to CR images having greater contrast resolution than conventional plain films, the digitized CR images can be further enhanced by computer manipulation before or after transmission to an interactive workstation. These digitized CR images as well as all other digital images (CT, MRI, and so forth) can be sent to a picture archiving and communication system and integrated into a radiology information system. This allows rapid retrieval (no lost films) and transmission of digital images and patient information within and between medical centers that are interconnected.

In the not too distant future, digitized CR images will likely be replaced by direct digital capture systems, also termed direct radiography (DR) systems. Unlike CR systems, which utilize phosphor imaging plates, DR systems send information from the detector directly to the workstation. We have recently begun using DR in acquiring scoliosis images at our institution. There are three advantages associated with DR as compared with conventional screen-film radiography: (1) a reduction in radiation exposure, (2) good visualization of all parts of the spine, owing to a variable contrast scale that allows adjustment of window width and level, and (3) a reduction in the time required for acquiring and processing the image for viewing by approximately 65 to 70 percent.

PATIENT PREPARATION FOR RADIOLOGIC EXAMINATIONS

Patient and Image Identification. Before a conventional radiograph or a CR image is obtained, the outpatient's identification must be checked and reconciled with the x-ray requisition. This is generally done by the radiology technologist, who queries the older child or the parents of the younger patient as to the patient's exact identity. Also, the radiology technologists will question the patient or the patient's parents as to their understanding of the radiographic examination ordered. Needless return visits to the radiology department may be circumvented by such simple questions as "Which side hurts?" or "Which leg did you break?"

An inpatient's identity must always be verified and checked with the patient's identification bracelet. If the inpatient is noncommunicative and not accompanied by a family member, nurse, or other medical attendant, and if the x-ray request seems inappropriate to the patient's diagnosis, the radiology technologist must check the medical chart, if available, or call the nurses' station for clarification of the request.

The patient's information—generally the patient's name, date of birth, medical number, and date of examination—can be printed on conventional film by an identification camera. This is done through a closed cassette outside the darkroom. Patient information for a CR image is entered via a radiology information system; or, if one is not in place, the radiology technologist types in the patient information during the laser reading.

Proper left and right markers should be placed on each film to help prevent treatment of the wrong anatomic part. This is extremely important if both left and right analogous anatomic structures are deformed and show no differences on visual inspection. A surgical procedure could be done on the wrong side—for example, the wrong clubhand could be operated on—if side markers are reversed. At our institution, each image is labeled with left- or right-side markers. Even when three views of the same hand, wrist, or ankle are on one film, each view is labeled with a side marker. This helps ensure proper labeling by forcing the technologist to recheck the side imaged before the next exposure.

PATIENT PROTECTION

Immobilization. Various immobilization techniques and devices are employed to obtain images in the young patient. The radiology technologist instructs the child's parents that immobilization is necessary (1) to obtain a diagnostic image, (2) to prevent physical injury to the patient, and (3) to decrease the rate of repeated studies, which decreases the radiation dose to the patient. If some explanation of the need for restraining young patients is not given to the patient's parents, the parents may view the procedure as abusive to their child.

Shielding of Reproductive Organs. X-rays may cause genetic mutations and chromosomal abnormalities. The damaging effects are proportional to the absorbed radiation dose, with no known threshold dose below which these effects do not occur. If genetic mutations develop in reproductive cells, they may not manifest for several generations. In essence, all future generations are at risk for genetic mutations in proportion to the cumulative radiation doses received by the total population's genetic pool. These genetic mutations will be randomly distributed, as the human population is an outbreeding one. To reduce the genetic effects of ionizing radiation, the concept of gonadal shielding was introduced in 1956 by the National Academy of Sciences Committee on Biological Effects of Atomic Radiation.

Gonadal shields are of two basic types, flat contact shields and shadow shields. The flat contact gonadal shields may be made by cutting 1.0-mm-thick lead vinyl sheeting into various sizes and shapes that are age and sex appropriate. These shields are placed on top of the patient or taped to the patient. The gonadal shield is simply positioned over the male patient's testes (Fig. 9–11). The female contact gonadal shield is placed so that the inferior margin is positioned at the pubis and the upper border extends to below the iliac crests (Fig. 9–12). Shadow shields are made of a radiopaque material that is attached to the x-ray tube head. The radiology technologist directs the shield to its proper position via a beam-defining light that illuminates the area to be imaged. When an x-ray exposure is made, a shadow of the shield projects over the gonads.

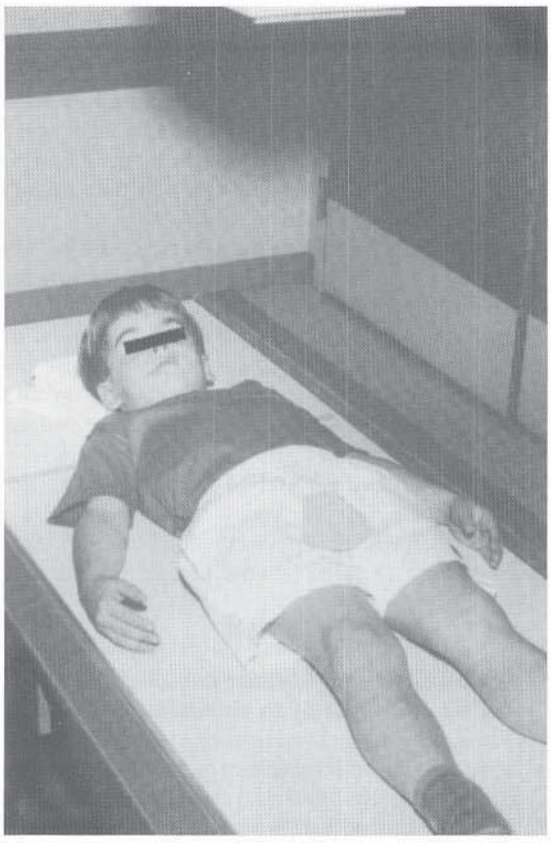

A

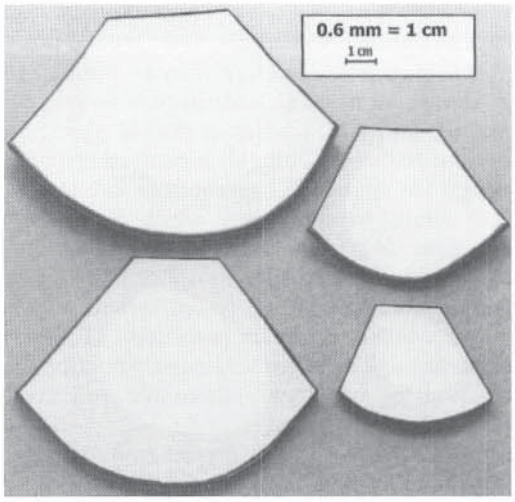

B

FIGURE 9–11 **A,** Proper positioning of male contact gonadal shield. **B,** Male contact gonadal shields of different sizes for use with patients of different ages. (From Godderidge C: Pediatric Imaging. Philadelphia, WB Saunders Co, 1995.)

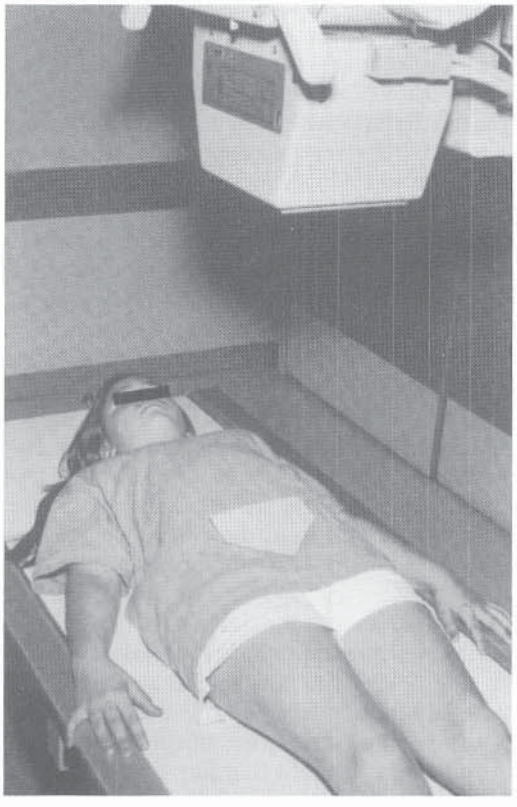

A

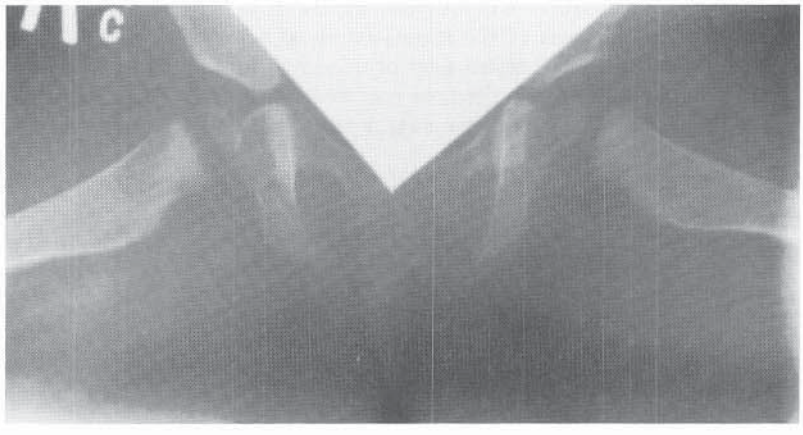

B

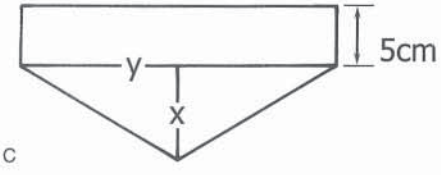

C

FIGURE 9–12 **A** and **B,** Properly positioned female gonadal shields. **C,** Scale for female contact gonadal shields. (Part A from Godderidge C: Pediatric Imaging. Philadelphia, WB Saunders Co, 1995. Parts B and C from D'Angio GJ, Tefft M: Radiation therapy in the management of children with gynecologic cancers. Ann NY Acad Sci 1967;142:675–693.)

Gonadal shields must be employed when the gonads are within 5 cm of the primary beam.[8] For most abdominal and pelvic imaging of the male, gonadal shields can be used with no loss of diagnostic information. Shielding of the variably placed intra-abdominal ovaries, however, may obscure pertinent information (Fig. 9–13). If two views of a female pelvis are required, one view is obtained with a gonadal shield and the other without the shield. Proper shielding decreases gonadal exposure by 95 percent in males and up to 50 percent in females.[12]

Shielding of Breast Tissue. X-rays not only are capable of causing genetic and chromosomal abnormalities, they can also induce cancer in somatic tissues. At particular risk is maturing female breast tissue, with the rate of breast cancer being appreciably higher after x-ray exposure during puberty than after irradiation in adult life.[2,3,5,10,11] To protect young scoliosis patients, who commonly receive multiple x-ray exposures during their adolescent years, a number of techniques have been devised to decrease radiation doses to breast tissue. These include using a posteroanterior (PA) projection, breast shields, fast rare-earth screen-film combinations, increased filtration in the x-ray tube collimator, and lower grid ratios and higher kilovoltages. Recently we have begun using DR at our institution to acquire scoliosis images. Use of this technique (DR) alone reduces the radiation dose by 75 to 85 percent of that of standard screen-film combinations.

Pregnancy Screening. All female patients age 12 years and older should complete a pregnancy information form that elicits the following: (1) menarchal status, (2) date of last menses, and (3) sexual activity. The form can be read to the patient by the technologist to ensure the patient's comprehension. If the possibility of pregnancy exists, radiographic procedures are not performed until the patient consults her ordering physician. The radiographic procedure is performed if the patient subsequently has a negative pregnancy test or if the ordering physician deems the x-ray examination necessary. In the latter event, all measures are employed to deliver the least ionizing radiation dose to the patient and fetus.

FIGURE 9–13 Intra-abdominal ovaries may be variably located. (From Godderidge C: Pediatric Imaging. Philadelphia, WB Saunders Co, 1995.)

REFERENCES

Conventional Radiographic Procedures, Normal Radiographic Variants of the Immature Skeleton, and Radiographic Technique

1. Blickman JG, Wilkinson RH, Graef JW: The radiologic "lead band" revisited. AJR Am J Roentgenol 1986;146:245.
2. Boice JD Jr, Monson RR: Breast cancer in women after repeated fluoroscopic examinations of the chest. J Natl Cancer Inst 1977;59:823.
3. Committee on the Biological Effects of Ionizing Radiations: The Effects on Populations of Low Levels of Ionizing Radiation. Washington, DC, National Academy Press, 1980.
4. Ewing J: A review and classification of bone sarcomas. Arch Surg 1922;4:485.
5. Gray JE, Hoffman AD, Peterson HA: Reduction of radiation exposure during radiography for scoliosis. J Bone Joint Surg 1983;65-A:5.
6. Huang HK: Elements of Digital Radiology. Englewood Cliffs, NJ, Prentice-Hall, 1987.
7. Madewell JE, Ragsdale BD, Sweet DE: Radiologic and pathologic analysis of solitary bone lesions. Part I. Internal margins. Radiol Clin North Am 1981;19:715.
8. Poznanski AK: Practical approaches to pediatric radiology. Chicago, Year Book Medical Publishers, 1976.
9. Swischuk LE: Anterior displacement of C2 in children: physiologic or pathologic? Radiology 1977;122:759.
10. Tokunaga M, Norman JE Jr, Asano M, et al: Malignant breast tumors among atomic bomb survivors, Hiroshima and Nagasaki 1950–74. J Natl Cancer Inst 1979;62:1347.
11. United Nations Scientific Committee on the Effects of Atomic Radiation (UNSCEAR): Sources and Effects of Ionizing Radiation: 1977 Report to the General Assembly. New York, United Nations, 1977.
12. United States Department of Health, Education and Welfare: Gonad Shielding in Diagnostic Radiology. Rockville, MD, DHEW, 1975.

Computed Tomography in Pediatric Orthopaedics

In 1917, Radon detailed the principles of image reconstruction from projections.[3] However, production of the first CT scanner would await many technological advances. Thus, it was not until 1970 that Hounsfield constructed the first CT prototype. Since its introduction by Hounsfield in 1973,[20] the acceptance and dissemination of CT throughout the medical field has advanced rapidly. CT has developed into an imaging tool that has significantly aided and enhanced the evaluation of multiple musculoskeletal disorders.[26,39]

CT is similar to conventional tomography in that images are acquired in planar fashion; however, this is where the similarity ends. CT images are generally acquired transaxially and are unhampered by overlying soft tissues and bowel gas.[3] Tissues are displayed clearly and contrast resolution is superb, clearly surpassing that of conventional radiography. The extent of disease is optimally evaluated, and the resolution between different tissue densities is excellent.[46] This superior contrast resolution allows quantitative evaluation of the skeleton and surrounding tissues. Additional information can be obtained with the injection of iodinated intravenous contrast material. This technique allows for opacification of vascular structures and enhancement of normal and pathologic tissues, and supplies physiologic information. CT is not operator dependent, and therefore the study is consistent and reproducible from one examination to the next. Parameters that can be accurately measured include length, area, density, and circumference. An interfaced workstation allows manipulation of the CT data so that multipla-

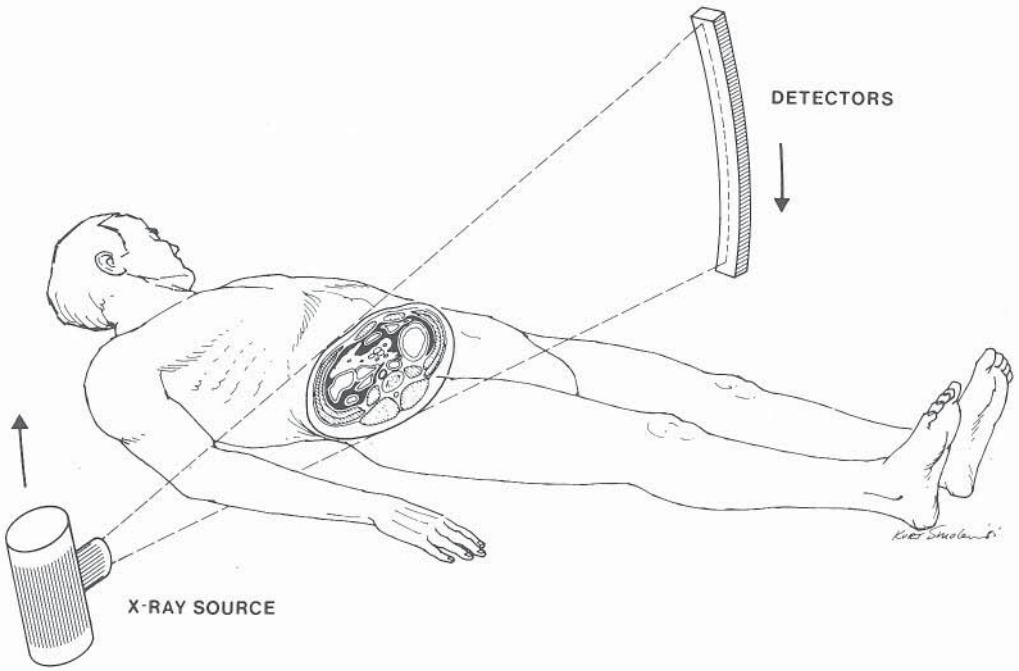

FIGURE 9–14 A CT scanner produces a cross-sectional image of the patient by confining its beam to a thin transaxial slice.[3] The amount of attenuation of x-rays is measured by detectors opposite the x-ray source. (From André M, Resnick D: Computed tomography. In Resnick D (ed): Diagnosis of Bone and Joint Disorders, 3rd ed, p 119. Philadelphia, WB Saunders Co, 1995.)

nar reformatting in sagittal, coronal, and oblique orientations can be done easily and quickly. Three-dimensional reconstructed images can also be generated, adding a wealth of information, particularly for preoperative planning, for the orthopaedic surgeon.[3,15,27–29,41]

THE CT SCANNER

The basic components of a CT scanner consist of a scanning gantry and patient couch, an x-ray tube and generator, and a computer processing and display system. During image acquisition, a highly collimated beam is passed through the patient in a predetermined section thickness and at varying angles. Rotating the tube about the patient while the table is stationary or moving creates the angles. As the tube rotates, detectors on the other side of the patient measure the amount of irradiation that passes through the patient's tissues (Fig. 9–14). From the data so generated, a computer determines the attenuation coefficient for the various tissues in a sample volume. The sample volume is termed a voxel and can vary in size from 0.2 × 0.2 × 1.0 mm to 10 mm. The pixel that is viewed in a two-dimensional image represents the voxel in which the depth is equal to the section thickness (Fig. 9–15). With the addition of multiple projections from numerous angles, the scanner computer is able to produce an image via a process termed filtered backprojection (Fig. 9–16). The image can be displayed on a monitor and then printed on film or distributed to a network for viewing and archiving. The CT scanner display computer converts the multiple attenuation values (in Hounsfield units, or HUs) to recognizable anatomy by assigning various shades of gray to the various HUs: black represents air and white represents bone (Fig. 9–17).[3,46]

The first-generation scanners were inefficient and slow and used a thin (pencil) beam x-ray source with a single detector. With this arrangement, a frame was moved in linear fashion while the x-ray source scanned through a tissue section; the detector moved in unison, recording numerous attenuation densities. After the first linear scan was obtained, the entire frame was rotated by a small angle to

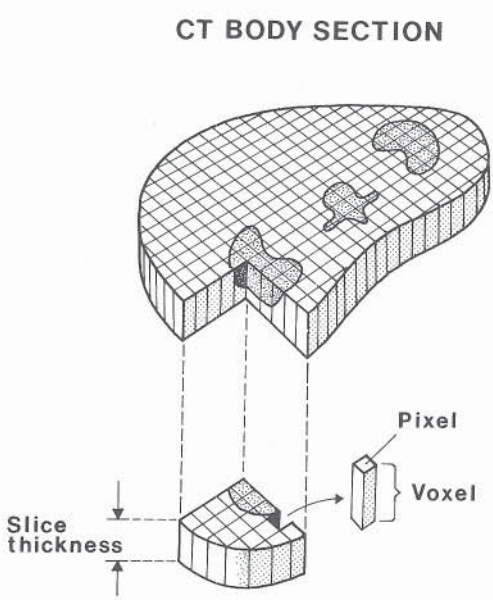

FIGURE 9–15 The CT image is a matrix of elements (pixels) that corresponds to a volume of tissue (voxel).[3] (From André M, Resnick D: Computed tomography. In Resnick D (ed): Diagnosis of Bone and Joint Disorders, 3rd ed, p 121. Philadelphia, WB Saunders Co, 1995.)

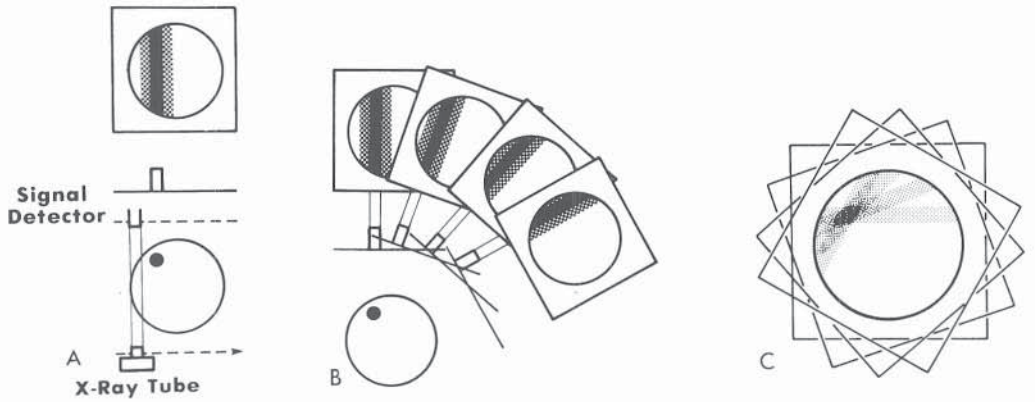

FIGURE 9–16 Reconstruction of an image from scan projections is shown schematically.[3] By translating the tube and detector (**A**), a single ray may produce a view. Multiple views are taken (**B**) and combined by the backprojection process (**C**) to form an image.[3] (From André M, Resnick D: Computed tomography. In Resnick D (ed): Diagnosis of Bone and Joint Disorders, 3rd ed, p 119. Philadelphia, WB Saunders Co, 1995.)

obtain another data set. Scan times (i.e., the time required to obtain the data for an image) were long, approximately 3 to 5 minutes per section (Fig. 9–18).[3,46]

Second-generation scanners used a similar arrangement; however, instead of a pencil beam x-ray source and a single detector, a fan-shaped x-ray beam with multiple detectors was utilized. Scan times decreased to as little as 20 seconds (see Fig. 9–18).[3,46]

Third-generation CT systems use a fan beam source and multiple detectors, but the detectors are arranged so that linear translation is no longer required. In these systems, a 360-degree continuous sweep is utilized with a pulsed fan beam. The design allows decreased scan times (1 second), decreased x-ray scatter, and increased contrast resolution. This arrangement, however, is prone to detector artifact and significant heat stress on the x-ray tube (see Fig. 9–18).[3,46]

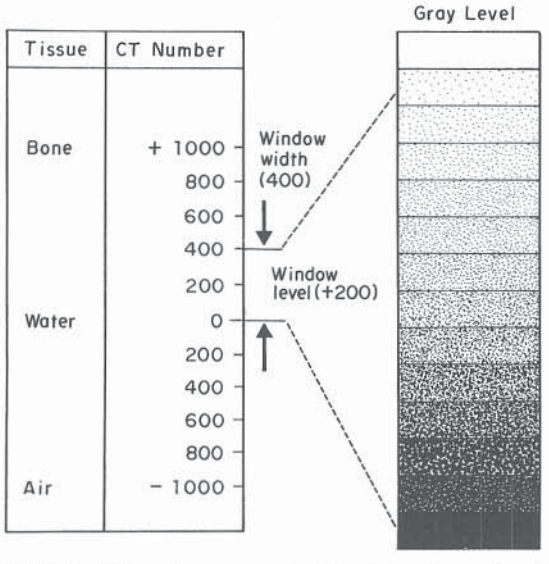

FIGURE 9–17 CT numbers are assigned a shade of gray for display. Windowing allows the operator to select the range of tissues viewed.[3] (From André M, Resnick D: Computed tomography. In Resnick D (ed): Diagnosis of Bone and Joint Disorders, 3rd ed, p 121. Philadelphia, WB Saunders Co, 1995.)

In fourth-generation systems, there is a stationary circular array of detectors within the scanning gantry. With this arrangement, only the x-ray tube rotates about the patient (see Fig. 9–18). The detector size and spacing decrease total detection efficiency, so that fourth-generation scanners have no significant advantage over third-generation systems.[3,46]

Slip ring technology can be applied to either third- or fourth-generation scanners.[3] An x-ray tube is continuously energized and rotated while the patient is moved through the scanning gantry at a predetermined rate (Fig. 9–19). Since the acquired data represent a volume of data rather than a set of individually stacked CT sections, thinner and overlapping sections can be generated from the data set.[46] The reconstructed images can then be used to produce high-quality multiplanar reformatted and three-dimensional images. Electrical connections between the stationary gantry and rotating slip ring are made via sliding contacts. CT scanners that employ slip ring technology are designated volume, helical, or spiral scanners (Fig. 9–20).[6,7,19,33] Volume scanners are readily applicable to evaluation of the pediatric patient, as the design permits rapid scan times—as little as 1 second.[11,42] The reconstruction time for these newer systems varies but can be as short as 1 second. The technology allows greater patient throughput, less sedation in younger and uncooperative children,[46,51] a decrease in the volume of intravenous contrast material,[9,46] decreased motion artifact,[10,46] and examinations that can be completed in a single breath-hold (e.g., chest CT).[22,46,49]

Shorter scan times are possible with an *electron beam* CT system (Fig. 9–21) that uses no mechanical motion. A conventional x-ray tube is not present in this system; instead, a scanning electron beam is moved on a tungsten target ring that is curved about the patient. Extremely rapid (subsecond) scans are obtained with this design. The speed of these scanners holds promise in regard to joint motion studies.[3]

PHYSICAL PRINCIPLES

Imaging quality in CT depends on several parameters. Some of these parameters are modifiable by the technologist; others, inherent to the CT scanner, are not.

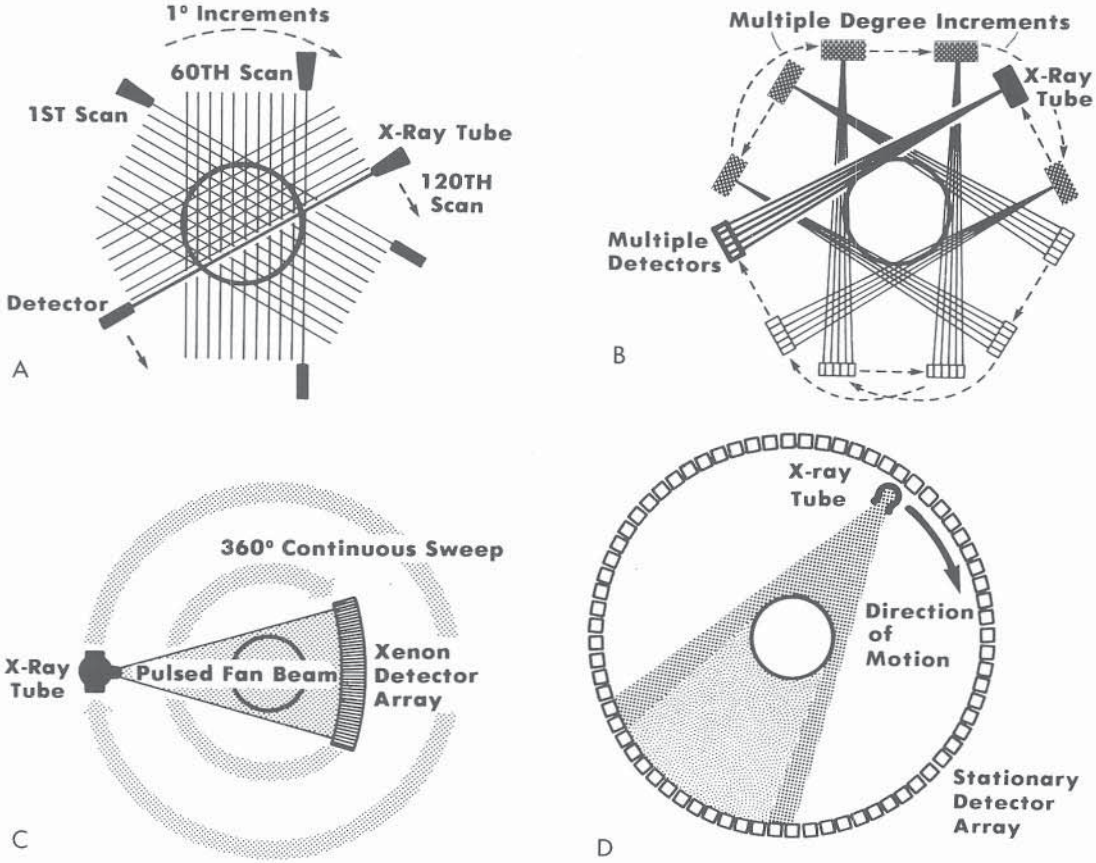

FIGURE 9–18 Schematic representation of first-generation (**A**), second-generation (**B**), third-generation (**C**), and fourth-generation (**D**) CT scanners.[3] (From André M, Resnick D: Computed tomography. In Resnick D (ed): Diagnosis of Bone and Joint Disorders, 3rd ed, p 120. Philadelphia, WB Saunders Co, 1995.)

Spatial resolution refers to the ability to resolve two objects that are close together as two separate entities. In CT, this is determined by multiple factors, some of which are not modifiable by the operator. Factors that cannot be changed by the operator include the number, size, and spacing of the CT detectors and the number of measurements that each detector acquires. Matrix size for the display of images (Fig. 9–22), reconstruction algorithms (e.g., smooth or sharp), size of the scan field, and section thickness are variables that can be changed by the operator.[3]

Contrast resolution, on the other hand, refers to the ability to display small differences in attenuation from pixel to pixel. The contrast resolution is directly determined by the composition and size of the tissue being studied, but it is also influenced by the radiation dose, scan time, pixel size, section thickness, and the reconstruction algorithms that are applied to the imaging process. *Noise* is the statistical fluctuation in pixel attenuation values that limits the ability to differentiate low-contrast objects. In conventional radiography, the image on a film equates to the sum total of the variable attenuation of an x-ray beam as it passes through the various overlying tissues. As such, plain film radiographs record differences in attenuation of only 10 percent. CT, on the other hand, can record differences in attenuation as little as 0.1 percent. The HU value is defined to be 0 for water, 1,000 for bone, and −1,000 for air (Table 9–1). Although the spatial resolution of CT is less than that of conventional radiography, the superior contrast resolution of CT allows much finer distinction between tissues. This superior contrast resolution is a distinct advantage of CT as compared with conventional radiography.[3,46]

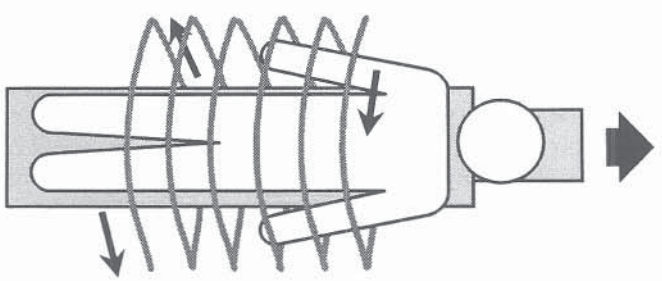

FIGURE 9–19 Volume scanning is accomplished with slip ring or electron beam scanners by moving the patient through the continuously rotating x-ray beam.[3] (From André M, Resnick D: Computed tomography. In Resnick D (ed): Diagnosis of Bone and Joint Disorders, 3rd ed, p 126. Philadelphia, WB Saunders Co, 1995.)

TECHNICAL CONSIDERATIONS

Before performing a CT examination, the radiologist and technologist should have a clear understanding of the clinical question that needs to be answered. Additionally, it is the

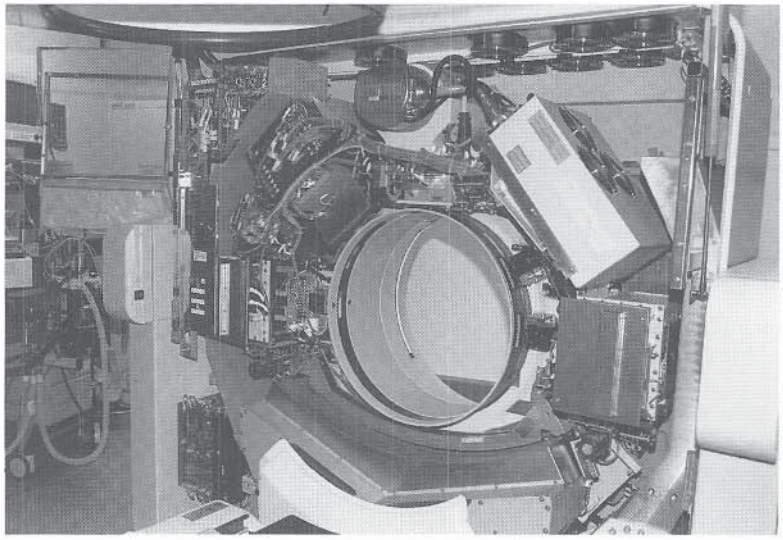

FIGURE 9–20 The covering of the CT scanner has been removed to show the x-ray tube mounted on its slip ring and other internal components of the scanning gantry. Slip ring technology allows the continuous tube rotation that is needed in volume scanning.

responsibility of the attending radiologist to determine that the requested examination is the appropriate study to answer the clinical question at hand. This is particularly important in imaging studies that are invasive or involve ionization radiation. It is usually the correlation of information from all available imaging studies—radiography, CT, MRI, and nuclear imaging—that provides for an accurate interpretation and diagnosis. That is not to say that all patients should undergo a battery of diagnostic examinations but that a tailored imaging evaluation should be performed that best addresses the clinical concern.

Before the CT study is performed, the radiologist should review plain film radiographs of the area to be studied. Although the radiograph may not contain all the diagnostic information needed by the radiologist and surgeon, it does allow for planning and individualization of the scanning process. The exact area that requires study, patient position, section thickness, table motion, radiation settings, gantry angling, and the need for multiplanar reformatting (usually in sagittal, coronal, or oblique planes) or three-dimensional images can usually be determined from the radiograph. The radiologist must be aware of the presence of foreign bodies (such as hardware), particularly metallic, that produce streak and beam hardening, as the imaging plan may have to be changed to keep artifacts to a minimum.

Standard scanning protocols developed by the radiologist make the examination process efficient. Ideally, all studies should be reviewed by the radiologist at the CT scanner

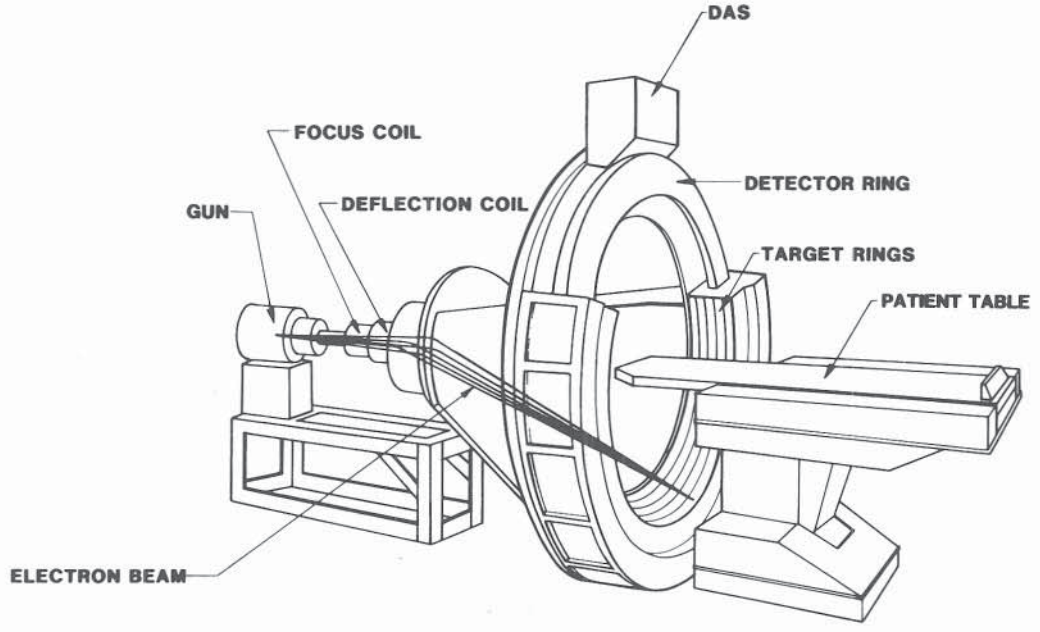

FIGURE 9–21 With no moving parts, a scanning electron beam system is capable of very short (50-msec) scans and rapid dynamic scanning.[3] (From André M, Resnick D: Computed tomography. In Resnick D (ed): Diagnosis of Bone and Joint Disorders, 3rd ed, p 121. Philadelphia, WB Saunders Co, 1995.)

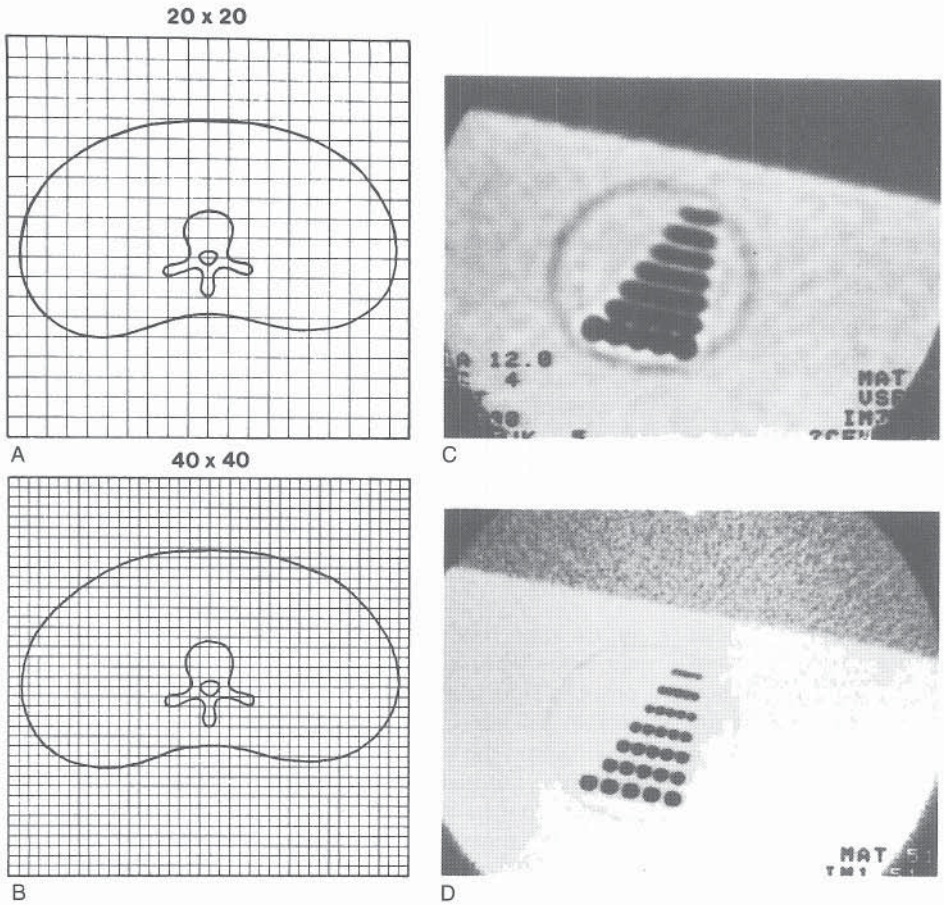

FIGURE 9–22 Decreasing the pixel size (from **A** to **B**) requires a larger matrix to cover the same cross-sectional area. Better resolution is seen in **D**, a 512 × 512 matrix, than in **C**, a 256 × 256 matrix.[3] (From André M, Resnick D: Computed tomography. In Resnick D (ed): Diagnosis of Bone and Joint Disorders, 3rd ed, p 123. Philadelphia, WB Saunders Co, 1995.)

console before the patient is removed from the scanning table. Additional imaging can then be performed if needed. Usually this obviates returning the patient to the x-ray department for additional CT study.

In general, special patient preparation is not needed for older, cooperative children. However, if intravenous or oral contrast agent administration or sedation is anticipated, the child should be placed on NPO status. The length of the NPO status varies slightly between institutions. Nonetheless, sedation protocols should be developed in conjunction with the anesthesia department.* Discussing the examination process with the patient and parents helps to alleviate unnecessary anxiety and confusion surrounding the CT examination. At times, it may be helpful to show the child the CT suite before performing the study. A television playing a child's favorite video program may be all that is needed to complete a short CT examination. Children less than 5 years old may need sedation, particularly if an uncomfortable stimulus such as a venipuncture is expected. Our current arrangement allows the radiology nurse to discuss with the parent or caregiver the type of examination to be done and what to expect (e.g., length of the study, anticipated discomfort). This helps the nurse to determine whether sedation will be needed. This type of assessment is best performed in person, but it can be done over the telephone. When the patient arrives for the scheduled appointment, a physical assessment is performed and documented by the radiology nurse. After consultation with the radiologist, the sedative, route, and dose are selected and the sedative is administered to the patient by the nurse in a sedation room that is free of distraction and noise. Sedation encounters of this type are conscious sedations. Nursing records on the type of sedation, dose, and its effectiveness are kept on all patients. This information is helpful if future procedures requiring sedation are anticipated. If the initial sedation fails, the study is rescheduled for a later date, when the child

TABLE 9–1 **Sample CT Numbers (Hounsfield Units) for Various Tissues**

Tissue	CT Number (HU)
Bone	1,000
Liver	40 to 60
White matter (brain)	46
Gray matter (brain)	43
Blood	40
Muscle	10 to 40
Kidney	30
Cerebrospinal fluid	15
Water	0
Fat	−50 to −100
Air	−1,000

From Philips Medical Systems: Basic Principles of MR Imaging, p 23. Shelton, CT, Philips Medical Systems, July 1998.

*See references 2, 8, 21, 23, 30, 31, 34, 35, 37, 44, 45, 47.

TABLE 9–2 **Pediatric Musculoskeletal Disorders That Are Readily Evaluated by CT**

Tarsal coalition (Fig. 9–23)[7,16,18]
Accessory navicular tarsal bone
Bipartite navicular tarsal bone
Conjugation of joints (e.g., hip,[13] shoulder)
Infection[3,8,23,50]
  Osteomyelitis
  Brodie abscess
  Soft tissue
Fracture (Fig. 9–24)[14,15,46]
Foreign body
Growth plate bar/arrest[3,33,46]
Bony deformity and anomaly
  Segmentation/fusion anomalies of the spine (Figs. 9–25 through 9–28)
  Craniovertebral junction anomalies
  Hand and foot deformity (e.g., clubhand/clubfoot)
Evaluation of bone length (e.g., leg length discrepancy)
Evaluation of rotational deformity (e.g., tibial torsion, femoral anteversion)
Osteoid osteoma[47]
Measurement of bony structures for preoperative planning (e.g., pedicle diameter/length for assessment of screw size/length)
Torticollis or other rotational deformity of the spine
Complex joint deformity[39]
Pseudoarthrosis (e.g., postoperative in situ spinal fusion)
Pin penetration into the joint (e.g., pins placed for femoral neck fracture or slipped capital femoral epiphysis) (Fig. 9–29)
Benign and malignant bone and soft tissue tumors (Fig. 9–30)[3]
Intraspinal pathology (e.g., diastematomyelia[48]) (Figs. 9–31 and 9–32)[44]
Postoperative assessment of bony structures (Fig. 9–33)
Spondylolysis and spondylolisthesis (Fig. 9–34)[3]

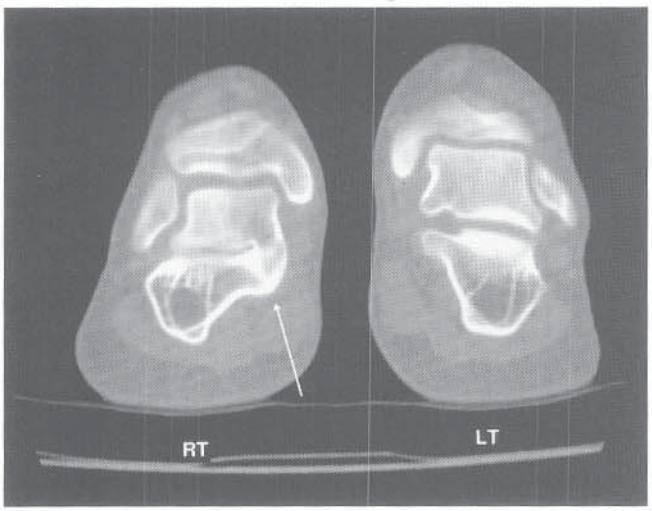

FIGURE 9–23 Coronal images of the hindfeet show a bony coalition on the right (*arrow*) at the middle facet of the subtalar joint. The normal left side is shown for comparison.

is sedated with the appropriate modification. Consultation with the anesthesiologist is obtained if necessary. If the second or third attempt at conscious sedation fails, the attending anesthesiologist will administer deep sedation or

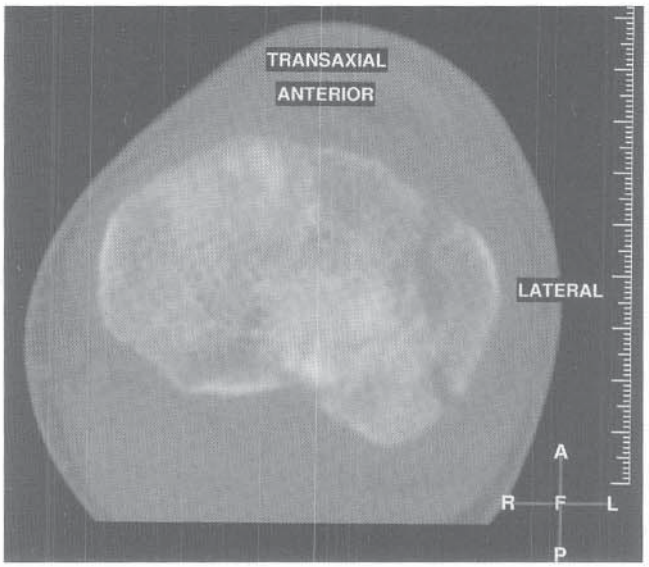

A

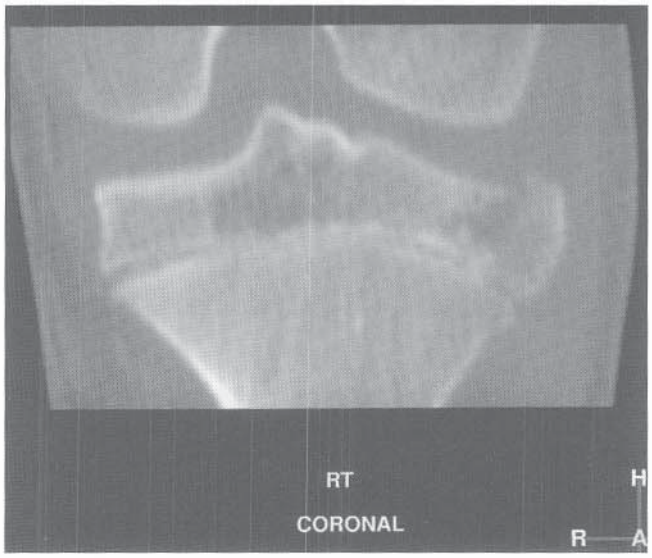

B

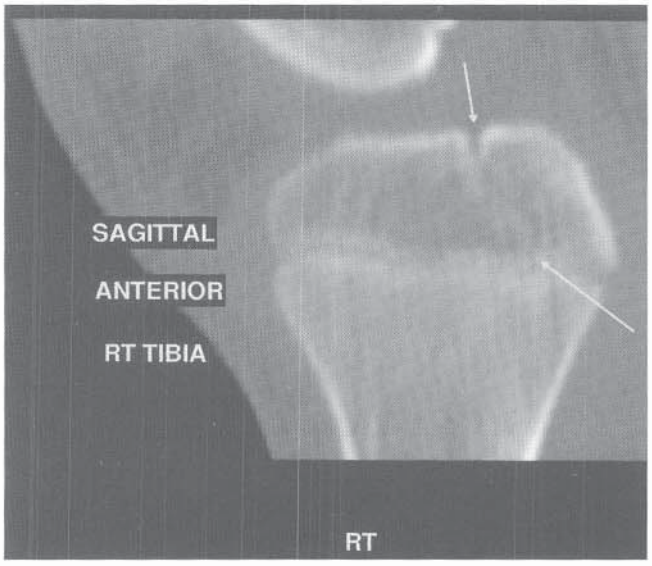

C

FIGURE 9–24 Transaxial (**A**), coronal (**B**), and sagittal (**C**) images of a lateral tibial plateau fracture accurately demonstrate the extent and position of the fracture fragments. Images in **B** and **C** were generated on a workstation directly interfaced with a volume scanner.

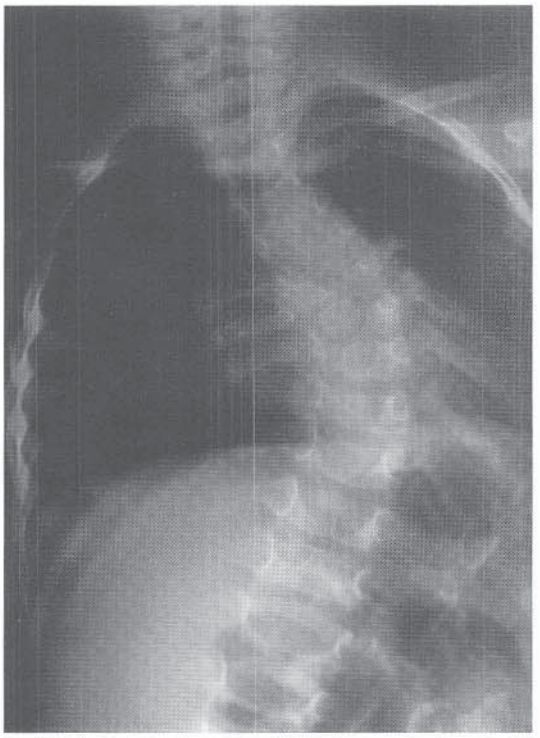

A

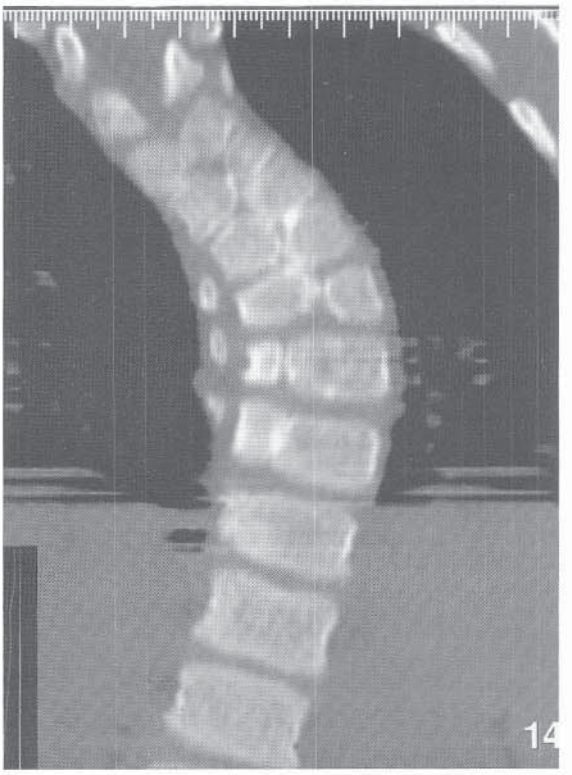

B

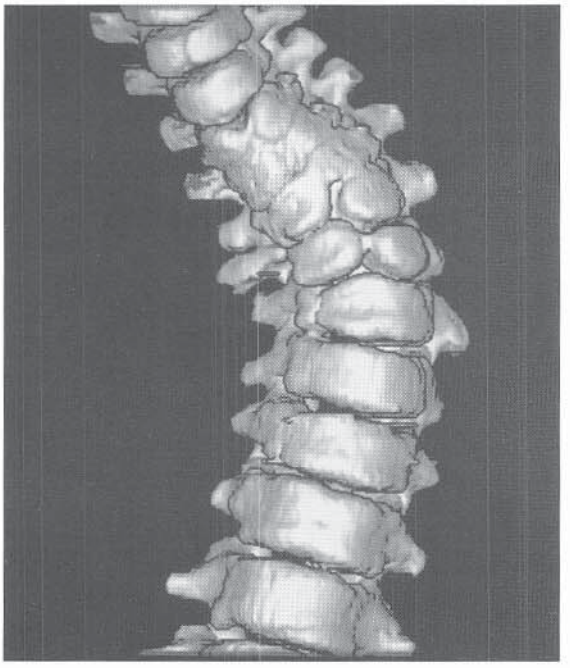

C

FIGURE 9–25 A coned view of the thoracic spine (**A**) shows multiple segmentation-fusion anomalies of the midthoracic spine. A curved multiplanar reformation in the coronal plane (**B**) and a three-dimensional image of the thoracic spine (**C**) accurately depict the nature of the anomalies.

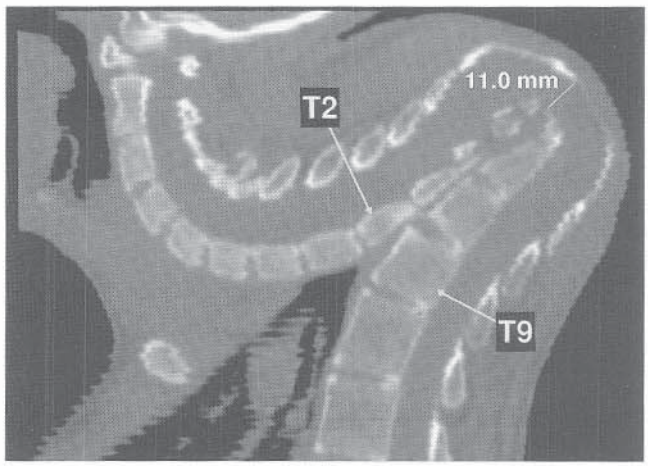

FIGURE 9–26 A 12-year-old girl with neurofibromatosis underwent a volume CT scan of a dysplastic thoracic kyphosis. A sagittal reconstruction vividly demonstrates the severity of the kyphosis and allows the spinal canal AP diameter to be measured precisely.

general anesthesia in the CT suite. In the design of the suite, it is vital to have the anesthesiologist's input so that oxygen, suction, nitrous oxide, electrical connections, and other required items can be placed in the appropriate location to facilitate the anesthesiologist's job.

RADIATION CONSIDERATIONS

CT scanners generally produce a radiation dose 49 times greater than that associated with conventional radiography but less than that of interventional procedures, which can use fluoroscopy extensively.[3] The radiation dose to the patient is best controlled by changing the milliampere settings of the x-ray tube and the time of the scan (seconds). The greater the milliampere setting and scan time, the greater the dose to the patient. However, increasing either factor will decrease imaging noise and may increase contrast resolution (i.e., improve image quality).[3] Thinner section thickness, overlapping sections, and smaller fields of view also increase the radiation dose, but in general, they also improve image quality.[3] Radiosensitive organs such as the lenses of the eye and the gonads should be shielded or avoided. Clearly the CT examination must be tailored to each patient's clinical problem so that an accurate diagnosis can be achieved with the lowest possible dose to the patient. For example, in infants who have undergone open or closed hip reduction with hip spica cast application, a minimum number of sections with low milliampere settings can reduce the radiation dose to the patient.[13] Although the lower milliampere setting may decrease the image quality, this is usually offset by the lower radiation dose to the patient. This philosophy embodies the ALARA principle, according to which one attempts to make an accurate diagnosis with a radiation dose that is *as low as reasonably achievable.*

CLINICAL APPLICATIONS

The multitude of clinical applications in musculoskeletal imaging where CT is useful are discussed in the chapters on the relevant anatomy. The present discussion concludes by reiterating that in the initial evaluation of any clinical problem, an appropriate history should be taken and a physical examination performed. These will then direct a logical diagnostic evaluation. Examples of pediatric musculoskeletal

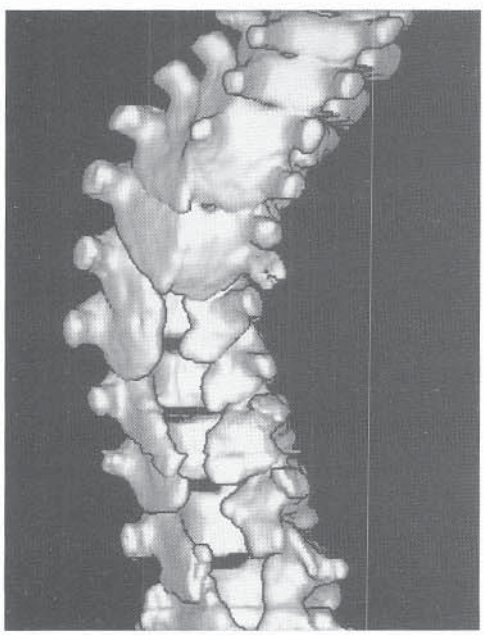

FIGURE 9–27 A three-dimensional image of the thoracic spine reveals levoscoliosis and several fused vertebrae in the upper and midthoracic spine. Dysraphic bony defects are identified in the mid- and distal thoracic spine.

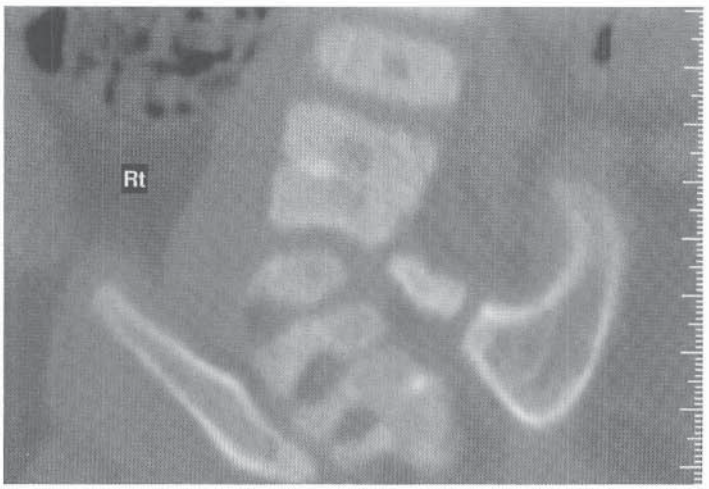

A

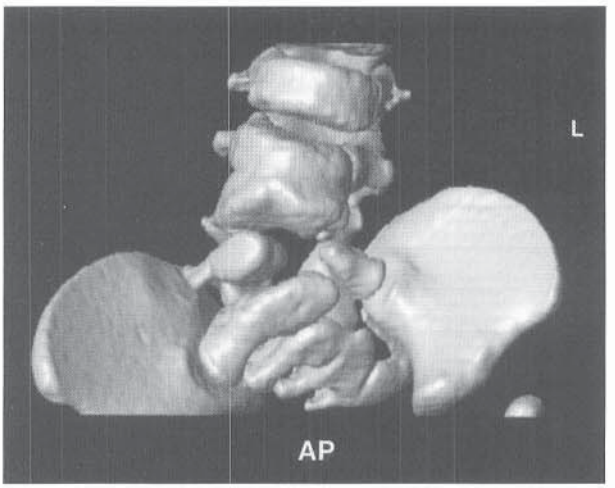

B

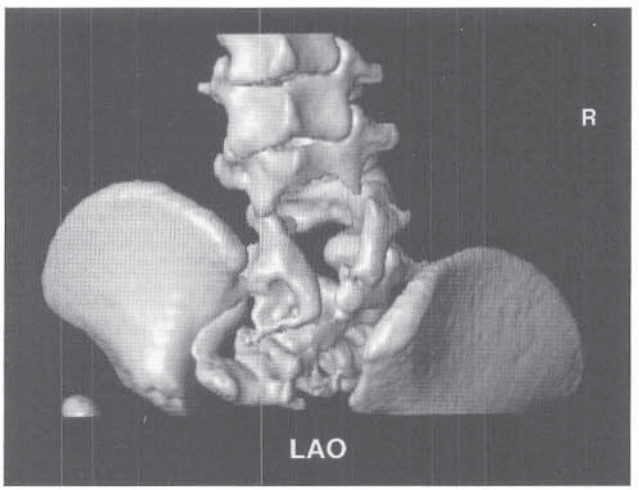

C

FIGURE 9–28 A coronal reconstruction (**A**) and three-dimensional images of the pelvis in the AP (**B**) and left anterior oblique (**C**) projections reveal complex bony deformity at the lumbosacral junction.

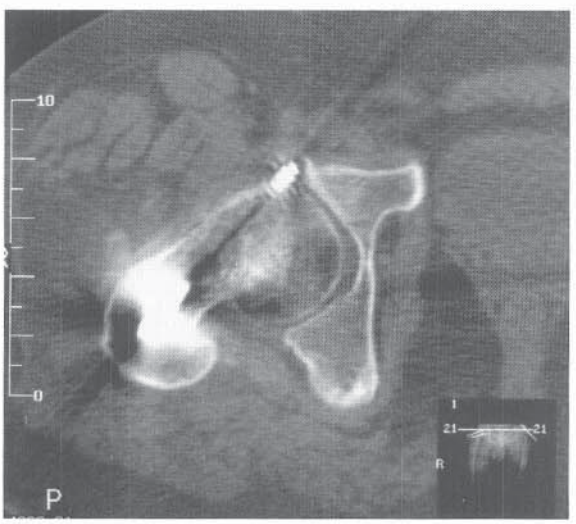

A

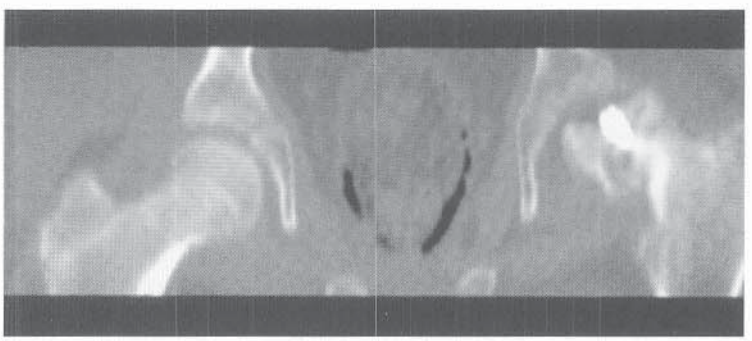

B

FIGURE 9–29 **A,** An axial image of the right hip in a patient with a slipped capital femoral epiphysis shows the distal tip of a screw impinging on the anterior aspect of the acetabulum. **B,** A coronal reconstruction of the hips in another patient shows avascular necrosis and pin penetration into the left hip joint.

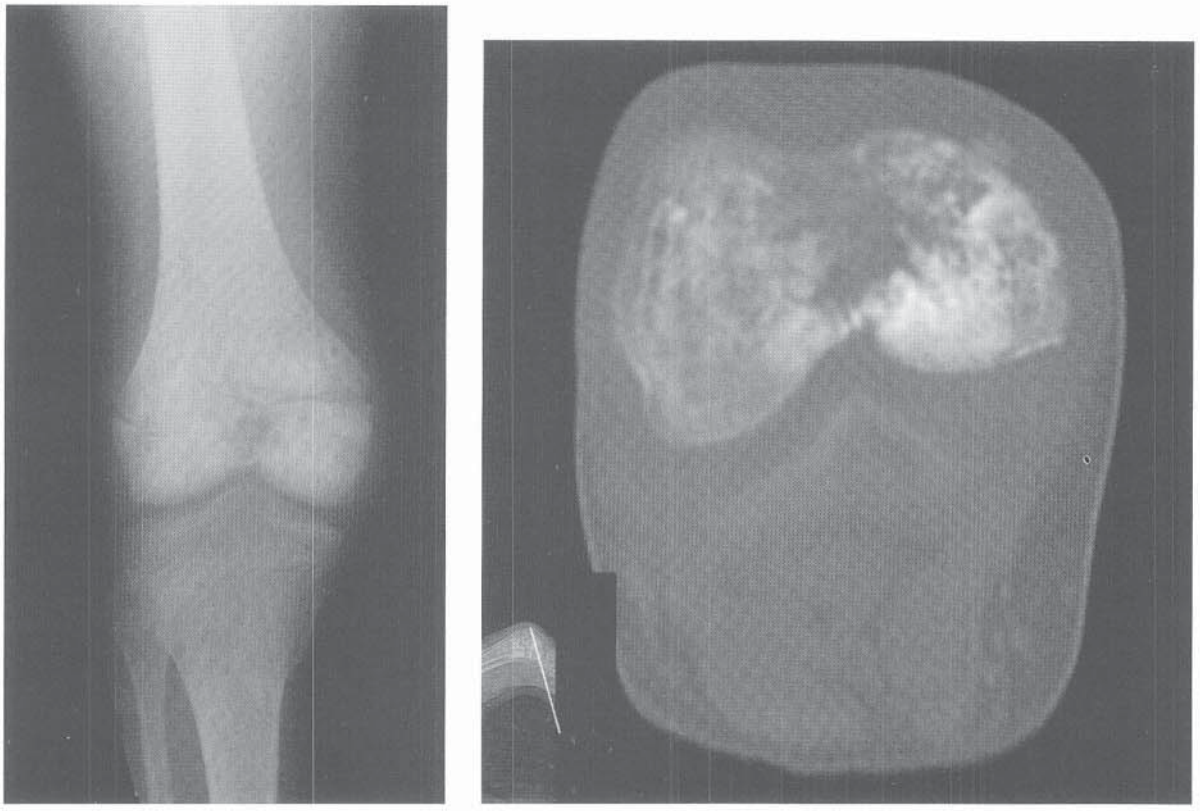

A B

FIGURE 9–30 Imaging findings in a patient with osteosarcoma. **A,** A radiograph of the right knee shows osteoblastic and lytic regions within the distal femoral metaphysis and epiphysis. **B,** A transaxial CT image of the distal femoral epiphysis reveals the osteoblastic and lytic areas of bony destruction to better advantage.

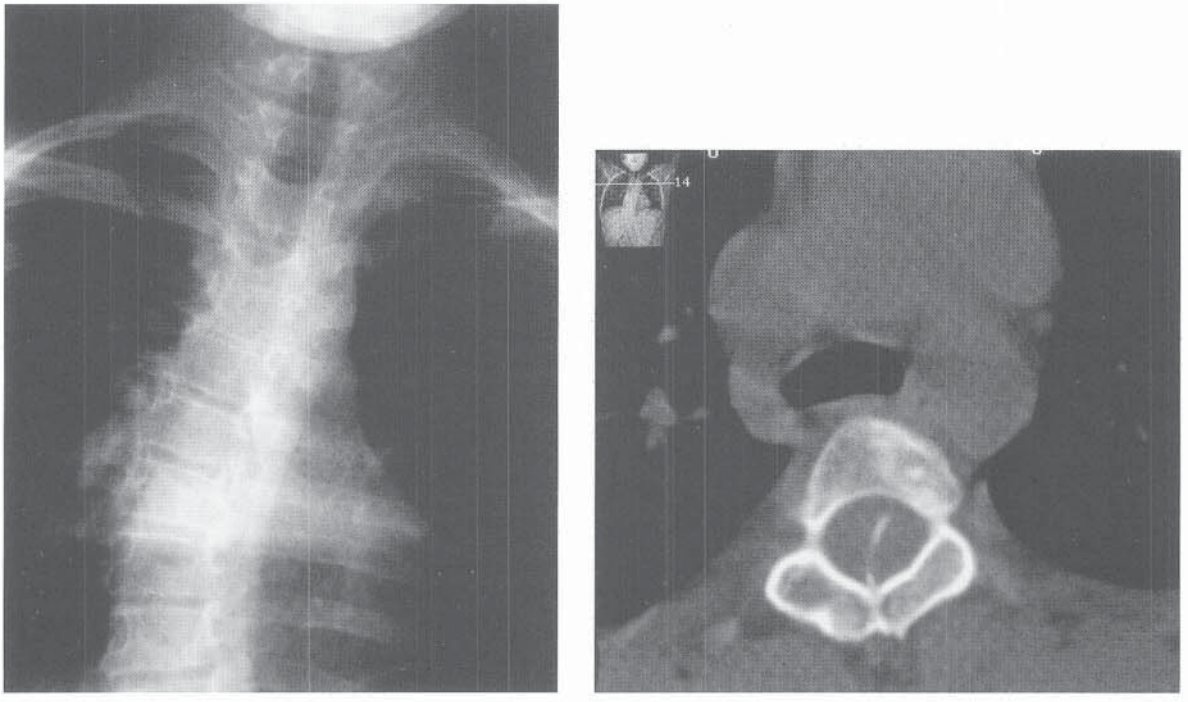

A B

FIGURE 9–31 Imaging findings in a patient with an abnormal neurologic examination. **A,** A coned radiograph of the thoracic spine shows mild dextroscoliosis. **B,** A CT scan that was obtained after an MRI study reveals a diastematomyelia and a midline bony spur in the spinal canal.

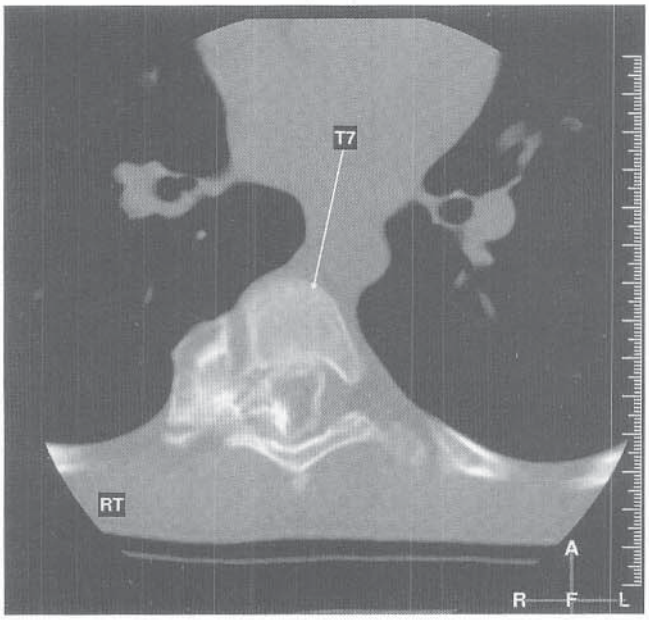

FIGURE 9–32 A transaxial section through T7 shows a large osteochondroma arising from the right rib head and extending through the adjacent neural foramen into the spinal canal.

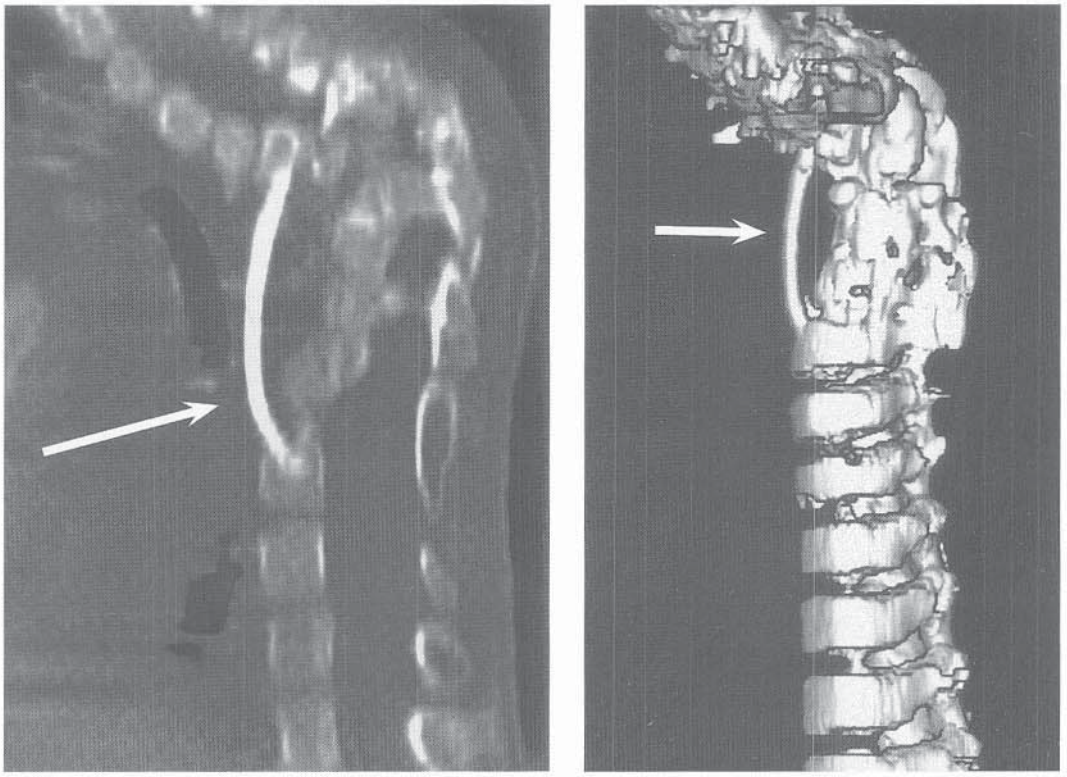

A B

FIGURE 9–33 CT findings in a patient with thoracic kyphosis. A sagittal reconstruction (**A**) and three-dimensional reconstruction (**B**) demonstrate an intact and properly positioned anterior rib strut graft (*arrow*).

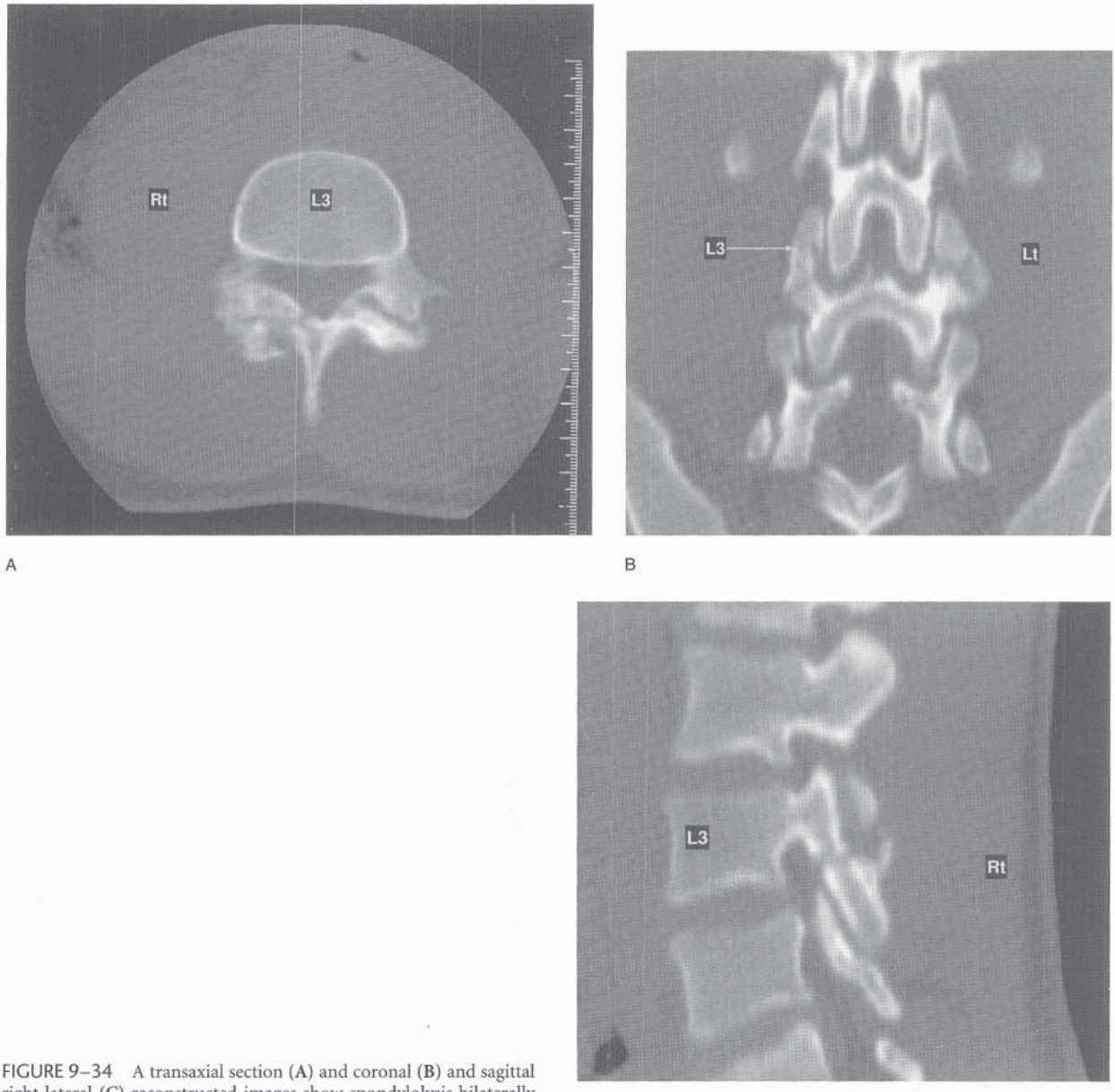

A B C

FIGURE 9–34 A transaxial section (**A**) and coronal (**B**) and sagittal right lateral (**C**) reconstructed images show spondylolysis bilaterally and minimal spondylolisthesis at L3.[46]

disorders that are readily evaluated by CT are listed in Table 9–2 and illustrated in Figures 9–23 through 9–34.

REFERENCES

Computed Tomography in Pediatric Orthopaedics

1. Aisen AM, Martel W, Braunstein EM, et al: MRI and CT evaluation of primary bone and soft tissue tumors. AJR Am J Roentgenol 1986;146:749.
2. Anderson RE, Osborn AG: Efficacy of simple sedation for pediatric computed tomography. Radiology 1997;124:739.
3. Andre M, Resnick D: Computed tomography. In Resnick D (ed): Diagnosis of Bone and Joint Disorders, 3rd ed, pp 118 ff. Philadelphia, WB Saunders Co, 1995.
4. Azouz IM, Greenspan A, Marton D: CT evaluation of primary epiphyseal bone abscesses. Skeletal Radiol 1993;22:17.
5. Baxter BS, Sorenson JA: Factors affecting the measurement of size and CT number in computed tomography. Invest Radiol 1981;16:337.
6. Brink JA, Davros WJ: Helical/spiral CT: technical principles. In Zeman R (ed): Helical/Spiral CT: A Practical Approach, pp 1–26. New York, McGraw-Hill Book Co, 1995.
7. Brink JA, Heiken JP, Wang G, et al: Helical CT: principles and technical considerations. Radiographics 1994;14:887.
8. Cook BA, Bass JW, Nomizou S, et al: Sedation of children for technical procedures: current standards of practice. Clin Pediatr 1992;31:137.
9. Costello P, Dupuy DE, Ecker CP, et al: Spiral CT of the thorax with reduced volume of contrast material: a comparative study. Radiology 1992;183:663.
10. Cox TD, White KS, Weinberger E, et al: Comparison of helical and conventional chest CT in the uncooperative pediatric patient. Pediatr Radiol 1995;25:347.
11. Dean LM, Taylor GA: Pediatric application of spiral CT. In Fishman EK, Jeffries RB Jr (eds): Spiral CT: Principles, Techniques and Clinical Applications, pp 159–166. New York, Raven Press, 1995.
12. DeCampo JF, Boldt DW: Computed tomography of partial growth plate arrest: initial experience. Skeletal Radiol 1986;15:526.
13. Eggli KO, King SH, Bloal DKB, et al: Low dose CT of developmental dysplasia of the hip after reduction: diagnostic accuracy and dosimetry. AJR Am J Roentgenol 1994;163:1441.

14. Feldman F, Singson RD, Rosenberg ZS, et al: Distal tibial triplane fractures: diagnosis with CT. Radiology 1987;164:429.
15. Fishman EK, Magid D, Ney DR, et al: Three-dimensional imaging. Radiology 1991;181:321.
16. Fredricks BJ, Boldt DW, Tress BM, et al: Diseases of the spinal canal in children: diagnosis with noncontrast CT scans. AJNR Am J Neuroradiol 1989;10:1233.
17. Gold RH, Hawkins RA, Katz RD: Bacterial osteomyelitis: findings on plain radiography, CT, MR, and scintigraphy. AJR Am J Roentgenol 1991;157:365.
18. Grogan DP, Love SM, Ogden JA, et al: Chondroosseous growth abnormalities after meningococcemia. J Bone Joint Surg 1989;71-A:920.
19. Heiken JP, Brink JA, Vannier MW: Spiral (helical) CT. Radiology 1993;189:647.
20. Hounsfield GH: Computerized transverse axial scanning (tomography). Part I. Description of system. Br J Radiol 1973;46:1016.
21. Hubbard AM, Markowitz RI, Kimmel B, et al: Sedation for pediatric patients undergoing CT and MRI. J Comput Assist Tomogr 1992;16:3.
22. Kalender WA, Seissler W, Klotz E, et al: Spiral volumetric CT with single-breath-hold technique, continuous transport, and continuous scanner rotation. Radiology 1990;176:181.
23. Keeter S, Benator RM, Weinberg SM, et al: Sedation in pediatric CT: national survey of current practice. Radiology 1990;175:745.
24. Kirks DR, Harwood-Nash, DCF: Computed tomography in pediatric radiology. Pediatric Ann 1980;9:53.
25. Klein MH, Shankman S: Osteoid osteoma: radiologic and pathologic correlation. Skeletal Radiol 1992;175:23.
26. Kleinman PK, Spevak MR: Advanced pediatric joint imaging. Radiol Clin North Am 1990;28:1073.
27. Lee DY, Choi IH, Lee CK, et al: Assessment of complex hip deformity using three-dimensional CT image. J Pediatr Orthop 1991;11:13.
28. Magid D, Fishman EK, Ney DR, et al: Acetabular and pelvic fractures in the pediatric patient: value of two- and three-dimensional imaging. J Pediatr Orthop 1992;12:621.
29. Magid D, Fishman EK, Sponseller PD, et al: 2D and 3D computed tomography of the pediatric hip. Radiographics 1988;8:901.
30. Manuli MA, Davies L: Rectal methohexital for sedation of children during imaging procedures. AJR Am J Roentgenol 1993;160:577.
31. Mitchell AA, Louik C, Lacouture P, et al: Risks to children from computed tomographic scan premedication. JAMA 1982;247:2385.
32. Murray K, Nixon GW: Epiphyseal growth plate: evaluation with modified coronal CT. Radiology 1988;166:263.
33. Napel SA: Basic principles of spiral CT. In Fishman EK, Jeffery RB Jr (eds): Spiral CT: Principles, Techniques and Clinical Applications, pp 1–9. New York, Raven Press, 1995.
34. Nelson MD Jr: Guidelines for the monitoring and care of children during and after sedation for imaging studies. AJR Am J Roentgenol 1993;160:581.
35. Pereira JK, Burrows PE, Richards HM, et al: Comparison of sedation regimens for pediatric outpatient CT. Pediatr Radiol 1993;23:341.
36. Pineda C, Resnick D, Greenway G: Diagnosis of tarsal coalition with computed tomography. Clin Orthop 1986;208:282.
37. Pruitt AW, Anyan WR, Kaufman RE, et al: American Academy of Pediatrics Committee on Drugs, Section on Anesthesiology: Guidelines for monitoring and management of pediatric patients during and after sedation for diagnostic and therapeutic procedures. Pediatrics 1992;89:1110.
38. Ram P, Martinez S, Korobkin M, et al: CT detection of intraosseous gas: a new sign of osteomyelitis. AJR Am J Roentgenol 1981;137:721.
39. Riddlesberger MM Jr, Kuhn JP: The role of computed tomography in diseases of the musculoskeletal system. J Comput Tomogr 1983;7:85.
40. Sarno RC, Carter BL, Bankoff MS, et al: Computed tomography in tarsal coalition. J Comput Assist Tomogr 1984;8:1155.
41. Scott WW Jr, Magid D, Fishman EK, et al: Three-dimensional imaging of acetabular trauma. J Orthop Trauma 1987;1:227.
42. Siegel MJ, Luker GD: Pediatric applications of helical (spiral) CT. Radiol Clin North Am 1995;33:997.
43. Stoskopf CA, Hernandez RJ, Kelikian A, et al: Technique: evaluation of tarsal coalition by computed tomography. J Pediatr Orthop 1984;4:365.
44. Strain JD, Harvey LA, Foley LC, et al: Intravenously administered pentobarbital sodium for sedation in pediatric CT. Radiology 1986;161:105.
45. Strain JD, Campbell JB, Harvey LA, et al: IV nembutal: safe sedation for children undergoing CT. AJNR Am J Neuroradiol 1988;9:955.
46. Taylor C, Kirks DR: Techniques. In Kirks DR, Griscom NT (eds): Practical Pediatric Imaging: Diagnostic Radiology of Infants and Children, 3rd ed. Philadelphia, Lippincott-Raven Publishers, 1998.
47. Thompson JR, Schneider S, Ashwal S, et al: The choice of sedation for computed tomography in children: a prospective evaluation. Radiology 1982;143:475.
48. Trefler M, Haughton VM: Patient dose and image quality in computed tomography. AJNR Am J Neuroradiol 1981;2:269.
49. Vock P, Soucek M, Daepp M, et al: Lung: spiral volumetric CT with single-breath-hold technique. Radiology 1990;176:864.
50. Weinstein MA, Rothner AD, Duchesneau P, et al: Computed tomography in diastematomyelia. Radiology 1975;118:609.
51. White KS: Reduced need for sedation in patients undergoing helical CT of the chest and abdomen. Pediatr Radiol 1995;25:344.
52. Young JWR, Bright RW, Whitley NO: Computed tomography in the evaluation of partial growth plate arrest in children. Skeletal Radiol 1986;15:530.

Magnetic Resonance Imaging in Pediatric Orthopaedics

MRI has had a significant impact on the imaging and diagnosis of musculoskeletal disorders since its development. Although MRI has not replaced CT, it holds many advantages for musculoskeletal imaging. These include (1) the ability to perform direct multiplanar imaging, (2) the provision of superb soft tissue contrast, (3) the capability of evaluating blood flow without the use of intravenous contrast agents, (4) the use of intravenous noniodinated contrast material, and (5) the ability to acquire images without ionizing radiation.[27,31] Of particular importance to the pediatric patient, MRI excels in evaluating the unossified cartilaginous skeleton, bone marrow, and soft tissues.[25]

HISTORY

As early as 1924, Pauli observed that many nuclei exhibit an angular momentum and a magnetic moment, and in fact behave as if they were small, charged, spinning spheres (Fig. 9–35).[35] Later, Bloch and Purcell independently observed

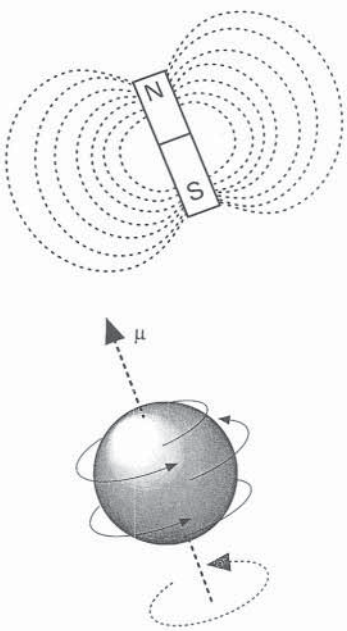

FIGURE 9–35 Rapidly spinning nuclei possessing a magnetic moment can be thought of as behaving like tiny bar magnets.[30] (From Philips Medical Systems: Basic Principles of MR Imaging, p 19. Shelton, CT, Philips Medical Systems, July 1998.)

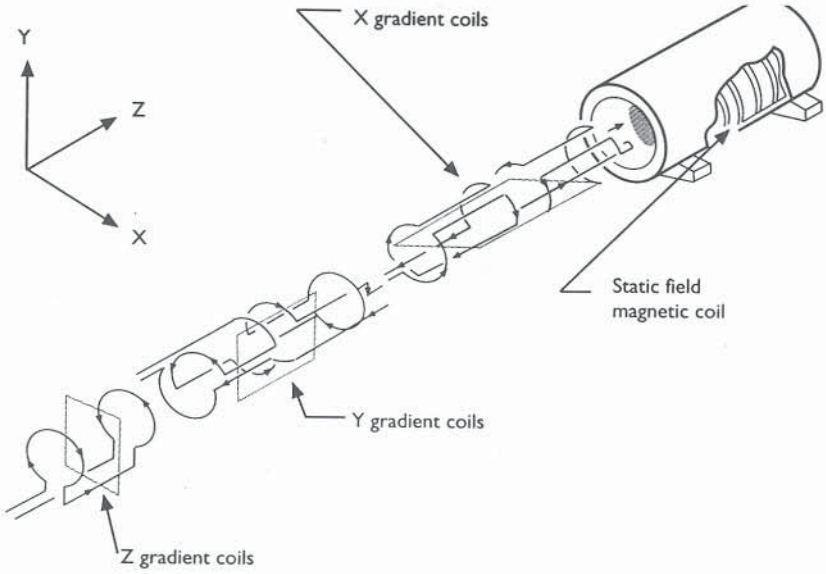

FIGURE 9–36 Typical coil arrangement (*x*, *y*, and *z* gradient coils) in an MR imager. (From Philips Medical Systems: Basic Principles of MR Imaging, p 20. Shelton, CT, Philips Medical Systems, July 1998.)

MR absorption in bulk materials, and in 1952 they shared the Nobel prize in physics for their work. During the 1950s and 1960s, MRI was mostly used by chemists and physicists to evaluate chemical structure, configuration, and reaction processes.[30] Jasper Johns measured MRI signals from live animals and in 1967 proposed human applications. In 1973, Paul Lauterbur modified an MRI spectrometer with a magnetic field to produce an image of inanimate objects—two tubes of water.[30] In 1974, Raymond Damadian produced a coarse MRI image of a rat tumor, an image that made its way to the cover of *Science* magazine.[35] Later, in 1976, Damadian produced a body image that took almost 4 hours to acquire,[8] and Sir Peter Mansfield reported imaging living humans.[30] Since then, MRI technology has progressed rapidly and has been readily accepted by physicians and patients.

BASIC PHYSICS

An in-depth discussion of the physical principles of MRI is beyond the scope of this text, and the reader is referred to other sources.[30]

MRI is noninvasive and does not use ionizating radiation. Unlike in radiography and CT, image production in MRI is based on the response of various nuclei to absorbed radiofrequency (RF) energy. Clinical MRI is based on the behavior of the hydrogen nucleus—abundant in the human body—in a magnetic field. The image, therefore, is predominantly a tomographic map of the distribution (i.e., density) of protons in the sampled tissue. Three gradient coils orthogonally positioned within the housing of the magnet create magnetic field gradients in the *x*, *y*, and *z* planes (Fig. 9–36). By energizing combinations of gradients, the operator can generate magnetic field gradients in any orientation. The gradients thus allow direct imaging in the axial, sagittal, coronal, and oblique planes. The magnetic field strength in MRI is much stronger than the earth's magnetic field—approximately 30,000 times stronger for a 1.5 Tesla (T) MRI system. The current that runs through the gradient coils is on the magnitude of several hundred amperes. This large force oscillates the mechanical switches in the gradient coils and results in the characteristic knocking noise that is heard during MRI.[8,30,35]

In simple terms, hydrogen nuclei (protons) in the human body are exposed to an external magnetic field (i.e., the bore of the magnet) (Fig. 9–37). While in this environment, the protons are pulsed with RF energy by RF coils. The absorbed energy reorients (i.e., flips) the hydrogen nuclei to a higher energy state. In the process, signal is generated by the protons. RF coils collect the signal emanating from the tipped protons, and the basic data necessary to form an image are acquired.[35]

After excitation, the protons gradually return to their

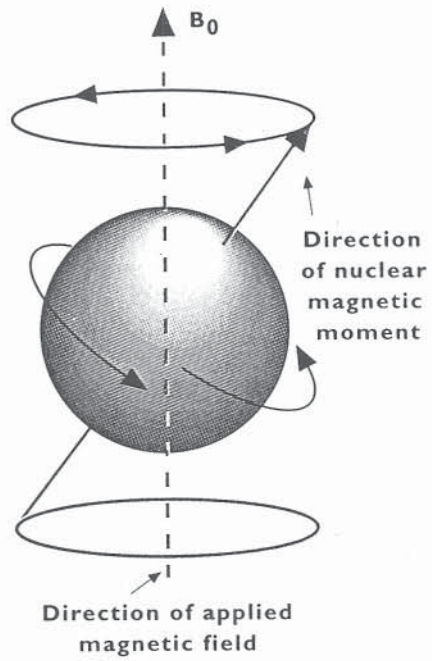

FIGURE 9–37 A spinning nucleus precesses about the axis of an applied magnetic field, analogous to a spinning top under the influence of Earth's magnetic field. (From Philips Medical Systems: Basic Principles of MR Imaging, p 22. Shelton, CT, Philips Medical Systems, July 1998.)

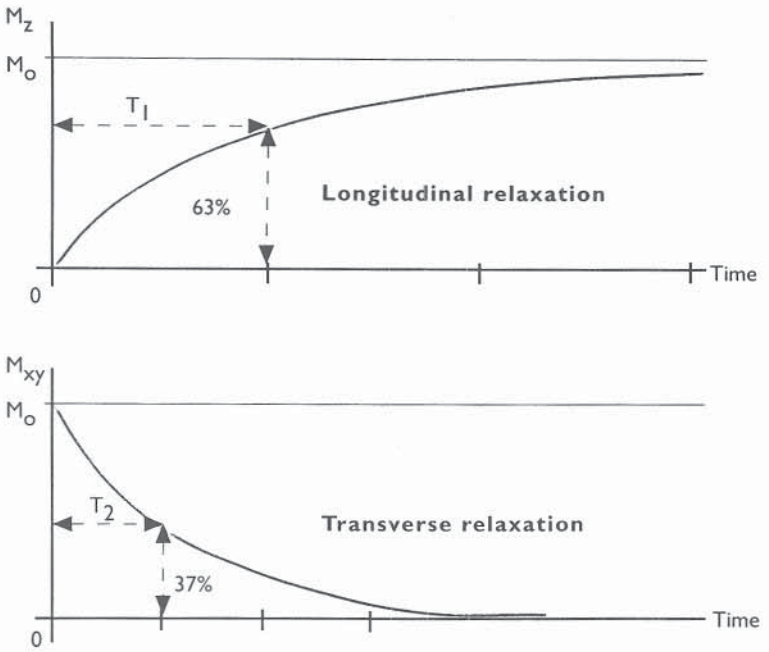

FIGURE 9–38 The longitudinal and transverse magnetization during relaxation. T1 is the time required for the longitudinal magnetization to return to 63 percent of its original value. T2 is the time required for the transverse magnetization to fall by 63 percent of its original value. T1 and T2 are independent. T2 is always shorter than T1. (From Philips Medical Systems: Basic Principles of MR Imaging, p 23. Shelton, CT, Philips Medical Systems, July 1998.)

original state (i.e., magnetization). T1 (longitudinal or spin-lattice relaxation time) is a time constant and represents the time necessary for the magnetization to return to 63 percent of its original value (Fig. 9–38). T2 (transverse or spin-spin relaxation time) is also a time constant and represents the period required for dephasing of the protons from their higher energy states (Fig. 9–38).

Depending on the frequency of the various RF pulses, slice selection is possible and allows for the spatial orientation necessary to form an image from a specific location in the patient.[30]

APPEARANCE OF THE MR IMAGE

For MR images to have clinical usefulness, contrast between the MR signal of various tissues is mandatory. Superior contrast resolution is one of the major advantages of MRI.[8] *Contrast* is defined as the difference in signal intensity of adjacent tissues. The intensity of the MR signal is based on several intrinsic and external factors. Some of the factors that are intrinsic to the patient include proton density, characteristic T1 and T2 relaxation times of tissues (discussed below), chemical shift (a term describing frequency alterations that protons exhibit based on their molecular environment), and motion or flow phenomena. The effect that the intrinsic parameters have on the image depends on the RF pulses and on the magnetic field gradients that are utilized, as well as on the timing of the data acquisition. Programmable factors are extrinsic to the patient and include (1) TR (*t*ime to *r*epetition)—the time period between the beginning of a pulse sequence and the beginning of the next identical pulse sequence, (2) TE (*t*ime to *e*cho)—the time between the beginning of a 90-degree RF pulse and the maximum amplitude of the first returning echo signal, and (3) the flip angle. Table 9–3 illustrates the image appearance based on TR and TE for spin-echo images; Table 9–4 shows the relationship between image intensities and the T1 and T2 values of a particular tissue.[8,30]

Images that are *T1 weighted* have a short TR (<800 msec) and a short TE (<30 msec).[35] In T1-weighted imaging, the short TR results in tissue contrast/differentiation that is based on T1 relaxation. For example, fat has a shorter T1 than water. Thus, after an RF pulse with a short TE, the protons in fat have recovered greater longitudinal magnetization than water, and therefore exhibit a stronger signal. Therefore, on a T1-weighted image, fat is bright (i.e., stronger signal) and water is dark (i.e., weaker signal).[35]

Images that are *T2 weighted* have a long TR (>2,000 msec) and a long TE (>60 msec). Because water has a longer T2 relaxation time than fat, there is more signal for the RF coil to collect after a long TE with water as compared to fat. Therefore, water is brighter (produces more signal) than fat (produces less signal) on a T2-weighted image.

TABLE 9–3 **Image Appearance as a Function of TR (Repetition Time) and TE (Echo Time) for Spin-Echo Images**

	Short TE	Long TE
Short TR	T1 weighted	Mixed contrast
Long TR	Proton density weighted	T2 weighted

From Philips Medical Systems: Basic Principles of MR Imaging. Shelton, CT, Philips Medical Systems, July 1998.

TABLE 9–4 **Relationship Between Image Intensities and T1 and T2 Values of a Tissue**

	Dark	Bright
T1 weighted image	Long T1	Short T1
T2 weighted image	Short T2	Long T2

From Philips Medical Systems: Basic Principles of MR Imaging, p 93. Shelton, CT, Philips Medical Systems, July 1998.

Proton density images have a long TR (>2,000 msec) and a short TE (<30 msec). The signal intensity of proton density images, therefore, is based primarily on the density of protons in the sampled tissue. Table 9–5 gives the relative signal intensities of various tissues on T1-weighted, proton density-weighted, and T2-weighted imaging.

The primary goal in pediatric MRI is to obtain diagnostic images with the highest possible resolution in the shortest period of time. Image quality is determined by several factors (signal-to-noise ratio [S/N], contrast-to-noise ratio, spatial and temporal resolution, and scanning parameters such as TR and TE). In general, obtaining images of the highest quality is a trade-off with time. In other words, those factors that increase image quality usually result in a lengthier examination. For example, a longer TR allows for more signal and greater section coverage but requires a longer acquisition time. An increase in the matrix size will increase the spatial resolution; however, the S/N within a given voxel will decrease, which can decrease image quality to a certain degree. Increasing the number of signal averages will improve the image quality but at the expense of increasing the imaging time.[30,35]

IMAGE INTERPRETATION

After obtaining the appropriate clinical information and inspecting the pertinent radiographs, the operator selects the sequences that best demonstrate the suspected pathology and the RF coil that best images the body part in question. At the end of the examination, placement of similar sequences (e.g. T1- and T2-weighted, proton density, and postenhanced images) in close proximity to one another facilitates perusal of lengthy examinations, particularly when the images are to be compared with images obtained in a previous study. A consistent and thorough search pattern should be adhered to so that pathology is not overlooked. The name, sex, and age of the patient should be noted. The appearance of the bone marrow and adjacent soft tissues (ligaments, tendons, cartilage, and vascular or neural structures) should be carefully examined with each sequence utilized. Routine identification of normal anatomic structures allows for rapid recognition of pathologic processes. If gadolinium was administered, the absence or presence of enhancement should be noted.

TABLE 9–5 **Relative Signal Intensity of Tissues**

Tissue	T1 Weighted	Proton Density Weighted	T2 Weighted
Cortical bone	Very low	Very low	Very low
Calcium	Very low	Very low	Very low
Yellow marrow	High	High	Intermediate
Red marrow	Low	Low	Intermediate
Tendon/ligament	Low	Low	Low
Fat	High	High	Intermediate
Muscle	Intermediate	Intermediate	Low
Most tumors	Intermediate	High	High

From André M, Resnick D: Computed tomography. In Resnick D (ed): Diagnosis of Bone and Joint Disorders, 3rd ed. Philadelphia, WB Saunders Co, 1995.

In general, T1-weighted imaging is best suited for demonstrating structural anatomy. For example, tethered cord, syringomyelia, dislocation/subluxation, tendon rupture, and other structural anomalies as well as normal anatomic structures are usually evaluated best on T1-weighted images. T2-weighted images, especially with fat suppression sequences, best demonstrate pathology due to the edema that often accompanies pathologic processes. Edema appears as an increase in signal intensity (i.e., a bright signal). As examples, with osteomyelitis, a bone bruise, or stress fracture, an increase in signal intensity accurately depicts the region of abnormality.

Short-tau inversion recovery (STIR) imaging suppresses fat signal (i.e., renders fat signal dark) and produces bright signal in regions of water, either normal or abnormal. Because STIR imaging is exquisitely sensitive to edema, it is advantageous in localizing the region of abnormality. Additional sequences and perhaps intravenous contrast agent administration can then be used to further characterize the pathology. For example, if one were imaging the pelvis in the

TABLE 9–6 **Common Indications for MRI**

- Bone marrow imaging
  - Normal marrow[5,37]
  - Pathologic marrow
    - Neoplasia (Fig. 9–39)
    - Osteomyelitis (Fig. 9–40)[16]
    - Replacement (Fig. 9–41)
    - Devascularization (e.g., Legg-Calvé-Perthes disease)[19]
    - Transient osteopenia about the hip
- Bone tumors and soft tissue masses[11,20]
  - Benign and malignant bone tumors (Fig. 9–42)
  - Soft tissue masses (Figs. 9–43 and 9–44)[5]
- Traumatic abnormalities[16,22]
  - Soft tissue injury
  - Bone injury
  - Epiphyseal and cartilaginous injury (Fig. 9–45)[4,13,17,18,21,34]
- Abnormalities of specific joints
  - Knee (Fig. 9–46)
  - Shoulder
  - Ankle
  - Elbow
  - Hip
  - Wrist
  - Temporomandibular joint
- Specific articular abnormalities
  - Osteoarthritis
  - Synovial inflammatory disorders
- Muscle abnormalities
  - Hypertrophy
  - Anomalous origin and/or insertion
  - Degeneration
  - Inflammation
  - Trauma
  - Neoplasm
- Skeletal deformity
  - Scoliosis (atypical) (Fig. 9–47)[3]
  - Kyphosis (Fig. 9–48)
  - Limb deformity[26]
- Intraspinal pathology
  - Disk disease
  - Tumor
  - Tethered spinal cord (Fig. 9–49)
  - Structural (i.e., syrinx) (Fig. 9–50)
  - Trauma

Modified from Resnick D (ed): Diagnosis of Bone and Joint Disorders. Philadelphia, WB Saunders Co, 1995.

A

B

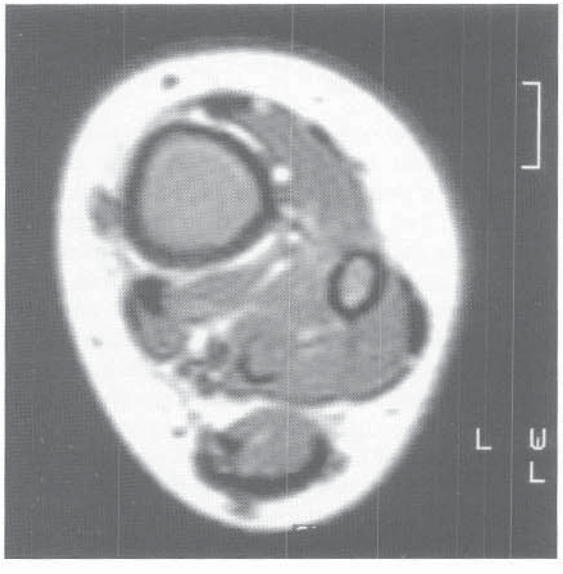

C

FIGURE 9–39 Imaging findings in a 6-year-old boy who presented with a history of ankle pain following trauma. **A,** A lateral radiograph demonstrated an abnormal region of increased density in the distal tibial metaphysis. **B** and **C,** Subsequent MRI revealed a diffuse marrow abnormality with homogenous increased signal intensity on a sagittal STIR image (B) and intermediate signal intensity on the transaxial T1-weighted image (C). Normally, most of the bone marrow in the imaged area of a 6-year-old child should be of decreased signal intensity on a STIR sequence and increased signal intensity on T1-weighted images (normal fatty marrow). In this patient, the conversion of yellow marrow to red marrow was due to acute lymphocytic leukemia. Red marrow is bright on STIR imaging and intermediate on T1-weighted imaging owing to the increased water content of hematopoietic marrow.

coronal plane for suspected septic arthritis or osteomyelitis, inflamed marrow, subperiosteal abscess, and hip effusion, as well as urine in the adjacent bladder, would all show bright signal intensity. Many other imaging sequences are available to the radiologist; however, most of the terminology is vendor specific. Therefore, it is best to consult the attending radiologist as to the sequences available on a particular scanner and the utility of each.

When interpreting an MRI examination, one must be aware of the patient's age, the imaging sequences used, and the normal and abnormal signal intensities of the tissues being evaluated. This is demonstrated well in bone marrow imaging. Infants have predominantly red (hematopoietic) marrow. On T1-weighted images, the red marrow is primarily dark, due to the abundance of water protons. On T2-weighted and STIR imaging, the marrow is therefore bright. As children age, there is a progressive and generally symmetric conversion of red marrow to fatty marrow beginning distally in the appendicular skeleton and proceeding proximally to the central (axial) skeletal structures. By age 6 years, the bony structures of the hands, feet, tibiae, fibulae, radii, and ulnae are predominantly yellow (fatty) marrow. However, hematopoietic marrow persists in the femora and axial skeleton. As an example, one is presented with a 6-year-old child with a 3-month history of dull, aching pain in the foot and ankle. Arthritis or a bone bruise is suspected clinically. Radiographs are obtained and are unrevealing. After selecting the appropriate coil, MRI is performed using T1- and T2-weighted axial and coronal images and sagittal STIR images. On evaluating the images the practitioner notes homogenous, dark-appearing marrow (low signal intensity) on the T1-weighted images and bright but homogeneous signal intensity on the T2 and STIR pulse sequences. In an infant or toddler, this appearance may be normal. However,

in a 6-year-old child, yellow marrow should be seen (i.e., bright on T1-weighted, intermediate on T2-weighted, and dark on STIR images). In fact, this MRI appearance is common in young patients with leukemia or other severe anemia (e.g., sickle cell disease or thalassemia). In these diseases, the MRI appearance of the marrow results from peripheral conversion of yellow marrow to red marrow (water abundant) in a stressful state requiring greater hematopoiesis.

In summary, the practitioner must be knowledgeable of (1) which sequences to use in various suspected diseases, (2) the patterns of signal intensity (bright, dark, intermediate) encountered in normal and pathologic states with each sequence used, and (3) the age-related changes in signal intensity exhibited by various tissues.

IMAGING ARTIFACTS

Artifacts in MRI are intrinsic or extrinsic to the MR system. Artifact recognition is vital to avoid obscuring or misdiagnosing artifact as pathology. Various scanning parameters can be altered to decrease or eliminate the offending artifact, thus optimizing the study.

Intrinsic artifacts result from acquisition or data handling difficulties inherent to the imaging system or the imaging chain. For example, *truncation* errors appear as ringing or parallel bands of high and low signal intensites and are due to the method of data manipulation at high-contrast interfaces. *Aliasing* or *wrap-around* occurs when the size of the imaged body part in the preparation direction is larger than the field of view. Another intrinsic artifact, *eddy current distortion,* is due to gradient switching during image acquisition and can lead to image degradation. Most current MRI systems incorporate means of compensating for these artifacts.[30]

Extrinsic artifacts are due to biologic processes within or caused by the patient. Gross motor movement of the patient is the most significant of these, particularly in pediatric imaging, and can result in severe image degradation. Additionally, respiratory and ocular motion, cardiac and blood vessel pulsation, swallowing, peristalsis of bowel, and CSF flow/pulsation can all lead to motion artifact. Multiple techniques have been developed to manage the various causes of motion artifact.[1,10,12,29,30,35]

Chemical shift artifact is very dependent on magnetic field strength and is seen at fat-water interfaces. This artifact produces hypointense and hyperintense lines at the boundaries between organs and surrounding fatty tissue.[30]

MR images are highly sensitive to small distortions in magnetic field homogeneity.[30] Ferromagnetic objects such as metallic prostheses, surgical wire, dental amalgam, and tiny shavings or filings from surgical saws and drill bits or screws can result in significant image distortion. Stainless steel anterior or posterior spinal instrumentation and biopsy needles can also cause magnetic and geometric distortion of the final image. Often the size of the distorted area is larger than the object that causes the distortion. If imaging will be necessary following surgical instrumentation (e.g., monitoring of spinal cord syrinx size following posterior spinal instrumentation), titanium (nonferromagnetic) instrumentation should be considered.[30]

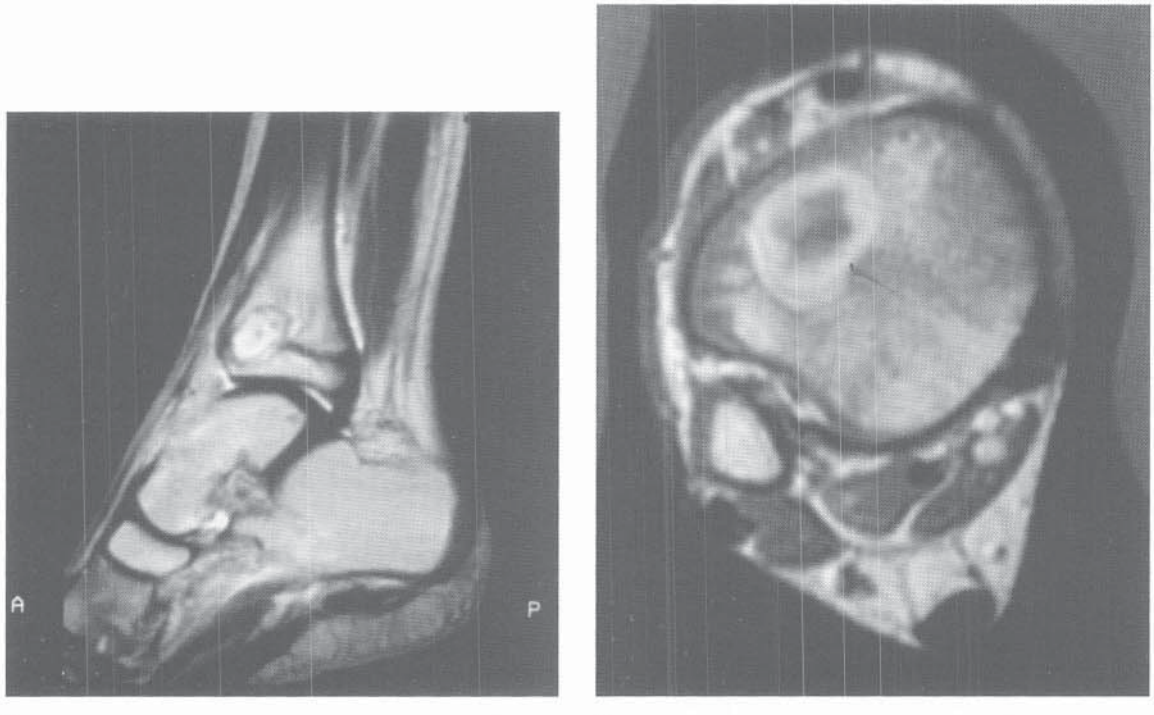

A B

FIGURE 9–40 Imaging findings in a 9-year-old boy with a 3-month history of dull, aching ankle pain. Plain films revealed a lucent region in the distal tibial metaphysis and epiphysis. **A,** A sagittal T2-weighted image accurately localized a high-signal-intensity lesion spanning the growth plate. **B,** A transaxial postgadolinium image of the distal tibial growth plate demonstrated peripheral enhancement with a nonperfused region centrally suggesting an intramedullary abscess. A Brodie's abscess was confirmed at surgery.

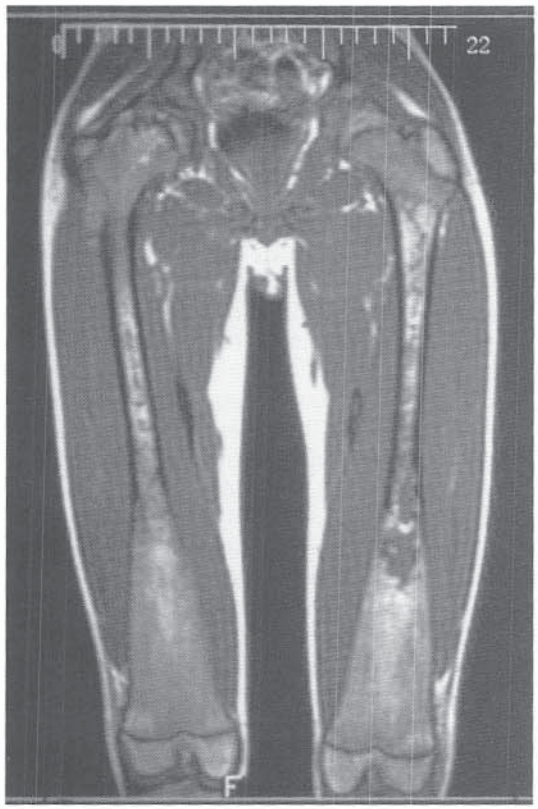

FIGURE 9–41 T1-weighted image in a 13-year-old boy with Gaucher's disease showing bilateral avascular necrosis of the hips and Erlenmeyer flask deformities of the distal femora. Abnormal regions of decreased signal intensity intermixed with regions of fatty marrow (bright signal) are seen in the proximal and midfemora, representing marrow replacement.

IMAGING ENHANCEMENT

Gadolinium (Gd^{3+}) is a paramagnetic ion (a compound with a small positive magnetic susceptibility) that is injected intravenously and serves to decrease the T1 relaxation time of the tissues where it accumulates. When gadolinium is used in conjunction with T1-weighted imaging, the acceleration in T1 relaxation time results in an *increase* in signal intensity (i.e., a brighter image) and is analogous to contrast enhancement in CT.[30]

For example, in the evaluation of tumor, gadolinium administration may result in tumor enhancement relative to the surrounding tissues, thus helping to differentiate tumor from edema. Additionally, intravenous contrast medium is helpful in imaging the postoperative back, where it can differentiate scar tissue from recurrent disk herniation.[32] In the evaluation of soft tissue or bony infection or abscess, a nonperfused region with surrounding enhancement can lead to the identification of a drainable fluid collection (i.e., the abscess). Intra-articular administration may enhance the conspicuity of certain lesions such as cartilaginous or tendinous tears (e.g., glenoid labrum or rotator cuff tear) but currently is not officially approved by the Food and Drug Administration.[27] Because of its toxicity, gadolinium is not injected as a free ion but is chelated to other molecules such as DTPA (diethylene triamine pentaacetic acid) to decrease its toxicity and allow clinical use.[30]

SAFETY PRECAUTIONS AND PATIENT PREPARATION

A primary safety issue in MRI is the strong magnetic field that is generated. A metallic object such as an oxygen canister

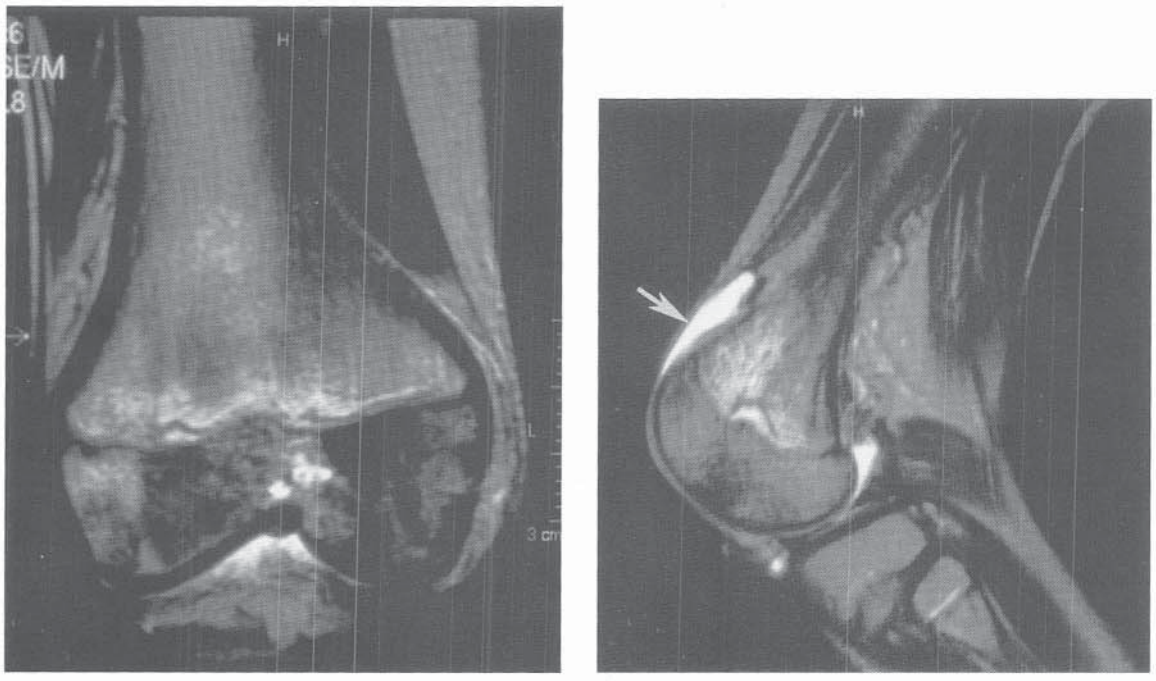

A B

FIGURE 9–42 Same patient as in Figure 9–30, with osteosarcoma. Coronal (**A**) and sagittal (**B**) STIR images show abnormal edema (bright signal) in the metaphysis and epiphysis of the distal femur. The abnormal dark signal in the epiphysis represents dense osteoblastic tumor. A small knee effusion (*arrow*) is noted in B.

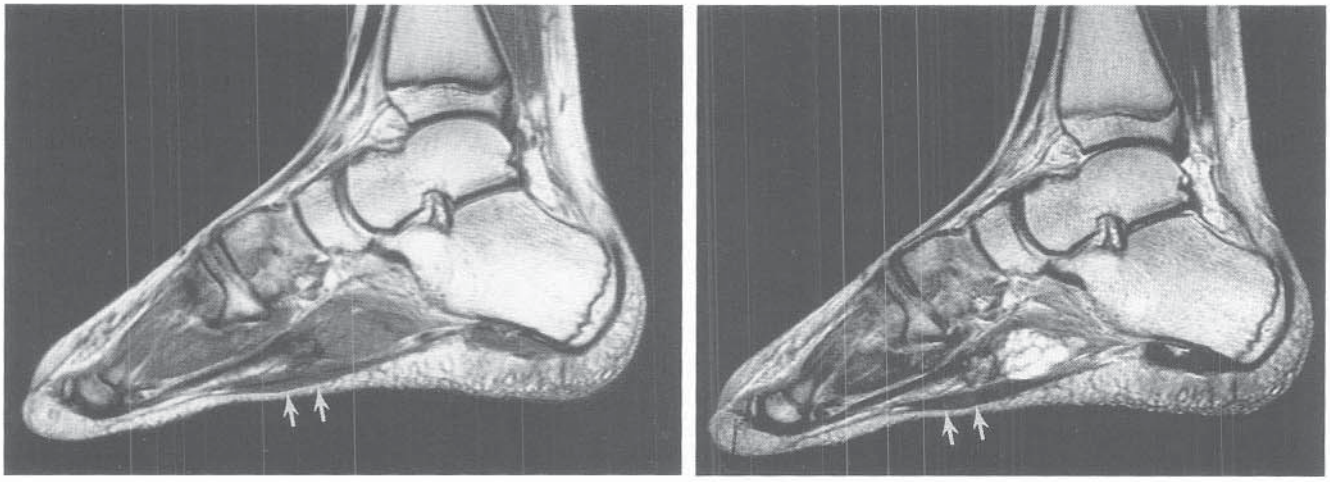

A B

FIGURE 9–43 A 13-year-old boy presented with a 3-month history of plantar left foot pain that was worsened by activity and improved with rest. **A,** A sagittal T1-weighted image revealed an ovoid, intermediate-signal-intensity mass deep to the flexor digitorum brevis muscle (*arrows*). The differential diagnosis would include a vascular lesion, a tumor associated with a tendon, an inflammatory process secondary to a foreign body, and a synovial sarcoma. **B,** A sagittal T2-weighted image showed abnormal cystlike regions of increased signal intensity, suggesting a venous malformation. Because the patient had persistent pain, a biopsy was performed and revealed a venous malformation.

or other ferromagnetic item can become a flying missile-like projectile capable of causing lethal harm. A nurse or other staff person should screen all patients before entering the MRI suite for watches, chains, bracelets, earrings, recent surgery, metallic implants or instrumentation, a pacemaker, or other metallic foreign bodies (e.g., tiny filings in the eye). If possible, the items should be removed.

As in CT, the key to a successful pediatric MRI examination is appropriate preparation of the patient. The child and caregiver should be forewarned of the loud knocking noise characteristic of image acquisition. If possible and thought to be helpful, the patient can be shown the scanner before the study is performed to help alleviate anxiety. The importance of not moving during the study should be stressed to patient and parents.

The radiology nurse should take the appropriate history. If sedation is anticipated, the patient should be NPO. The length of the NPO status depends on the age of the child (see computed tomography section). Neonates and infants less than 3 months old often fall asleep after a feeding with swaddling, obviating the need for sedation. However, patients between ages 3 months and 5 to 6 years will usually need sedation to remain still for the entire examination.[36] Older, cooperative patients generally do not need sedation. Abundant literature is available on sedation guidelines in children[2,6,15,23,28,33]; however, the procedures followed should be tailored to the patient population and developed in conjunction with the attending anesthesiologist.

Monitoring children in an MRI setting requires magnet-compatible equipment (e.g., pulse oximeters, electrocardiograph, noninvasive blood pressure monitor, ventilators) that will not produce image artifacts.[36] The MRI technologist

FIGURE 9–44 A transaxial STIR image showing a mass in the lateral aspect of the right gluteus maximus muscle characterized by inhomogeneously increased signal intensity. Multiple regions of increased signal intensity are seen in the peripheral subcutaneous tissues. A vascular malformation was suggested. At arteriography, a vascular malformation was identified and embolized.

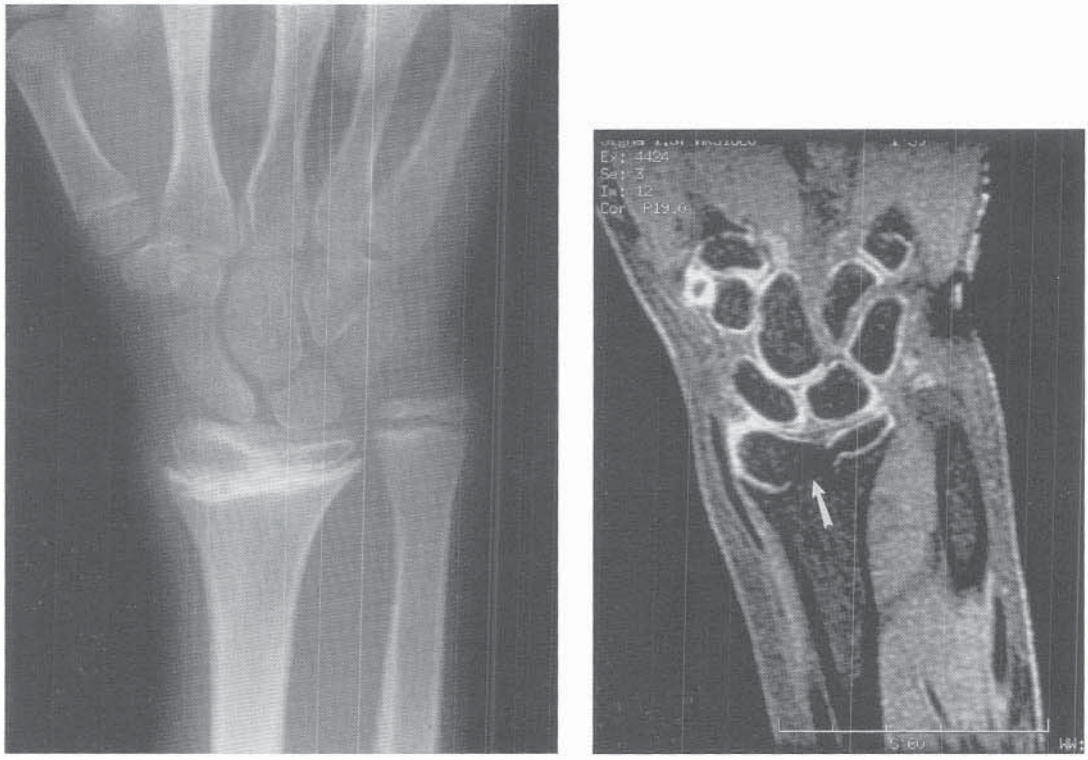

A B

FIGURE 9–45 Imaging findings several months following trauma. Imaging was performed to address the clinical question of partial closure of the distal radial growth plate. **A,** PA radiograph of the wrist showed slight narrowing of the central portion of the distal radial growth plate and increased density of the adjacent metaphysis. **B,** A coronal fat-saturated spoiled gradient echo image of the wrist demonstrated loss of the increased signal intensity of cartilage at the central portion of the growth plate (*arrow*), confirming a growth plate bar.

should be certain that the child is restrained, comfortable, and appropriately positioned for the examination. It is vital that the technologist and the radiologist have a clear understanding of the clinical question to be answered. Scanning protocols are helpful for patient throughput. However, MRI studies in children should be closely monitored by the radiologist to ensure that all appropriate sequences have been performed to address the clinical concern. It is imperative that all prior imaging studies, particularly plain radiographs, be available to the radiologist for planning the imaging strategy (e.g., patient position, region of interest, imaging planes, pulse sequences, contrast administration, type of coil, and the like). To expedite patient throughput, it is best to address these issues before the patient arrives in the radiology department. Correlation of the clinical history, previous imaging studies (particularly radiographs), and MRI findings usually guides the practitioner to the correct diagnosis. Radiographs of the area in question should always be available to the radiologist, not only for planning, but also for interpretation of the MRI examination.

INDICATIONS FOR MRI IN PEDIATRIC MUSCULOSKELETAL DISEASE

MRI has not replaced CT in musculoskeletal imaging but has influenced the practitioner's ability to confidently identify normal anatomy and a multitude of pathologic processes. Its capacity to demonstrate anatomy and disease states in varied planes without the use of ionizing radiation is extremely advantageous in evaluating the pediatric patient.

MRI has proved valuable in various pathologic states such as tumor assessment. The extent of disease can be more accurately determined, thereby allowing limb-sparing procedures to be performed instead of amputation. By comparing the slope values from sequential postcontrast MR images, the surgeon can differentiate tumor from nonneoplastic edema, a useful feature in planning limb salvage procedures.[24]

Evaluation of joints for internal derangement is enhanced with MRI, which in many cases has replaced arthrography. For example, in the knee, meniscal and ligamentous pathology can be documented well. In some cases, intra-articular injection of gadolinium increases the conspicuity of meniscal and ligamentous tears. The identification of ligamentous injury in the absence of radiographic findings (e.g., cervical trauma) has been enhanced. Intra-articular disease such as pigmented villonodular synovitis, pannus formation associated with rheumatologic disorders, and joint cartilage destruction, as seen in hemophiliac arthropathy, are all imaged well. Although injury to the rotator cuff of the shoulder is more common in the adult, it is readily evaluated in children with MRI.

In children, MRI has rapidly progressed to the forefront in the evaluation of lesions located in the spinal canal or cord. Lesions such as tethered cord, syrinx, diastematomye-

lia, intraspinal lipoma, spinal cord hematoma or transection, and spinal cord tumors such as hemangioma, astrocytoma, and drop metastasis are easily evaluated with MRI. Spinal cord impingement due to vertebral subluxation (e.g., Down syndrome) or cervical kyphosis (seen, for example, in neurofibromatosis, diastrophic dysplasia, and Larsen's syndrome) are superbly delineated. Disk herniation, diskitis, and paravertebral pathology (e.g., infectious inflammatory processes, tumor, hemorrhage [e.g., psoas hematoma/abscess]) are all exquisitely depicted. Cartilaginous imaging is clearly a distinct advantage of MRI compared to CT. For example, fracture extension through the cartilaginous epiphysis into the joint of the young child's elbow is easily assessed.

MRI also excels in bone marrow and soft tissue imaging owing to its superior contrast resolution. This allows excellent delineation of both focal and diffuse disease. Osteomyelitis, avascular necrosis, marrow replacement with tumor, storage disorders such as Gaucher's disease, and primary bony tumors such as osteosarcoma and Ewing's sarcoma are demonstrated well. The diffuse nature of certain pathologic processes such as myositis and vascular malformations is also defined well.

Soft tissue infection (cellulitis, phlegmon, abscess) and soft tissue tumors such as lipoma, rhabdomyosarcoma, and extraosseous Ewing's sarcoma are all superbly imaged.

Although MRI is extremely sensitive in depicting pathologic tissues, it may not be specific as to the etiology. Many disease processes manifest with an increase in free tissue water—that is, edema. For example, tumor, infection, trauma, and other afflictions may all produce edema that is easily detected with MRI. However, the identification of edema does not correlate with a specific diagnosis. The excellent contrast resolution of MRI can at times lead to an overestimation of disease aggressiveness. For example, in

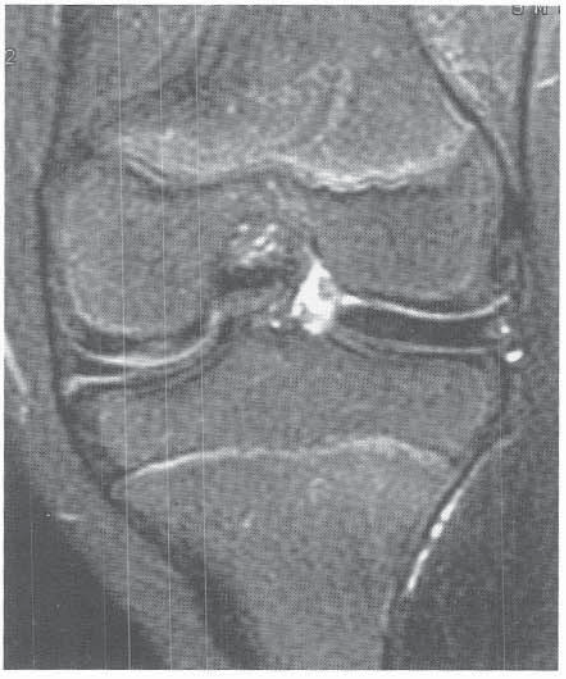

A

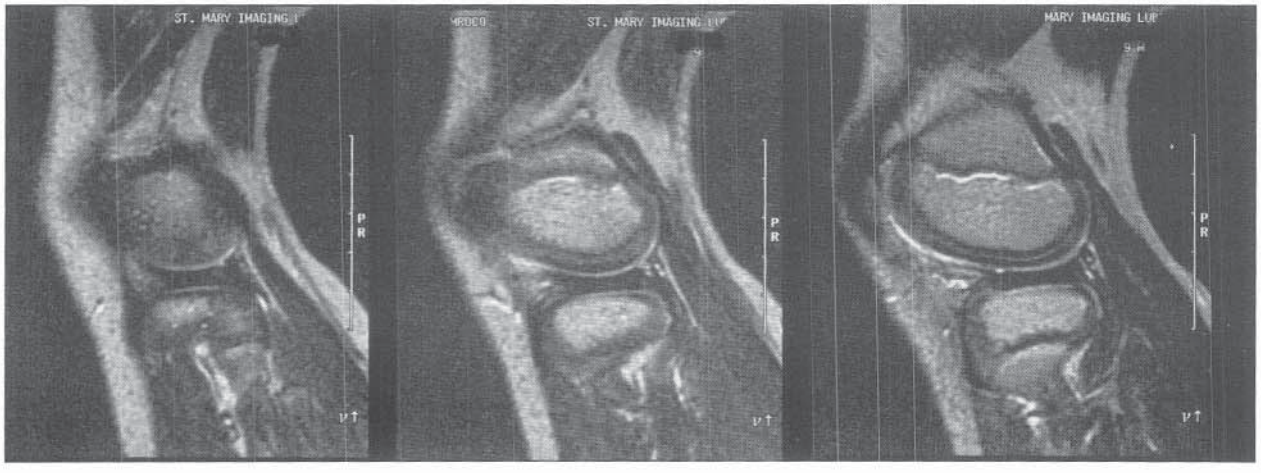

B

FIGURE 9–46 Imaging findings in a 9-year-old boy with knee pain. **A,** A coronal, heavily T2-weighted image revealed increased height of the lateral meniscus. **B,** Sagittal T2-weighted images obtained through the lateral meniscus demonstrated a continuous or bow-tie appearance on three consecutive images. The findings were consistent with a lateral discoid meniscus.

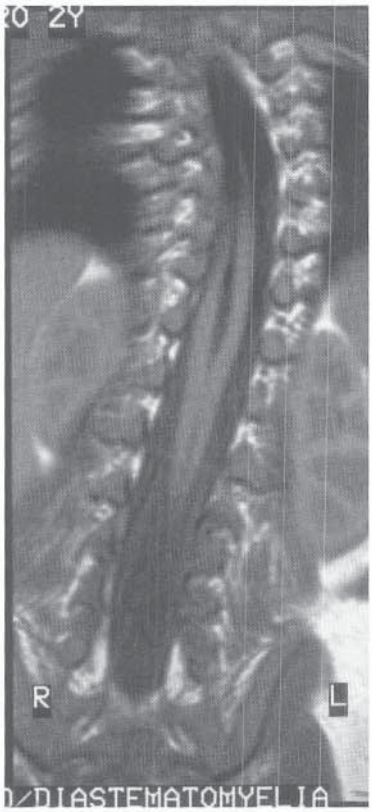

A

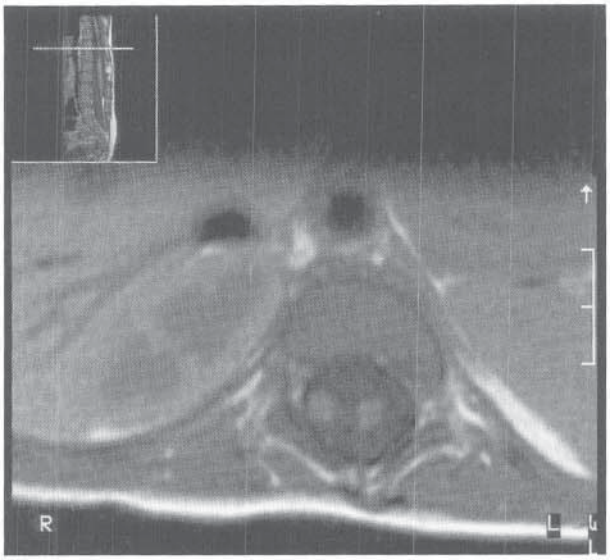

B

FIGURE 9–47 MRI findings in a 2-year-old boy with a thoracic levoscoliosis and abnormal neurologic examination. Coronal (**A**) and transaxial (**B**) T1-weighted images of the spine showed a diastematomyelia.

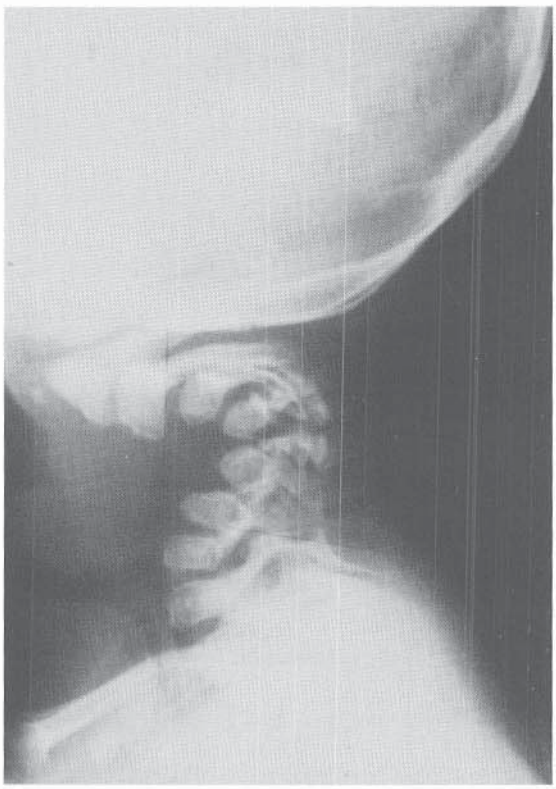

A

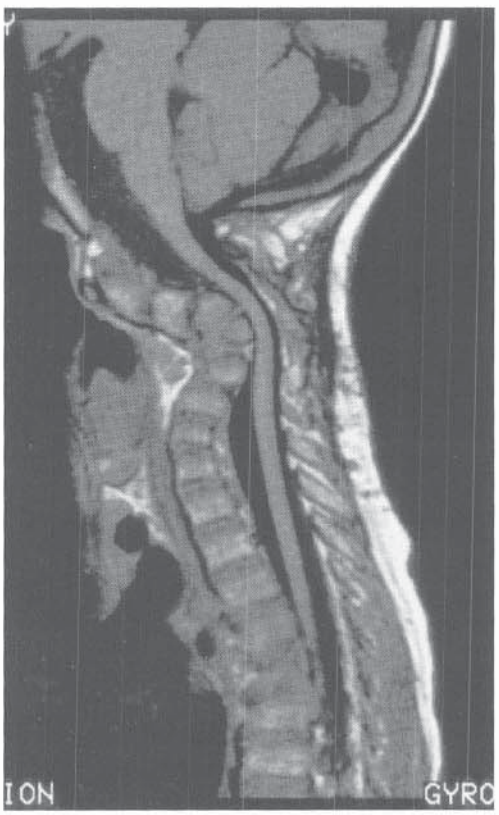

B

FIGURE 9–48 Imaging findings in a 10-year-old girl with diastrophic dwarfism. **A,** A lateral cervical spine radiograph showed severe kyphosis. **B,** A sagittal T1-weighted MR image showed cervical kyphosis, narrowing of the AD diameter of the spinal canal, and impingement of the spinal cord.

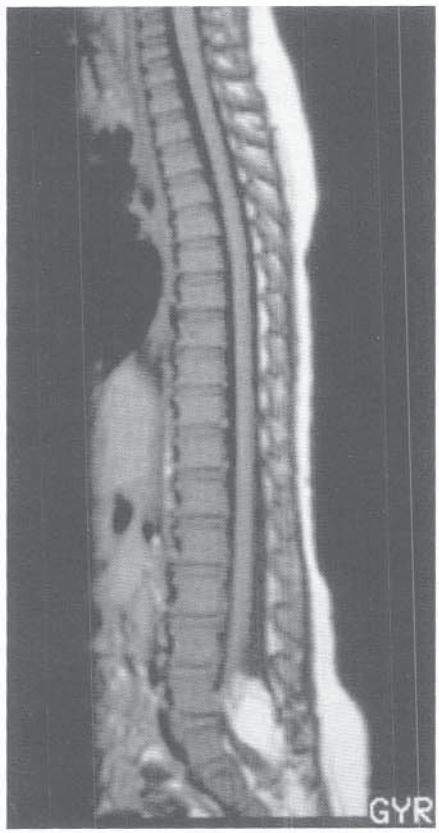

A

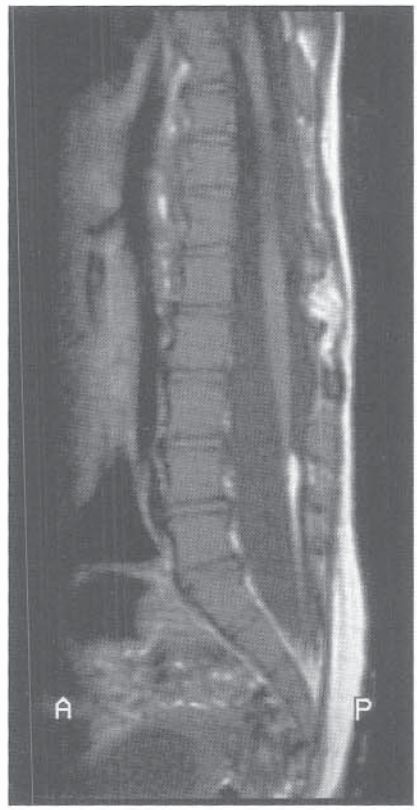

B

FIGURE 9–49 MRI findings in two patients with abnormal neurologic examinations. **A,** A sagittal T1-weighted image in one patient revealed a tethered cord with intraspinal lipoma. **B,** A sagittal T1-weighted image in the other patient demonstrated a low-lying conus with a tethering thickened fatty filum.

FIGURE 9–50 A sagittal T1-weighted MR image of the cervical and upper thoracic spine demonstrating a syrinx spanning the mid- to lower cervical spinal cord.

osteoid osteoma or stress fracture, an intense soft tissue reaction manifesting as abnormal high signal intensity can be found in the surrounding soft tissues. This appearance may lead to the incorrect diagnosis of an aggressive and perhaps malignant lesion with extensive extraosseous extension. The clinical history of night pain relieved by nonsteroidal agents or of trauma and correlation with plain radiographic or CT findings will usually disclose the true nature of this process. Additionally, in regard to myositis ossificans, MRI often demonstrates a diffuse intramuscular aggressive-appearing process, leading one to suspect a malignant soft tissue tumor. However, the history of trauma and previous radiographs or CT scans showing an early thin shell of peripheral bone often lead to the correct diagnosis on initial radiographic evaluation.

MRI is misused when the pertinent clinical history and correlative radiographs are not available for review at the time of imaging planning and interpretation. To avoid misdiagnosis and patient mismanagement, the clinical record and previous imaging studies should *always* be available to the radiologist. Their importance is illustrated by the scenario of the young patient who presents with left hip pain of approximately 1 week's duration. AP radiographs show a questionable focal bony lesion in the proximal femur. MRI is then ordered and performed without the pertinent history. At the time of image planning and interpretation, the plain films are unavailable. The MRI examination shows abnormal bright signal on the T2-weighted images with intense surrounding extraosseous edema, and tumor is suspected. Subsequently the history of a fall and limping are discovered. In retrospect, orthogonal or oblique films or fluoroscopy with spot filming would have demonstrated a nondisplaced fracture with early new bone formation. Thus, an extensive and expensive workup could have been avoided had the appropriate history and films been available and reviewed prior to MRI. As in any diagnostic evaluation, a tailored imaging pathway that most easily and cost-effectively allows the diagnosis to be made is preferred.

Although MRI has assumed a prominent role in imaging a number of pathologic conditions, it should not be used as the first-line examination. MRI is relatively lengthy and costly compared to other imaging modalities. In general, MRI should be performed to answer or evaluate a *specific* question. For example, the precise history of "atypical scoliosis" with a request to "rule out tethered cord/syrinx" is preferred over the nonspecific note of "back pain." Imaging parameters and protocols are usually developed to evaluate specific disease processes. Therefore, the pertinent question needs to be asked to obtain the correct answer.

Many indications for MRI have arisen since its early development, although not as the first-line examination. The common indications are listed in Table 9–6, and the relevant MRI appearances for some are shown in Figures 9–39 through 9–50.

REFERENCES

Magnetic Resonance Imaging in Pediatric Orthopaedics

1. Bailes DR, Gilerdale DJ, Bydder GM, et al: Respiratory ordered phase encoding (ROPE): a method for reducing respiratory motion artifacts in MR imaging. J Comput Assist Tomogr 1985;9:835.
2. Ball WS, Bisset GS III: Proper sedation essential to MR imaging in children. Diagn Imaging 1990;12:108.
3. Barnes PD, Brody JD, Jaramillo D, et al: Atypical idiopathic scoliosis: MR imaging evaluation. Radiology 1993;186:247.
4. Barnewolt CE, Shapiro F, Jaramillo D: Normal gadolinium-enhanced images of the developing appendicular skeleton. Part 1. Cartilaginous epiphysis and physis. AJR Am J Roentgenol 1997;169:183.
5. Bissett GS III: MR imaging of soft-tissue masses in children. MRI Clin North Am 1996;4:697.
6. Bissett GS III, Ball WS Jr: Preparation, sedation, and monitoring of the pediatric patient in the magnetic resonance suite. Semin Ultrasound CT MR 1991;12:376.
7. Bruxton RB: Magnetic resonance imaging: technical considerations. In Resnick D (ed): Diagnosis of Bone and Joint Disorders, 3rd ed, pp 170–190. Philadelphia, WB Saunders Co, 1995.
8. Bushong SC: Magnetic Resonance Imaging: Physical and Biological Principles, St. Louis, CV Mosby Co, 1988.
9. Dwek JR, Shapiro F, Laor T, et al: Normal gadolinium-enhanced MR images of the developing appendicular skeleton. Part 2. Epiphyseal and metaphyseal marrow. AJR Am J Roentgenol 1997;169:191.
10. Felmlee JP, Ehman RL: Spatial presaturation: a method for suppression of flow artifacts and improving depiction of vascular anatomy in MR imaging. Radiology 1987;164:559.
11. Fletcher BD, Hanna SL: Pediatric musculoskeletal lesions simulating neoplasms. MRI Clin North Am 1996;4:721.
12. Haacke EM, Lenz GW: Improving MR image quality in the presence of motion by using rephasing gradients. AJR Am J Roentgenol 1987;148:1251.
13. Havranek P, Lizler J: Magnetic resonance imaging in the evaluation of partial growth arrest after physeal injuries in children. J Bone Joint Surg 1991;73-A:1234.
14. Horowitz AL: MRI Physics for Radiologists. New York, Springer-Verlag, 1995.
15. Hubbard AM, Markowitz RI, Kimmel B, et al: Sedation for pediatric patients undergoing CT and MRI. J Comput Assist Tomogr 1992;16:3.
16. Jaramillo D: Pediatric musculoskeletal MR imaging and CT: infection and trauma. In Current Concepts: A Categorical Course in Pediatric Radiology, pp 125–134. Oak Brook, IL, Society of Pediatric Radiologists, 1994.
17. Jaramillo D, Hoffer FA: Cartilaginous epiphysis and growth plate: normal and abnormal MR imaging findings. AJR 1992;158:1105.
18. Jaramillo D, Hoffer FA, Shapiro F, et al: MR imaging of fractures of the growth plate. AJR Am J Roentgenol 1990;155:1261.
19. Jaramillo D, Kasser JR, Villegas-Medina OL, et al: Cartilaginous abnormalities and growth disturbances in Legg-Calvé-Perthes disease: evaluation with MR imaging. Radiology 1995;197:767.
20. Jaramillo D, Laor T, Gebhardt MC: Pediatric musculoskeletal neoplasms: evaluation with MR imaging. MRI Clin North Am 1996;4:749.
21. Jaramillo D, Laor T, Zaleske DJ: Indirect trauma to the growth plate: results of MR imaging after epiphyseal and metaphyseal injury in rabbits. Radiology 1993;187:171.
22. Jaramillo D, Shapiro F: Musculoskeletal trauma in children. MRI Clin North Am 1998;6:521.
23. Karlik SJ, Heatherley T, Pavan F, et al: Patient anesthesia and monitoring on a 1.5-T MRI installation. Magn Reson Med 1988;7:210.
24. Lang P, Honda G, Roberts T, et al: Musculoskeletal neoplasm: perineoplastic edema versus tumor on dynamic postcontrast MR images with spatial mapping of instantaneous enhancement rates. Radiology 1995;197:831.
25. Laor T, Chung T, Hoffer FA, et al: Musculoskeletal magnetic resonance imaging: how we do it. Pediatr Radiol 1996;26:695.
26. Laor T, Jaramillo D, Hoffer FA, et al: MR imaging in congenital lower limb deformities. Pediatr Radiol 1996;26:381.
27. McEnery KW, Murphy WA Jr: Magnetic resonance imaging: practical considerations. In Resnick D (ed): Diagnosis of Bone and Joint Disorders, 3rd ed. Philadelphia, WB Saunders Co, 1995.
28. Merrick PA, Case BJ, Jagjivan B, et al: Care of pediatric patients sedated with pentobarbital sodium in MRI. Pediatr Nurs 1991;17:34.
29. Mitchell DG, Vinitski S, Burk DL Jr, et al: Motion artifact reduction in MR imaging of the abdomen: gradient moment nulling versus respiratory-sorted phase encoding. Radiology 1988;169:155.
30. Philips Medical Systems: Basic Principles of MR Imaging. Philips Medical Systems, Shelton, CT, July 1998.
31. Rawson JV, Siegel MJ: Techniques and strategies in pediatric body MR imaging. MRI Clin North Am 1996;4:589.

32. Ross JS, Delamarter R, Hueftle MG, et al: Gadolinium-DTPA-enhanced MR imaging of the postoperative lumbar spine: time course and mechanism of enhancement. AJR Am J Roentgenol 1989;152:825.
33. Sheppard JK, Hall-Craggs MA, Griffin JP, et al: Sedation in children scanned with high field magnetic resonance: the experience at the Hospital for Sick Children, Great Ormond Street. Br J Radiol 1990;63:794.
34. Smith BG, Rand F, Jaramillo D, et al: Early MR imaging of lower-extremity physeal fracture-separations: a preliminary report. J Pediatr Orthop 1994;14:526.
35. Taylor C, Kirks DR: Techniques. In Kirks DR, Griscom NT (eds): Practical Pediatric Imaging: Diagnostic Radiology of Infants and Children, 3rd ed, pp 44 ff. Philadelphia, Lippincott-Raven, 1998.
36. Techniques and Strategies in Pediatric Body MR Imaging. MRI Clin North Am 1996;4:4.
37. Zawin JK, Jaramillo D: Conversion of bone marrow in the humerus, sternum, and clavicle: changes with age on MR images. Radiology 1993;188:159.

Ultrasonography

The advent of high-resolution, real-time ultrasound equipment has led to expanded application in the musculoskeletal system. Ultrasound is particularly useful in pediatrics, for several reasons: no ionizing radiation is used; images are acquired in real time, allowing ultrasound to be used in crying or uncooperative children; imaging can be performed in infinite planes, increasing the understanding of spatial relationships; small patient size results in improved imaging; equipment portability allows imaging to be done at the bedside or in the operating room; and ultrasound is relatively inexpensive compared to other cross-sectional imaging modalities such as CT and MRI, making it useful in multiple follow-up examinations or in screening.

PHYSICS

Ultrasound is sound above the audible range, generally greater than 20 kilohertz (kHz). Diagnostic ultrasound operates in a frequency range of 1 to 20 megahertz (MHz). The sound is created in the transducer crystal by the piezoelectric effect, whereby ceramic crystal elements are deformed in the presence of an applied electric current, establishing vibratory energy. The emitted sound is dependent on the crystal thickness and its resonant frequency. The returning sound wave then deforms the crystal, generating an electric pulse that is used to create an image.

Transmitted sound energy may be reflected, refracted, scattered, or absorbed. Reflection occurs at interfaces of different impedance. Acoustic impedance is related to the product of tissue density and the speed of sound in that tissue. The amount of reflection depends on the impedance difference and the angle of incidence of the sound wave. Refraction is a change in direction of the sound wave at an oblique interface. Scattering occurs at irregular interfaces and is also due to the heterogeneity of biologic tissues. Absorption is the conversion of sound energy into thermal energy. Deeper echoes are electronically amplified to compensate for their decreasing intensity from reflection, scattering, and absorption.

IMAGE GENERATION

The returning sound pulses were originally displayed in graphic form as the amplitude of the echo versus time, known as A-mode. Later, the echoes were displayed as dots, with greater brightness corresponding to increased amplitude. This is known as B-mode imaging. The time required for the signal to return to the transducer could be converted to depth, or distance, based on the speed of sound in soft tissue (1,540 m/sec). Two-dimensional displays were created by sweeping the transducer across the patient and "painting" an image. An articulated arm attached to the transducer determined its location and orientation.

Current equipment generates two-dimensional gray-scale images in real time with freely moving, hand-held transducers. Mechanical transducers contain a single large crystal that oscillates, creating a wedge-shaped image. Array transducers contain multiple small crystal elements adjacent to one another. By triggering these elements in various sequences and combinations, the operator can electronically steer and focus the ultrasound beam. A phased array transducer utilizes all of its elements for each pulse. This type of transducer produces a large field of view in deeper tissues but a small field of view superficially. A linear array transducer utilizes a limited number of elements in each pulse. This provides higher resolution and a larger field of view in superficial tissues, but the deep field of view is limited.

DOPPLER IMAGING

Ultrasound images are based on gray-scale reconstruction of amplitude data. The Doppler technique relies on frequency data. Sound reflected from a moving target undergoes a change in frequency. The difference between the transmitted and received frequencies is the Doppler shift. This effect is experienced when a siren apparently changes pitch as it approaches, and then passes, a stationary observer. The early Doppler probes utilized separate crystals for transmitting and receiving, and produced a continuous signal. This technology proved sensitive for the detection of blood flow but could not provide depth localization. The development of pulsed Doppler technology, which sends a short pulse, then listens for the echo, enabled this localization. By varying the time delay for echo acquisition, the operator can select the depth of the returning signal. Duplex Doppler ultrasound uses the gray-scale image as a road map. A cursor is positioned within the image to select a region for Doppler interrogation. This technique is reliable and useful but can be quite time-consuming when studying many small vessels or a single large vessel.

Color Doppler imaging is sensitive to Doppler signals within a large field of view. This technique analyzes amplitude, frequency, and phase information and displays a color map over the gray-scale image. Stationary objects, with no phase shift, are assigned a shade of gray based on the amplitude of the echo. Color choices are based on the phase shift of the echo, indicating motion toward or away from the transducer. The color shade is assigned by frequency shift, indicating relative speed of the moving object. Additional refinements are constantly being developed, such as harmonic imaging, which listens for echoes at resonant frequencies different from the transmitted frequency, thus eliminating much of the noise artifact. Sonographic contrast materials are currently being tested and show great promise.

APPLICATIONS

Ultrasound has become the imaging method of choice for the evaluation of developmental dysplasia of the hip (DDH). Cartilaginous and other soft tissue structures can be demonstrated that are not visible radiographically. Mass screening is controversial because of the associated cost and limited manpower and equipment. Ultrasound is performed selectively in infants at increased risk for pathology and in those being followed during treatment.

The standard ultrasound examination combines a static assessment of hip position and acetabular morphology with a dynamic assessment during modified Barlow and Ortolani maneuvers. The hip is examined from the lateral approach with the femur in both extension and flexion. Ossified structures are highly echogenic, with posterior shadowing. Cartilaginous structures are hypoechoic with finely stippled echoes. Normally the cartilaginous epiphysis rests against the acetabulum, with at least 50 percent medial to the axis of the ilium. The labrum, joint capsule, and triradiate cartilage may be seen. In pathologic hips, subluxation, increased motion with stress maneuvers, pulvinar, dislocation, and acetabular dysplasia may be demonstrated. A child undergoing treatment may be examined while in the flexion-abduction harness.

Hip ultrasound is performed in older children to assess joint effusions. With the child supine and the hip in neutral position, the hip is imaged from an anterior approach and parallel to the femoral neck. The contralateral hip is imaged for comparison. The joint capsule is echogenic and parallels the anterior cortex, resulting in a concave configuration. Joint effusions of as little as 1 mL may be seen as a distention of the joint space, with a convex, anteriorly bowed capsule. The echogenicity of the fluid is variable and cannot be used as a guide in distinguishing septic arthritis from toxic synovitis. Ultrasound may be used to guide joint aspiration (Fig. 9–51).

Ultrasound of the hip is also useful in evaluating patients with proximal femoral focal deficiency. In this disorder there is a variable degree of underdevelopment of the proximal femur, from mild shortening to near total absence. Treatment decisions are often based on the presence or absence of the femoral head and its location. The cartilaginous epiphysis can be imaged sonographically before it becomes radiographically evident (Fig. 9–52).

The indications for ultrasound in the evaluation of musculoskeletal disorders and soft tissue masses are continually expanding. The ability to differentiate solid and cystic masses noninvasively and to document any blood flow associated with them ensures a growing role for ultrasound in pediatric

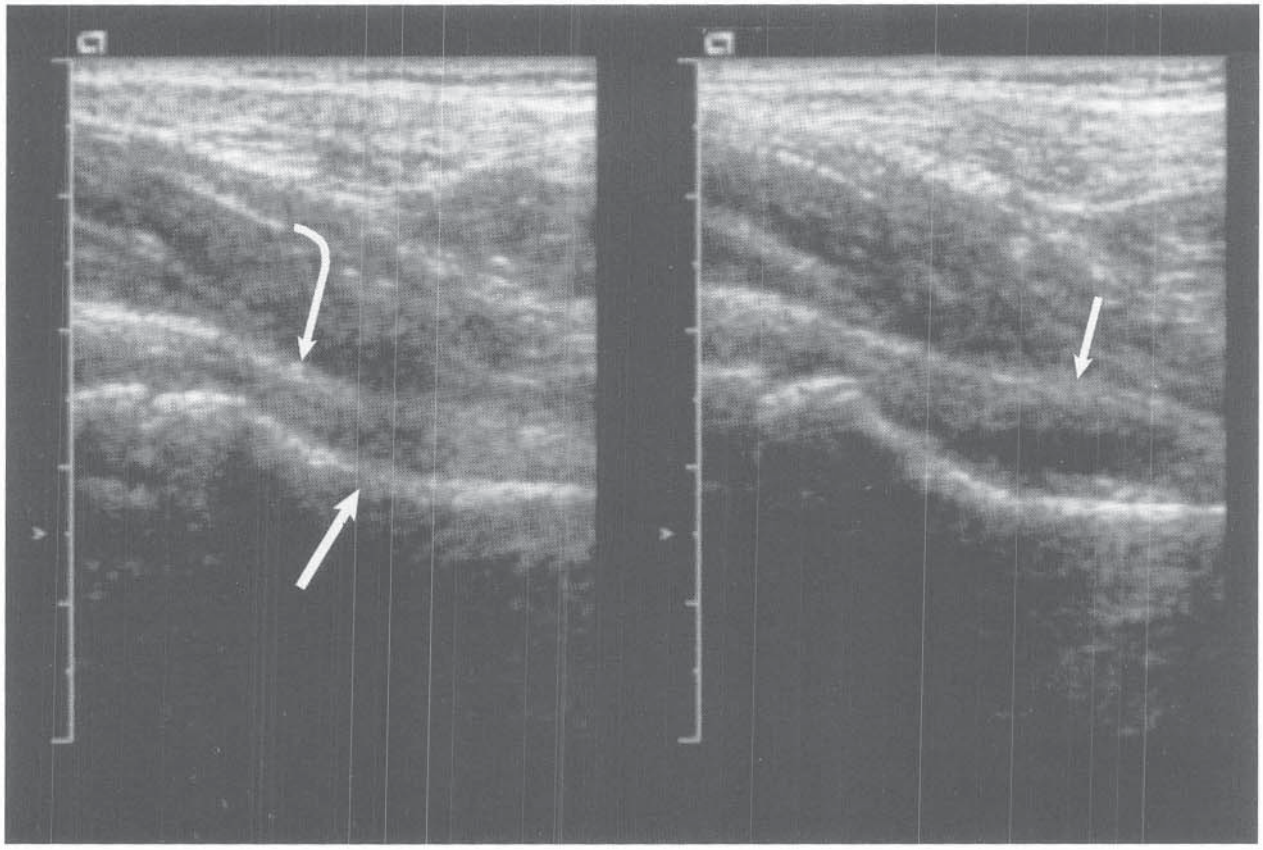

A B

FIGURE 9–51 Ultrasound findings in normal and pathologic hip joint capsules. **A,** Normal hip capsule. The scan was performed anterior to the left femoral neck and demonstrates the echogenic joint capsule paralleling the concave cortical margin. *Straight arrow* points to the cortex; *curved arrow* points to the joint capsule. **B,** Joint effusion from toxic synovitis. The sonogram shows bowing of the anterior joint capsule with fluid between it and the femoral neck. *Straight arrow* points to the distorted joint capsule.

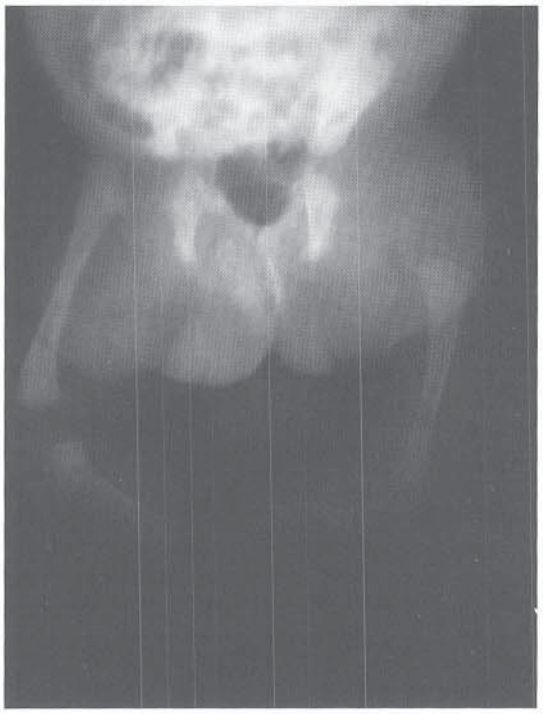

A

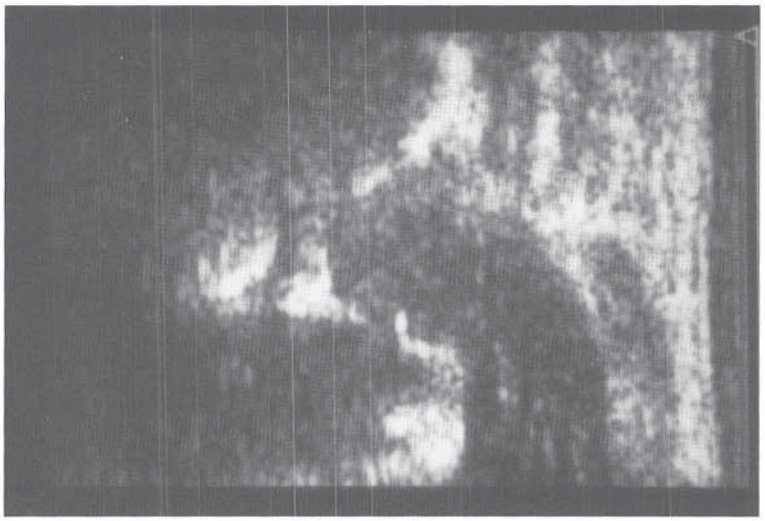

B

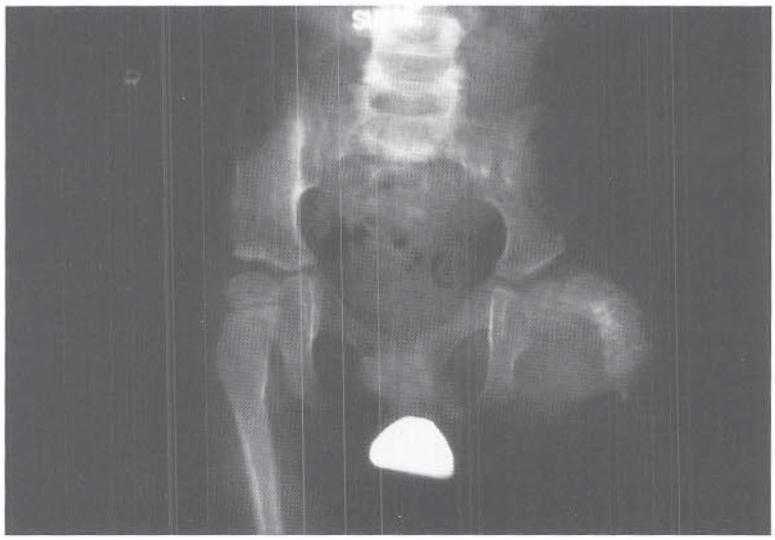

C

FIGURE 9–52 Imaging findings in proximal focal femoral deficiency. **A,** Pelvic radiograph obtained at age 4 weeks shows a lack of ossification of the short left femur. **B,** Left hip sonogram obtained at age 4 weeks shows the bowed cartilaginous anlage of the left femur conjugating with the acetabulum. **C,** Radiograph obtained at age 6 years shows ossification of the deformed, but conjugated, left femur.

imaging. Additional uses are described in the chapters on specific conditions.

Nuclear Imaging

Diagnostic nuclear imaging differs from other radiographic techniques in two important ways: it displays physiologic information rather than purely anatomic information, and it relies on the emission of energy from the patient rather than the transmission of energy through the patient. Nuclear imaging is accomplished with the use of various radiopharmaceuticals. These compounds may be administered in oral, intravenous, gaseous, or aerosolized forms. Once administered, they demonstrate an affinity for specific physiologic processes, such as osteoblastic activity, hepatic function and biliary excretion, phagocytic activity, renal filtration and excretion, or myocardial activity. Because the compounds are bound to selected radioactive isotopes, the resulting images serve as a guide to physiologic and pathologic localization and processing.

Radioactivity is produced by the spontaneous disintegration of the nucleus of a radioactive atom. The nucleus, a collection of protons and neutrons, may decay from an unstable, high-energy state to a lower energy state through the release of energy in the form of alpha, beta, or gamma rays. The moment of decay for individual atoms is unpredictable, but the overall rate of decay of a larger sample is constant and is referred to as its half-life. This is the time it takes for half the sample to decay, and it is unique for every radioactive species. Alpha decay releases a helium nucleus (two protons and two neutrons) from the atom. This is of little diagnostic interest as these large, energetic particles deliver a large radiation dose locally and can travel only micrometers in soft tissues. Beta decay releases an electron (or positron) from the nucleus and is the most frequent decay observed in nature. These particles travel millimeters in tissue. Electromagnetic radiation in the form of photons

(gamma ray) is produced when a nucleus decreases its energy state without any change in its number of protons and neutrons. Gamma rays are optimal for medical imaging since a large enough proportion can escape the patient to be detected, and a lower dose is delivered to the soft tissues.

Emitted gamma rays are imaged with the use of a specialized camera with three main components. A scintillation crystal made of thallium-activated sodium iodide converts gamma photons into light photons. A photomultiplier tube converts these light photons into electrical impulses. The processing unit amplifies the electrical pulse and selects those of appropriate energy for recording, helping to reduce background noise.

The most commonly used radiopharmaceutical for skeletal imaging is a technetium 99m-labeled phosphate compound, such as methylene diphosphonate (MDP). Tc-99m is a readily available material with a half-life of 6 hours. It is a metastable isomer (hence the *m* suffix) that decays by gamma emission to Tc-99. The half-life is convenient for diagnostic purposes, and its photon energy of 140 keV is excellent for imaging with the scintillation camera. The phosphate moiety determines the compound's fate within the body. As it circulates and diffuses throughout the tissues, it becomes absorbed to hydroxyapatite crystals. This tracer is distributed in relation to blood flow and metabolic activity. The gamma emission from the Tc-99m label allows localiza-

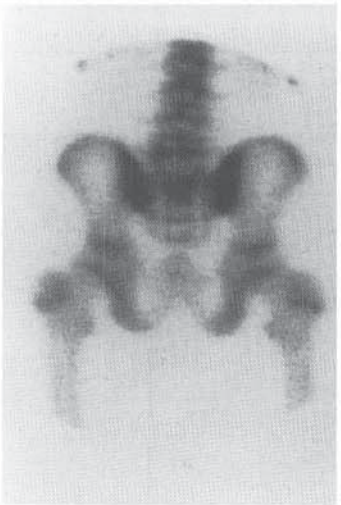

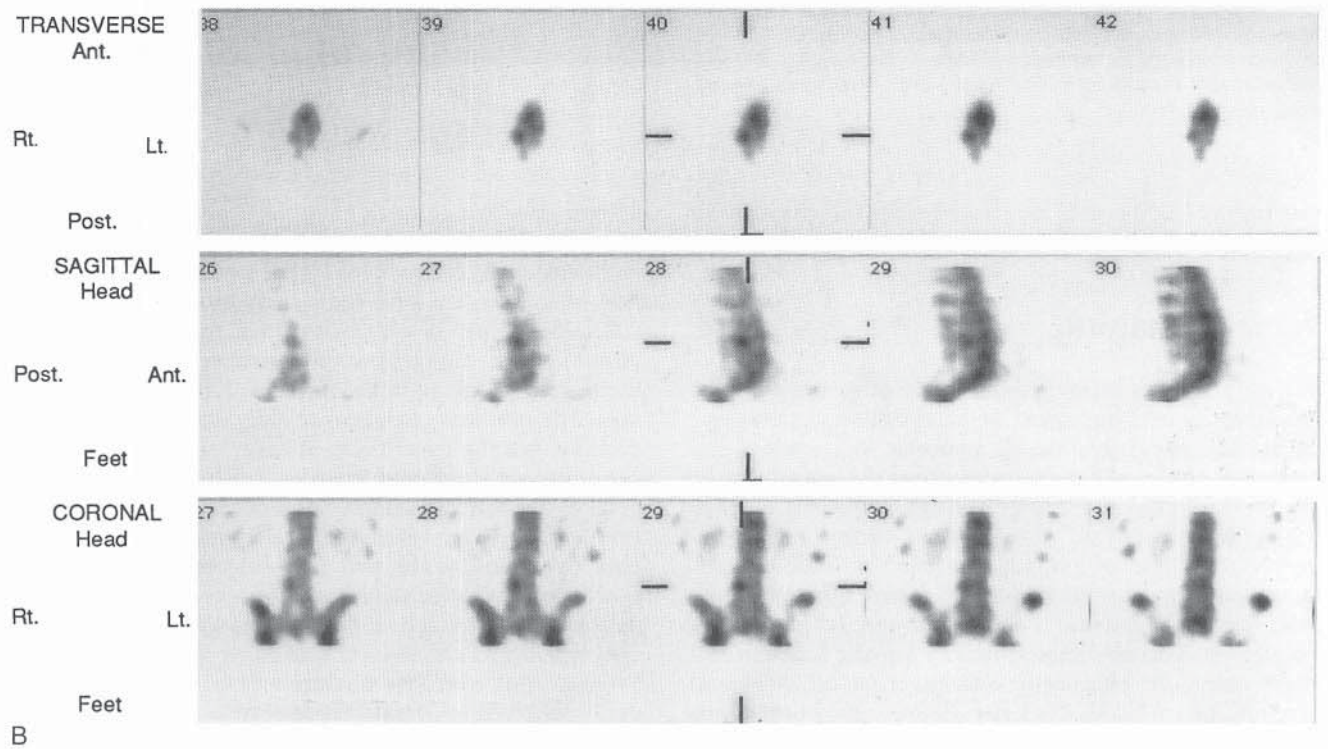

FIGURE 9–53 Stress fracture of the pars interarticularis of L4 in an adolescent athlete with low back pain. **A,** The posterior planar scan performed with ^{99m}Tc-MDP was normal. **B,** Abnormal focal uptake involving the region of the right pedicle and lamina of L4 was seen with SPECT imaging. The intensity of the uptake and its location amid the posterior neural bony elements are diagnostic of a stress fracture reaction. (From Treves ST, Connolly LP, O'Tuama LA, et al: Pediatrics. In Wagner HN (ed): Principles of Nuclear Medicine. Philadelphia, WB Saunders Co, 1995.)

tion of this phosphate tracer. Other agents, such as gallium 67 and white blood cells labeled with indium 111 or Tc-99m for the diagnosis of infection, are utilized less frequently. Thallium 201 may be used to diagnose and monitor bone tumors.

Imaging with these bone-seeking tracers offers advantages over other imaging methods because of the physiologic data obtained and the high sensitivity of the tracers to pathologic processes. Conventional radiography requires up to 50 percent of bone's calcium content to be lost before the loss is detectable. Periosteal reaction does not become apparent for 7 to 10 days. Bone scintigraphy becomes positive in only 24 to 48 hours following infection and trauma. An exception is the occasionally normal or decreased activity that may be seen in acute osteomyelitis. This "cold bone scan" may be due to a high-pressure abscess or an inflammatory response that occludes local blood vessels. When symptoms persist, the study should be repeated in 2 to 3 days, or a gallium study may be performed.

Although bone scintigraphy has a high sensitivity, its specificity is low, as bone is limited in its response to injury. Benign and malignant processes cannot be distinguished solely by skeletal scintigraphy.

Bone scintigraphy is not usually the initial imaging modality for patients with musculoskeletal problems. Plain radiographs are typically obtained first. Scintigraphy is a useful adjunct when the radiographs are normal but the history and clinical examination make a skeletal disorder likely. The imaging sequence will include one or more of the following: a radionuclide angiogram, or blood flow image, obtained during injection; early imaging, or blood pool imaging, performed within 15 minutes; a bone phase, obtained at 2 to 4 hours, when the activity is seen principally in the skeleton, with clearance from the blood and soft tissues; and 24-hour imaging, which may improve diagnostic certainty, as background activity continues to fall over time. As with all pediatric imaging, radionuclide scintigraphy requires careful technique, patient positioning, and immobilization. Sedation may be necessary in patients unable to cooperate.

Magnification is an indispensable technique in pediatric nuclear imaging. Pinhole and converging collimators improve the relatively low resolution of the scintillation camera and are better than electronic image enlargement, which does not change the resolution. Single-photon emission computed tomography (SPECT) can increase lesion detection. As in conventional CT, a rotating camera obtains three-dimensional data that can be displayed as sections in any plane and can be reformatted into a three-dimensional representation. Although spatial resolution is not improved fundamentally, the separation of overlapping structures and the removal of out-of-plane information increase image contrast. This technique is particularly important in detecting lesions of the spine, femoral neck, and small bones of the extremities (Fig. 9–53). The decision to perform SPECT imaging should be made in consultation with the radiologist.

Indications for the use of skeletal scintigraphy include the evaluation and differentiation of osteomyelitis, cellulitis, and septic arthritis. Aseptic necrosis can be diagnosed and revascularization followed scintigraphically. Bone scanning is useful in trauma for diagnosing occult fractures, toddler fractures, and stress fractures, and can be used as an adjunct to a conventional skeletal survey in cases of suspected child abuse (Fig. 9–54). Both benign and malignant lesions, such as fibrous dysplasia, osteoid osteoma, osteosarcoma, and

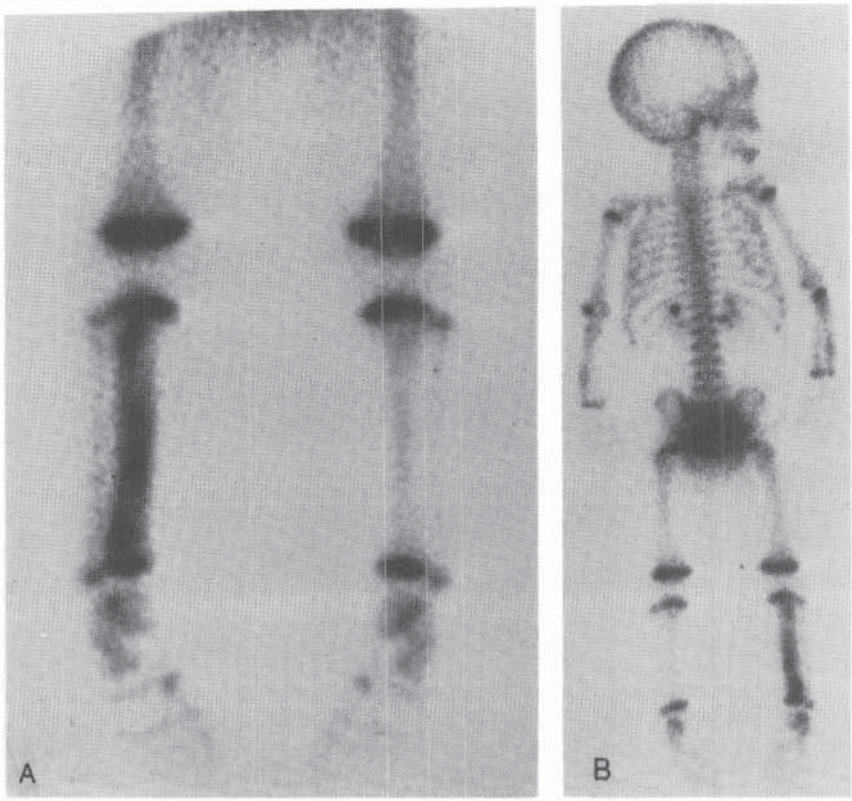

FIGURE 9–54 Scintigraphic findings in battered child syndrome. **A,** An anterior scintiphoto of the lower extremities of a child who sustained the sudden onset of a limp revealed increased uptake in the right tibia, suggesting a toddler's fracture. **B,** A posterior whole-body scintiphoto revealed abnormal uptake in both forearms and an epitrochlear fracture of the left arm. Multiple rib abnormalities are suggested as well. Psychosocial evaluation uncovered evidence of child abuse. (From Harcke HT, Mandell GA: Musculoskeletal scintigraphy. In Miller JH, Gelfand MJ (eds): Pediatric Nuclear Imaging. Philadelphia, WB Saunders Co, 1994.)

metastatic disease, are within the realm of scintigraphy. Specific indications and findings are discussed in the relevant chapters.

ADDITIONAL READING

Ultrasonography and Nuclear Imaging

Alazraki N: Radionuclide techniques. In Resnick D (ed): Diagnosis of Bone and Joint Disorders, 3rd ed. Philadelphia, WB Saunders Co, 1995.

Chung T, Kirks DR: Techniques. In Kirks DR, Griscom NT (eds): Practical Pediatric Imaging: Diagnostic Radiology of Infants and Children, 3rd ed. Philadelphia, Lippincott-Raven, 1998.

Harcke HT, Imaging techniques and applications. In Morrissy RT, Weinstein SL (eds): Lovell and Winter's Pediatric Orthopaedics, 4th ed. Philadelphia, Lippincott-Raven, 1996.

Harcke HT: Mandell GA: Musculoskeletal scintigraphy. In Miller JH, Gelfand MJ (eds): Pediatric Nuclear Imaging. Philadelphia, WB Saunders Co, 1994.

Mack LA, Scheible W: Diagnostic ultrasonography. In Resnick D (ed): Diagnosis of Bone and Joint Disorders, 3rd ed. Philadelphia, WB Saunders Co, 1995.

Treves ST (ed): Pediatric Nuclear Medicine, 2nd ed. New York, Springer-Verlag, 1995.